DESIGN ANALYSIS AND FABRICATION OF MICROSTRIP PATCH ANTENNAS FOR WLAN APPLICATIONS USING APERTURE COUPLING FEED

A thesis submitted in partial fulfillment of the requirements

for the award of degree of

MASTER OF ENGINEERING

In

Electronics and Communication

Submitted By

Gunjan

Roll No. 801261008

Under guidance of

Ms. Amanpreet Kaur

Assistant Professor, ECED

T.U., Patiala

Department of Electronics and Communication Engineering

THAPAR UNIVERSITY, PATIALA

June 2014

CERTIFICATE

I hereby declare that the work which is being presented in the thesis entitled, **"DESIGN ANALYSIS AND FABRICATION OF MICROSTRIP PATCH ANTENNAS FOR WLAN APPLICATIONS USING APERTURE COUPLING FEED"** in partial fulfillment of the requirement for the award of degree of M.E in Electronics and Communication submitted in Electronics and Communication Engineering Department of Thapar University, Patiala is an authentic record of my own work carried out under the supervision of Ms. Amanpreet Kaur, Assistant Professor, ECED.

The matter presented in this thesis has not been submitted in any other University/Institute for the award of degree.

Date: 26th June, 2014

(GUNJAN)

ROLL NO: 801261008

It is certified that the above statement made by the student is correct to the best of my knowledge and belief.

(Ms. Amanpreet Kaur)
Assistant Professor
ECED, Thapar University

Countersigned By:-

Dr. Sanjay Sharma
Professor & Head
ECED, Thapar University
Patiala, 147004

Dr. S.K. Mohapatra
Dean of Academic Affairs
Thapar University
Patiala, 147004

ABSTRACT

As of today, Wi-Fi (also known as WLAN) has become a standard in most computers. Almost every modern mobile, and other gadgets are being implemented with Wi-Fi technology. Wi-Fi makes it possible for the user to connect to the internet or a LAN (Local Area Network) through a wireless connection (hence the name WLAN-Wireless Local Area Network). Wireless communications have been developed widely and rapidly in the modern world especially during the last two decades. The future development of the personal communication devices will aim to provide image, speech and data communications at any time, and anywhere around the world. This indicates that the future communication terminal antennas must meet the requirements of multi-band or wideband to sufficiently cover the possible operating bands. However, the difficulty of antenna design increases when the number of operating frequency bands increases. In addition, for miniaturizing the wireless communication system, the antenna must also be small enough to be placed inside the system. However, in order to transmit and receive more information large bandwidths are required, and bandwidth enhancement is currently a popular research area. Therefore the advantages of microstrip antennas made them a perfect candidate for use in the wireless local area network (WLAN) applications. Though bound by certain disadvantages, microstrip patch antennas can be tailored so they can be used in the new high-speed broadband WLAN systems. In the thesis work the analysis of aperture coupled microstrip antenna is done using transmission line model. A single band aperture coupled microstrip antenna is designed at 5.8 GHz for WLAN applications. Then a dual band aperture coupled microstrip antenna is designed at 3.692 GHz and 5.2 GHz for WLAN applications by cutting the slits in the rectangular shaped patch and its bandwidth is improved by placing the stubs with the feedline. Then a broadband aperture coupled microstrip antenna is designed at 12.5 GHz for DBS applications. Thereafter a dual band aperture coupled stacked microstrip antenna is designed at 3.455 GHz and 5.2 GHz for wireless applications and its bandwidth is improved by introducing an air gap between the ground plane and the upper layer substrate. The fabrication of the broadband aperture coupled microstrip antenna at 12.5 GHz for DBS applications is done and the fabricated antenna is tested by the VNA model no N5222A of Agilent Technologies, whose frequency range is from 10 MHz to 26.5 GHz.

ACKNOWLEDGEMENT

To discover, analyze and to present something new is to venture on an untraded path towards and unexplored destination is an arduous adventure unless one gets a true torch bearer to show the way. I would have never succeeded in completing my task without the cooperation, encouragement and help provided to me by various people. Words are often too less to reveals one's deep regards. I take this opportunity to express my profound sense of gratitude and respect to all those who helped me through the duration of this thesis. I acknowledge with gratitude and humility my indebtedness to **Ms. Amanpreet Kaur, Assistant Professor,** Electronics and Communication Engineering Department, Thapar University, Patiala, under whose guidance I had the privilege to complete this thesis. I wish to express my deep gratitude towards her for providing individual guidance and support throughout the thesis work.

I convey my sincere thanks to **Head of the Department, Dr. Sanjay Sharma** as well as **PG Coordinator, Dr. Kulbir Singh, Associate Professor,** Electronics and Communication Engineering Department, entire faculty and staff of Electronics and Communication Engineering Department for their encouragement and cooperation.

My greatest thanks are to all who wished me success especially my parents. Above all I render my gratitude to the Almighty who bestowed self-confidence, ability and strength in me to complete this work for not letting me down at the time of crisis and showing me the silver lining in the dark clouds. I do not find enough words with which I can express my feelings of thanks to my dear friends for their help, inspiration and moral support which went a long way in successful competition of the present study.

Also, I would like to give special thanks to **Dr. C.C. Tripathi, Associate Professor**, Electronics and Communication Engineering Department, UIET Kurukshetra for giving the permission to test my fabricated antenna at their institute.

(Gunjan)

INDEX

LIST OF FIGURES

LIST OF TABLES

ABBREVIATIONS

ACMA	Aperture Coupled Microstrip Antenna
ACSMPA	Aperture Coupled Stacked Microstrip Patch Antenna
AMTS	Advanced Mobile Telephone System
CDMA	Code Division Multiple Access
CST	Computer Simulation Technology
DBS	Direct Broadcast Satellite
DTH	Direct to Home
GSM	Global System for Mobile communications
iDEN	Integrated Digital Enhanced Network
IMTS	Improved Mobile Telephone Service
IrDA	Infrared Data Association
ITU	International Telecommunication Union
MMS	Multimedia Media Messages
MPA	Microstrip Patch Antenna
OFDM	Orthogonal Frequency Division Multiplexing
PDC	Personal Digital Cellular
PTT	Push to Talk
RFID	Radio Frequency Identification
SAR	Specific Absorption Rate
TDMA	Time Division Multiple Access
WLAN	Wireless Local Area Network
WiMAX	Worldwide Interoperability for Microwave Access
VNA	Vector Network Analyzer

CHAPTER-1

INTRODUCTION

1.1 Overview of Wireless Communication

Wireless communication may be defined as the transfer of information between two or more points that are not connected by an electrical conductor. It is the fastest growing segment of the communication industry. Therefore it has attracted the attention of the media and the imagination of the public. The long distance communications were impractical to implement with the use of wires. Wireless operations permit services that make the long distance communication possible without the use of wires. The first wireless networks were developed in the pre-industrial age. These systems transmitted information over line of sight distances using smoke signals, torch signaling, flashing mirrors, signal flares or semaphore flags. An elaborate set of signal combinations was developed to convey complex messages with these rudimentary signals. Observation stations were built on hilltops and along roads to relay these messages over large distances. These early communication networks were replaced first by the telegraph network (invented by Samuel Morse in 1838) and later by the telephone (invented by Alexander Graham Bell and Thomas Augustus Watson in 1876). In 1895, a few decades after the telephone was invented, Marconi demonstrated the first radio transmission from the Isle of Wight to a tugboat 18 miles away, and radio communications was born. Radio technology advanced rapidly to enable transmissions over larger distances with better quality, less power, and smaller, cheaper devices, thereby enabling public and private radio communications, television, and wireless networking [1].

Different modes of wireless communications are:

1. Radio – Radio is the radiation of electromagnetic signals through atmosphere or free space. The frequency of radio signals are from about 3KHz to 300KHz. It includes radio communications, microwave communications, for example long range line of sight via highly directional antennas, or short range communications.

2. Free space optical – Free space optical communication is an optical communication technology that uses light propagating in free space (air, outer space, vacuum, or something

similar) to wirelessly transmit data for telecommunications or computer networking. This is in contrast with using solids such as in the optical fiber cable or in an optical transmission line. This technology is useful where the physical connections are impractical due to high costs or other considerations. Light, visible and infrared (IR) is used in for example consumer IR devices such as remote controls or via Infrared Data Association (IrDA).

3. Sonic – It is especially ultrasonic short range communication which involves the transmission and reception of sound.

4. Electromagnetic Induction – It is the short range communication that has been used in biomedical situations such as pacemakers and for short range RFID (Radio Frequency Identification) tags [1].

1.2 Generations of Mobile Wireless Communication System

Mobile Wireless Technology has become very popular as it has simplified the communication. It provides high speed services to the users. In past few years, Mobile Wireless Technology has experienced different generations of Technology mainly from 0G to 4G. In present the implementation work of 5G is going on. In the following the features of each generation are presented [2].

0G or Mobile Radio Telephone Systems preceded modern cellular mobile telephony technology. Since they were the predecessors of the first generation of cellular telephones, these systems are sometimes retroactively referred to as pre cellular (or sometimes zero generation) systems. Technologies used in pre cellular systems included the PTT (Push to Talk), MTS (Mobile Telephone System), IMTS (Improved Mobile Telephone Service), and AMTS (Advanced Mobile Telephone System) systems [2].

1G or First Generation of Wireless Telephone Technology or Mobile Telecommunications was introduced in the 1980s. These were the analog telecommunication standards. One such standard is NMT (Nordic Mobile Telephone). The others standards include AMPS (Advanced Mobile Phone System), C-450, TACS (Total Access Communications System), Radiocom 2000 and RTMI. There were multiple systems in JAPAN. NTT (Nippon Telegraph and Telephone corporation) developed three standards namely TZ-801, TZ-802 and TZ-803. DDI (Daini Denden Planning, Inc.) used

JTACS (Japan Total Access Communications System) standard. 1G speed vary from 28kbps to 56kbps [2].

2G or Second Generation of Wireless Telephone Technology was launched on the GSM (Global System for Mobile Communications) standard in 1991. 2G technologies enabled mobile phone networks to provide the services like text messages, picture messages and MMS (Multi Media Messages). On the basis of multiplexing used 2G technologies can be divided into TDMA (Time Division Multiple Access) based and CDMA (Code Division Multiple Access) based standards. The main 2G standards are GSM, IS-95 (Interim Standard-95) or cdmaOne, PDC (Personal Digital Cellular), iDEN (Integrated Digital Enhanced Network) and IS-136 or D-AMPA. The data transmission rate of the 2G is about 64kbps. The 2G systems superseded by 2.5G (GPRS), 2.75G (EDGE), 3G and 4G [2].

3G or Third Generation of Wireless Telephone Technology or Mobile Telecommunications is based on a set of standards which are used for mobile devices. 3G has applications in wireless voice telephony, mobile internet access, fixed wireless internet access, video calls and mobile TV. The third generation support services which provide an information transfer rate of at least 200kbps. Later on 3G released often denoted 3.5G and 3.75G provide mobile broadband access of several Mbps to smart phones and mobile modems in laptop computers. The first release of the 3GPP LTE (third Generation Partnership Project Long Term Evolution) standard does not completely fulfill the ITU 4G requirements called IMT-Advanced. First release LTE is not backward compatible with 3G, but it is a pre-4G technology. Its evolution LTE Advanced is a 4G technology. WiMAX (Worldwide Interoperability for Microwave Access) is another technology verging on or marketed as 4G [2].

4G or Fourth Generation of Mobile Telecommunications Technology succeeded 3G. A 4G system in addition to the usual voice and other services of 3G provides mobile ultra broadband internet access with USB wireless modems to laptops, smart phones and other mobile devices. 4G find applications in mobile web access, IP telephony, gaming services, video conferencing, high definition mobile TV, cloud computing and 3D television. The

4Gsystems use OFDM (Orthogonal Frequency Division Multiplexing) and accomplish data transmission at the rate of 20Mbps [2].

Table 1.1 below shows various generations of mobile wireless communication system and a comparison between them.

Technology / Features	**1G**	**2G/2.5G**	**3G**	**4G**	**5G**
Start/ Deployment	1970/ 1984	1980/ 1999	1990/ 2002	2000/ 2010	2010/ 2015
Data Bandwidth	2Kbps	14.4-64Kbps	2Mbps	200Mbps to 1Gbps for low mobility	1Gbps and higher
Standards	AMPS	2G:TDMA, CDMA,GSM 2.5G:GPRS, EDGE,1xRTT	WCDMA, CDMA-2000	Single unified standard	Single unified standard
Technology	Analog cellular technology	Digital cellular technology	Broad bandwidth CDMA, IP technology	Unified IP and seamless combination of broadband, LAN/WAN/ PAN and WLAN	Unified IP and seamless combination of broadband LAN/WAN/PAN/ WLAN and wwww
Service	Mobile telephony (Voice)	2G:Digital voice, short messaging 2.5G:Higher capacity	Integrated high quality audio, video and	Dynamic information access, wearable devices	Dynamic information access, wearable devices with AI capabilities

		packetized data	data		
Multiplexing	FDMA	TDMA, CDMA	CDMA	CDMA	CDMA
Switching	Circuit	2G:Circuit 2.5G:Circuit for access network & air interface; packet for core network and data	Packet except circuit for air interface	All packet	All packet
Core Network	PSTN	PSTN	Packet network	Internet	Internet
Handoff	Horizontal	Horizontal	Horizontal	Horizontal and Vertical	Horizontal and Vertical

Table 1.1 Comparison of All Generations of Mobile Technologies [2]

1.3 WLAN (Wireless Local Area Network)

In 1997, IEEE (Institute of Electrical and Electronics Engineers) created the very first WLAN standard. They called it 802.11 after the name of the group formed to oversee its development. It supported a maximum network bandwidth of 2Mbps which is too slow for most applications. For this reason ordinary 802.11 wireless products are no longer manufactured and to improve the above standard four subsets of Ethernet based protocol standard were included [2].

WLANs have become popular in the home due to ease of installation, and in commercial complexes offering wireless access to their customers. Wireless LANs have a great deal of applications. Modern implementations of WLANs range from small in-home networks to large campus-sized ones to completely mobile networks on airplanes and trains. Users can access the Internet from WLAN hotspots in restaurants, hotels, and now with portable devices that connect to 3G or 4G networks [2].

Table 1.2 below shows the different WLAN standards available and a comparison between them [2].

WLAN					
Standard	**802.11 Legacy**	**802.11a**	**802.11b (Wi-Fi)**	**802.11g**	**802.11n**
Frequency Band	2.4GHz	5.8GHz	2.4GHz	2.4GHz	2.4-5.8GHz
Maximum Range	~70 meters	~100 meters	~100 meters	~110 meters	~160 meters
Maximum Data Rate	2Mbps	54Mbps	11Mbps	54Mbps	248Mbps
Access Method	DSSS,FHSS	OFDM	DSSS,CCK	OFDM	MIMO-OFDM
Modulation Method	GFSK,BPSK, DBPSK, DQPSK	BPSK,QPSK, 16-QAM, 64-QAM	DPSK,DBPSK, DQPSK	BPSK,QPSK, 16-QAM, 64-QAM, DBPSK and DQPSK	BPSK, QPSK, 16-QAM, 64-QAM

Table 1.2 Comparison of Different WLAN Standards [2]

1.4 WiMAX (Worldwide Interoperability for Microwave Access)

WiMAX is a wireless communication standard which was designed to provide data rates at 30 to 40 Mbps, with the 2011 update providing up to 1Gbps for fixed stations. The name WiMAX was created by the WiMAX Forum which was formed in June 2001 to promote conformity and interoperability of the standard [2].

Table 1.3 below shows different WiMAX standards available and a comparison between them [2].

Standard	IEEE 802.16	IEEE 802.16d/802.16-2004 (Fixed WiMAX)	IEEE 802.16e/ 802.16e-2005 (Mobile WiMAX)
Spectrum	10-66 GHz	2-11 GHz	2-6 GHz
Application	Backhaul	Wireless DSL and Backhaul	Mobile Internet
Channel	Line of sight only	Non line of sight	Non line of sight
Bit Rate	32-134 Mbps at 28 MHz channelization	Up to 75Mbps at 20-MHz channelization	Up to 15Mbps at 5-MHz channelization
Modulation	QPSK, 16-QAM & 64-QAM	OFDM 256, OFDMA–2048, QPSK, 16-QAM, 64-QAM	Same as 802.16d, Scalable OFDMA
Mobility	Fixed	Fixed	Pedestrian mobility, regional roaming
Channel Bandwidths	20, 25, & 28 MHz	Selectable channel band--width between 1.5 & 20 MHz	Same as 802.16d
Typical Cell Radius	1-3 miles	3-5 miles(up to 30 miles depending on tower height, antenna gain & transmit power)	1-3 miles

Table 1.3 Comparison of Different WiMAX Standards [2]

WiMAX refers to interoperable implementations of the IEEE 802.16 family of wireless-networks standards ratified by the WiMAX Forum. Similarly, Wi-Fi refers to interoperable

implementations of the IEEE 802.11 Wireless LAN standards certified by the Wi-Fi Alliance. WiMAX can be used for a number of applications including broadband connections, cellular backhaul, hotspots, etc. It is similar to Wi-Fi, but it can enable usage at much greater distances [2].

1.5 Direct Broadcast Satellite

DBS (Direct Broadcast Satellite) broadcasts satellite television for home reception application purposes. DBS service refers to either free channels or commercial services available from one orbital position of any country. DBS refers to the transmitted services by the satellite in particular frequency bands. DBS is also known as BSS (Broadcasting Satellite Service) by the ITU (International Telecommunication Union). DTH (Direct to Home) is broader term than DBS. DTH occurred even earlier than the DBS. DTH is used for those services which require lower power satellites and larger dishes. DBS relatively requires smaller dishes. For the purpose of global radio spectrum management the ITU has divided the whole world in three regions. Each region has a set of frequency allocation. These regions are [2]:

1. ITU Region 3 which has frequency allocation from 11.7 GHz to 12.2 GHz. Asia and Australia comes under this region.

2. ITU Region 1 has frequency allocation from 10.7 GHz to 12.75 GHz. And it includes Europe, Russia and Africa.

3. ITU Region 2 has frequency allocation from 12.2 GHz to 12.7 GHz. It includes North and South America.

1.6 Need of Antenna

The IEEE Standard Definitions of terms for Antennas (IEEE Std 145-1983) defines the antenna or aerial as “a means for radiating or receiving radio waves.” In other words the antenna is the transitional structure between free-space and a guiding device. The guiding device or transmission line may take the form of a coaxial line or a hollow pipe (waveguide), and it is used to transport electromagnetic energy from the transmitting source to the antenna, or from the antenna to the receiver. In the former case, we have a transmitting antenna and in the latter a receiving antenna. Antennas are required by any radio receiver or transmitter to couple its electrical connection to the electromagnetic field. Radio waves are electromagnetic

waves which carry signals through the air or through space, at the speed of light [3]. Different types of antenna are available in the market starting from the simple wire antennas to the more complicated antennas as shown in Table 1.4 below:

Types of Antenna Available in the Market		
Wire Antennas	A Wire Antenna is simply a straight wire of length $\frac{\lambda}{2}$ (dipole antenna) and $\frac{\lambda}{4}$ (monopole antenna), where λ is the signal wavelength.	Short Dipole Antenna, Dipole Antenna, Half Dipole Antenna, Broadband Dipoles, Monopole Antenna, Folded Dipole Antenna and Loop Antenna
Travelling Wave Antennas	A Travelling Wave Antenna is a class of antenna that use a travelling wave on a guiding structure as the main radiating mechanism.	Helical Antennas, Yagi-Uda Antennas and Spiral Antennas
Reflector Antennas	Reflector Antennas reflect the electromagnetic waves. These antennas provide very high gain.	Corner Reflector, Parabolic Reflector (Dish Antenna)
Microstrip Antennas	Microstrip Antennas have a metal trace bonded to an insulating dielectric substrate, such as a PCB, with a continuous metal layer bonded to the opposite side of the substrate which forms a ground plane.	Rectangular Microstrip (Patch) Antennas, Planar Inverted-F Antennas (PIFA)
Log Periodic Antennas	Log Periodic Antennas' performance is periodic as a function of the logarithm of the frequency.	Bow Tie Antennas, Log Periodic Antennas, Log Periodic Dipole Array
Aperture Antennas	Aperture Antennas contain some sort of opening through which electromagnetic waves are transmitted or received.	Slot Antenna, Cavity-Backed Slot Antenna, Inverted-F Antenna, Slotted Waveguide Antenna, Horn Antenna, Vivaldi Antenna, Telescopes

Table 1.4 Different Types of Antennas

The major requirement in the present wireless world is to have the size of antenna as small as possible, so out of all the available structures in terms of WLAN and WiMAX applications are considered, the microstrip antennas serve the most optimum choice. Also the microstrip antennas require low cost materials, simple and inexpensive fabrication techniques for their commercial system applications.

1.7 Microstrip Patch Antenna

A microstrip patch antenna (MPA) consists of a conducting patch of any planar or non-planar geometry on one side of a dielectric substrate with a ground plane on other side as shown in Figure 1.1 as:

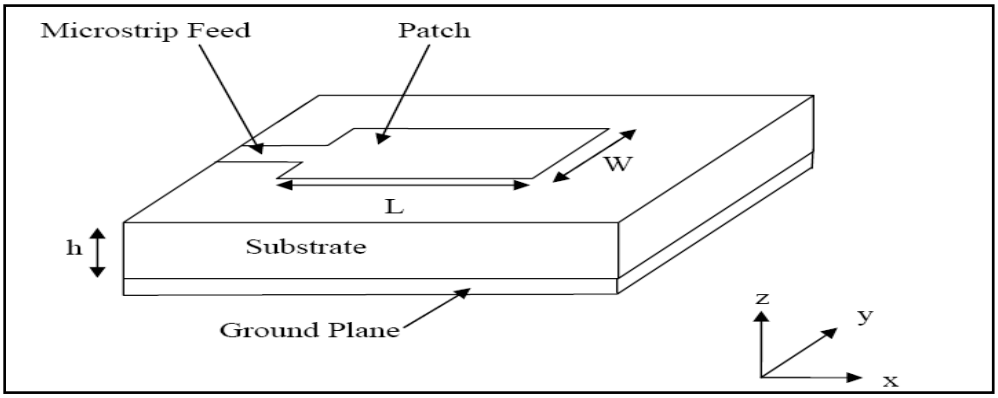

Figure 1.1 Microstrip Patch Antenna [3]

Due to its planar configuration and ease of integration with microstrip technology, the microstrip patch antenna has been heavily studied. There are different structures of microstrip antennas, but on the whole we have four basic parts in the antenna are the patch, dielectric substrate, ground plane and the feedline. The rectangular and circular patches are the basic and most commonly used microstrip antennas. These patches are used for the simplest and the most demanding applications. The microstrip patch antennas are well known for their performance and their robust design, fabrication and their extent usage. The advantages of this microstrip patch antenna are to overcome their de-merits such as easy to design, light weight etc., the applications are in the various fields such as in the medical applications, satellites and of course even in the military systems just like in the rockets, aircrafts missiles etc. A feedline is used to excite to radiate by direct or indirect contact.

There are many different techniques of feeding and four most popular techniques are coaxial probe feed, microstrip line, aperture coupling and proximity coupling [3].

A comparison between different feeding techniques has been given in Table 1.5 and based on the comparison aperture coupled technique to feed the Microstrip Antennas has been chosen in this thesis work.

Characteristics	Microstrip Line Feed	Coaxial Feed	Aperture Coupled Feed	Proximity Coupled Feed
Spurious feed radiations	More	More	Less	Minimum
Reliability	Better	Poor due to soldering	Good	Good
Ease of fabrication	Easy	Soldering and drilling needed	Alignment required	Alignment required
Impedance Matching	Easy	Easy	Easy	Easy
Bandwidth (achieved with impedance matching)	2-5%	2-5%	2-5%	13%

Table 1.5 Comparison of Different Feeding Techniques of MPA [3]

The selection of aperture coupled technique to feed the Microstrip Patch Antennas in this thesis work are due to the useful features and recent development related to this excitation method listed below as:

- Provides impedance bandwidths ranging from 5% to 50%
- The independent selection of antenna and feed substrate materials
- The two-layer construction shields radiating aperture from feed network
- The increased substrate space for antenna elements and feed lines
- Convenient integration for active arrays
- Theoretically zero cross polarization in principle planes

- Many possible variations in patch shape, aperture shape, feed line type, radomes etc.
- Extension to aperture coupled microstrip line couplers, waveguide transitions, dielectric resonators etc

1.8 Methods of Analysis

The most popular models for the analysis of Microstrip Patch Antennas are the transmission line model, cavity model, and full wave model (which include primarily integral equations/Moment Method). The transmission line model is the simplest of all and it gives good physical insight but it is less accurate. The cavity model is more accurate and gives good physical insight but is complex in nature. The full wave models are extremely accurate, versatile and can treat single elements, finite and infinite arrays, stacked elements, arbitrary shaped elements and coupling. These give less insight as compared to the two models mentioned above and are far more complex in nature [3].

1.8.1 Transmission Line Model

This model represents the Microstrip Antenna by two slots of width W and height h, separated by a transmission line of length L as shown in Figure 1.2. The microstrip is essentially non-homogeneous line of two dielectrics, typically the substrate and air.

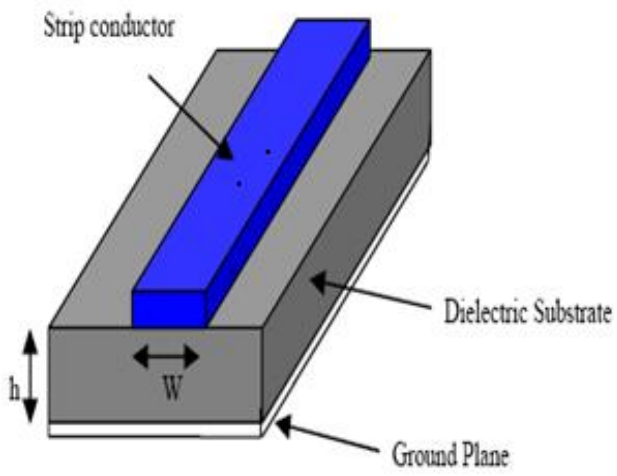

Figure 1.2 Microstrip Line [3]

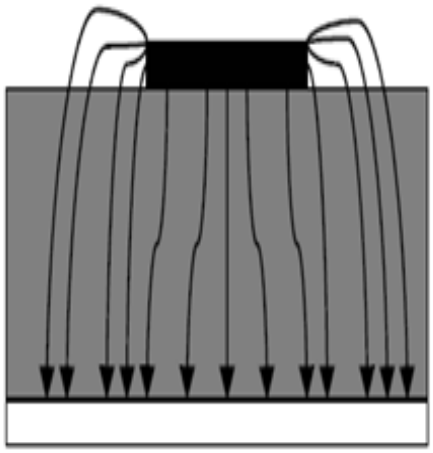

Figure 1.3 Electric field line [3]

Hence, as seen from Figure 1.3 most of the electric field lines reside in the substrate and parts of some lines in air. As a result, this transmission line cannot support pure transverse electric-

magnetic (TEM) mode of transmission, since the phase velocities would be different in the air and the substrate. Instead, the dominant mode of propagation would be the quasi-TEM mode. Hence, an effective dielectric constant (ε_{reff}) must be obtained in order to account for the fringing and the wave propagation in the line. The value of ε_{reff} is slightly less than ε_r because the fringing fields around the periphery of the patch are not confined in the dielectric substrate but are also spread in the air as shown in Figure 1.3 above. The expression for ε_{reff} is given as [3]:

$$\varepsilon_{reff} = \frac{\varepsilon_r + 1}{2} + \frac{\varepsilon_r - 1}{2}\left[1 + 12\frac{h}{w}\right]^{-1/2} \quad (1.1)$$

Where ε_{reff} is effective dielectric constant, ε_r is dielectric constant of substrate, h is height of dielectric substrate and w is width of the patch. Consider Figure 1.1 which shows a rectangular microstrip patch antenna of length L, width W resting on a substrate of height h. The co-ordinate axis is selected such that the length is along the x direction, width is along the y direction and the height is along the z direction.

In order to operate in the fundamental TM_{10} mode, the length of the patch must be slightly less than λ/2 where λ is the wavelength in the dielectric medium and is equal to $\lambda_0/\varepsilon_{reff}$ where λ_0 is the free space wavelength. The TM_{10} mode implies that the field varies one λ/2 cycles along the length, and there is no variation along the width of the patch. In the Figure 1.4 shown below, the microstrip patch antenna is represented by two slots, separated by a transmission line of length L and open circuited at both the ends. Along the width of the patch, the voltage is maximum and current is minimum due to the open ends. The fields at the edges can be resolved into normal and tangential components with respect to the ground plane. It is seen from Figure 1.5 that the normal components of the electric field at the two edges along the width are in opposite directions and thus out of phase since the patch is λ/2 long and hence they cancel each other in the broadside direction. The tangential components as shown in Figure 1.5, which are in phase, means that the resulting fields combine to give maximum radiated field [3].

Hence the edges along the width can be represented as two radiating slots, which are λ/2 apart and excited in phase and radiating in the half space above ground plane. The fringing

fields along the width can be modeled as radiating slots and electrically the patch of the microstrip antenna looks greater than its physical dimensions [3].

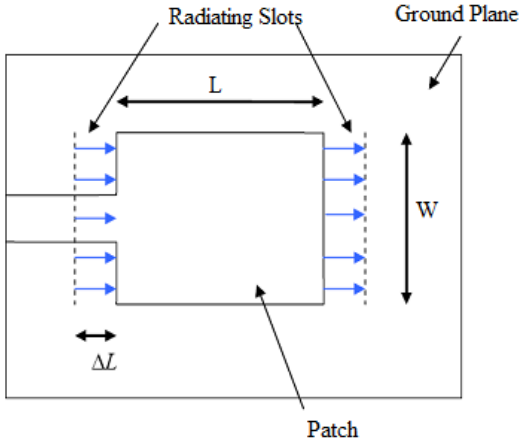

Figure 1.4 Top View of Antenna [3]

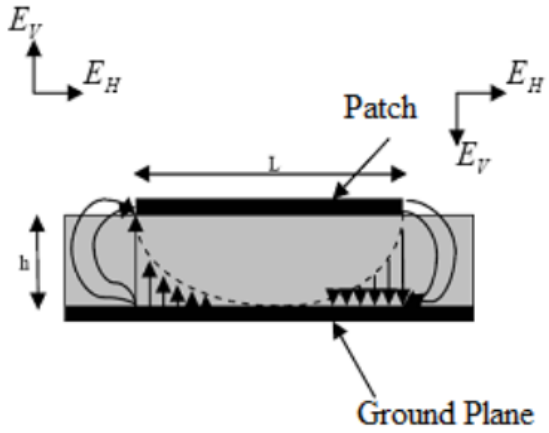

Figure 1.5 Side View of Antenna [3]

The dimension of the patch along its length have now been extended on each end by a distance ΔL [3].

$$\Delta L = 0.412h \cdot \frac{\left(\varepsilon_{reff} + 0.3\right)\left(\frac{W}{h} + 0.264\right)}{\left(\varepsilon_{reff} - 0.258\right)\left(\frac{W}{h} + 0.8\right)} \tag{1.2}$$

The effective length of the patch L_{eff} now becomes,

$$L_{eff} = L + 2\Delta L \tag{1.3}$$

For a given resonance frequency f_0, the effective length is given by [3] as,

$$L_{eff} = \frac{c}{2f_0\sqrt{\varepsilon_r}} \tag{1.4}$$

For a rectangular microstrip patch antenna, the resonance frequency for any TM_{mn} mode f_0

$$f_0 = \frac{c}{2\sqrt{\varepsilon_{eff}\left[\left(\frac{m}{L}\right)^2 + \left(\frac{n}{W}\right)^2\right]}} \tag{1.5}$$

Where m and n are modes along L and W respectively. The width W is given by [3] as,

$$W = \frac{c}{2f_0\sqrt{\frac{\varepsilon_r + 1}{2}}} \tag{1.6}$$

This model is related to only those ground planes which are infinite. For practical considerations, it is necessary that there should be a finite ground plane. It is found that for both infinite and finite ground planes same results can be obtained if the dimensions of the ground is greater than the patch dimensions by nearly six times the thickness of the substrate all around periphery same. Therefore, the length and width of ground is given as [3]:

$$L_g = 6h + L \tag{1.7}$$

$$W_g = 6h + W \tag{1.8}$$

1.9 Parameters for the Analysis of Microstrip Antenna Performance

1.9.1 Return Loss

It is the difference between forward and reflected power, in dB, generally measured at the input to the coaxial cable connected to the antenna. If the power transmitted by the source is P_t and the power reflected back is P_r, then return loss in dB is given by

$$R_L(dB) = 10\log_{10}\frac{P_t}{P_r} \tag{1.9}$$

Return loss should be as large a negative number as possible. Return loss is related to reflection coefficient as follows [4]

$$R_L(dB) = -20\log_{10}|\Gamma| \tag{1.10}$$

The $|\Gamma|$ is the ratio of reflected voltage to the incident voltage and it is related to the load impedance and characteristic impedance as follows

$$|\Gamma| = \frac{V_0^-}{V_0^+} = \frac{Z_L - Z_o}{Z_L + Z_o} \tag{1.11}$$

Where $|\Gamma|$ is reflection coefficient, V_o^- is reflected voltage, V_o^+ is incident voltage, Z_L is load impedance and Z_o is characteristic impedance.

1.9.2 Smith Chart

It was invented by Philip H. Smith. It is a graphical aid or monogram specializing in radio frequency engineering to assist in solving problems with transmission lines and matching circuits. Normalized scaling allows the Smith Chart to be used for problems involving any characteristics impedance or system impedance, although by the far most commonly used is 50 ohm [4].

Figure 1.6 below represents the smith chart of the single band antenna resonating at 5.812 GHz showing its impedance at 5.812 GHz.

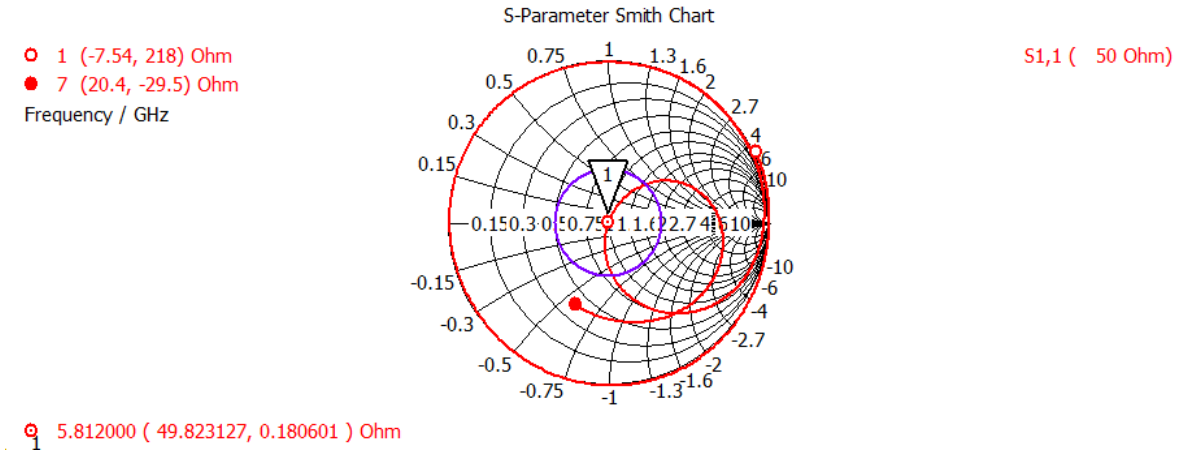

Figure 1.6 Smith Chart of the Single Band Antenna Resonating at 5.812 GHz

1.9.3 Directivity

It is defined as the ratio of radiation intensity in a given direction from the antenna to the radiation intensity averaged over all the directions. The average radiation intensity is equal to the total power radiated by the antenna divided by 4π. If the direction is not specified, the direction of maximum radiation intensity is implied. The directivity of the non- isotropic source is equal to the ratio of its radiation intensity in a given direction over that of an isotropic source. In numerical form, directivity is given by [4]:

$$D = \frac{U}{U_o} = 4\pi \frac{U_{max}}{P_{rad}} \tag{1.12}$$

Where U is radiation intensity (W/unit solid angle), U_o is maximum radiation intensity (W/unit solid angle) and P_{rad} is total power radiated (W)

1.9.4 Gain

It is defined as the ratio of the intensity, in a given direction, to the radiation intensity that would be obtained if the power accepted by the antenna is radiated isotropically. The radiation intensity corresponding to the isotropically radiated power is equal to power accepted (input) by the antenna divided by 4π. When the direction is not stated, the power gain is usually taken in the direction of maximum radiation. It is given by [4]:

$$\text{Gain} = 4\pi \frac{radiation\ \ intensity}{total\ \ input\ \ power} \tag{1.13}$$

1.9.5 Realized Gain

The realized gain is defined by Gain $*$ $(1 - S_{11}^2)$, it includes the impedance mismatch loss.

1.9.6 Beam Width

The beam-width (or angular width) is defined as the angle between two directions where the radiation is dropped by 3 dB regarding the radiation in main lobe direction. This angle is located in a plane containing the main lobe direction [4].

1.9.7 Radiation Pattern

The radiation pattern refers to the directional (angular) dependence of the strength of the radio waves from the antenna. An antenna radiation pattern or antenna pattern may be defined as the graphical representation properties of the antenna as a function of space coordinates. The radiation pattern is a graphical depiction of the relative field strength transmitted from or received by the antenna so the antenna radiation patterns are taken at one frequency. The patterns are usually presented in polar or form with a dB strength scale [4].

Since a Microstrip Patch Antenna radiates normal to its patch surface, the radiation pattern for elevation angle $\varphi = 0$ and $\varphi = 90$ degrees would be important. Figure (a), (b) below shows the radiation pattern of the gain of the single band antenna at 5.8 GHz for $\varphi = 0$ and $\varphi = 90$ degrees respectively. The maximum gain is obtained in the broadside direction and this is measured to be 6.9 dBi for both $\varphi = 0$ and $\varphi = 90$ degrees.

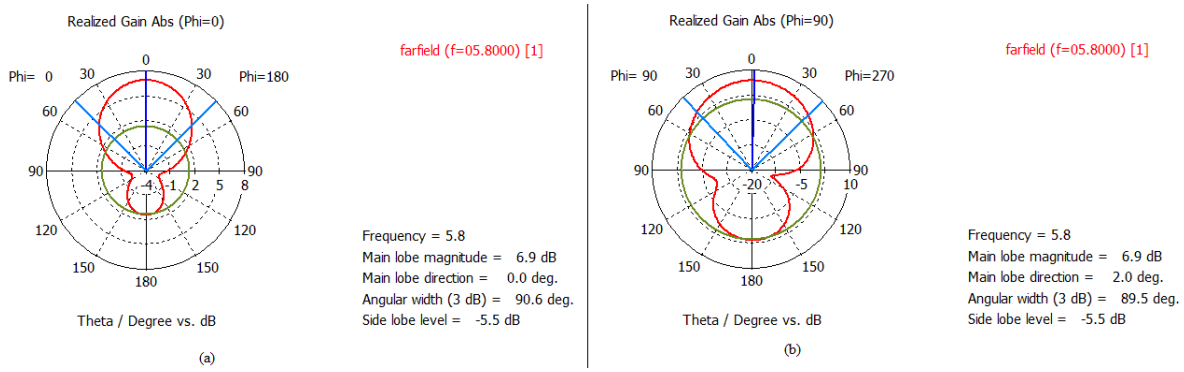

Figure 1.7 Radiation Pattern of the Gain of the Single Band Antenna Resonating at 5.8 GHz for (a)$\varphi = 0$, (b)$\varphi = 90$ Degree

1.9.8 Bandwidth

It is defined as the range of frequencies within which the performance of the antenna, with respect to some characteristic, conforms to a specified standard. The bandwidth can be considered to be the range of frequencies, on either side of a center frequency, where antenna

characteristics (such as input impedance, radiation pattern, beam width, polarization, side lobe level, gain, beam direction and radiation efficiency) are within an acceptable value of those at center frequency. The bandwidth is given as [4] :

$$BW = f_H - f_L \quad (1.14)$$

Where f_H is upper -10 dB frequency value and f_L is lower -10 dB frequency value on S_{11} plot of the antenna.

1.9.9 Efficiency

It is used to take into account losses at the input terminals and within the structure of the antenna. Such losses are due to

- Reflection because of mismatch between the transmission line and antenna
- I^2R losses (conduction and dielectric)

In general, the overall efficiency can be written as

$$e_o = e_r \times e_c \times e_d \quad (1.15)$$

Where e_o is total efficiency, e_r is reflection efficiency, e_c is conduction efficiency and e_d is dielectric efficiency.

An antenna with significant bandwidth with return loss below -10 dB, VSWR of less than 2, feed point impedance of 50 ohm with uniform patch surface current distribution with high directivity and high gain is generally required for efficient performance of an antenna [4].

1.10 Work Covered in the Thesis

The thesis covered the basic principles of design of single band aperture coupled microstrip patch antenna and parametric study of the designed antenna for WLAN applications, the design and simulation of dual band aperture coupled microstrip antenna and improvement of its bandwidth by placing stubs with the feedline, the design and simulation of broadband aperture coupled microstrip antenna for DBS applications and the design and simulation of dual band aperture coupled stacked microstrip antenna and enhancement of its bandwidth by introducing an air gap between the ground plane and the upper layer substrate. Also the fabrication and testing of broadband aperture coupled microstrip patch antenna has been done.

1.11 Thesis Organization

The thesis is divided into eight chapters listed below:

CHAPTER 1 is dedicated to overview of wireless communications and basics of Microstrip Patch Antenna.

CHAPTER 2 includes the literature survey of Microstrip Patch Antennas and the brief ideas about enhancement of the antenna's bandwidth. This chapter also covers the research gaps.

CHAPTER 3 describes the mathematical analysis of Aperture Coupled Microstrip Antenna. It also includes the design and simulation of the Single Band Aperture Coupled Microstrip Antenna used for WLAN applications and its parametric study.

CHAPTER 4 presents the Dual Band Aperture Coupled Microstrip Patch Antenna with the slits cut in the rectangular patch and then bandwidth improvement by placing stubs with the feedline. The nominal antenna has applications in WLAN frequency band.

CHAPTER 5 includes the designing of the Broadband Aperture Coupled Microstrip Patch Antenna for DBS applications with high gain and directivity values.

CHAPTER 6 describes the design of Dual Band Aperture Coupled Stacked Microstrip Patch Antenna for WLAN applications and enhancement of the bandwidth of the antenna by introducing an air gap of 3 mm between the ground plane and the upper layer substrate.

CHAPTER 7 is dedicated to the fabrication and testing of Broadband Aperture Coupled Microstrip Antenna at 12.5 GHz for DBS applications

CHAPTER 8 is dedicated to conclusion and future work.

1.12 Conclusion

In this chapter the overview of wireless communication and microstrip patch antenna has been studied. The design procedure for the microstrip patch antenna has also been studied. The parameters which affect the performance of the microstrip antenna has been discussed.

CHAPTER-2

LITERATURE SURVEY

In order to carry out the research work, the first step was to study the research papers. Papers related to the work were chosen and studied. With the help of literature review, it becomes clearer to perform this project. Researched papers are described below:

2.1 Progress of Aperture Coupled Microstrip Antenna

In 1990, D. M. Pozar et al proposed that the frequency response of the antenna can be controlled by adjusting the size of the coupling aperture. Also by the proper arrangement of the size of the coupling aperture frequency selective surface can be made to pass linear or dual polarized wave [5].

In 1991, W. Chujo et al discussed that aperture coupled microstrip antenna instead of fulfilling the requirements like light weight, thin substrate and ease of fabrication and compatibility with multi-layered feed networks also provide wide bandwidth for mobile satellite communication use as compare to inline and coaxial technique [6].

In 1995, H. Lee et al proposed an antenna with a U-slot in the patch and shows that an antenna with U-slot can provide impedance bandwidth in excess of 30% for an air substrate thickness of about $0.08\lambda_0$ and in excess of 20% for the microwave substrates of similar thickness [7].

In 1995, L. Giauffret et al presented a CPW fed aperture coupled microstrip antenna has a large bandwidth with high gain and low cross polarization levels and is also compact with only one substrate and can be easily connected to both passive and active components [8].

In 1996, K. P. Ray et al showed a new hour glass shaped aperture configuration which was capable for providing maximum coupling and increased bandwidth as compare to other aperture shapes [9].

In 1996, E. Nishiyama et al designed an antenna with two parasitic elements. One parasitic element increases the bandwidth and other is to increase gain [10].

In 1997, W. P. Harokopus et al concluded that Smart antennas are required to increase the coverage of the base station for personal communication systems. Although they provide high gain and coverage over the whole cell but still microstrip antennas are preferred as they provide high gain and coverage but are also flat in appearance and provide dual polarization.

It reduces weight, while yielding excellent electrical performance. The dual polarization provides the required bandwidth to cover the entire transmit and receive bands [11].

In 1998, D. M. Pozar et al proposed that for many wireless applications, bandwidths of 10-15% are required and can be easily achieved by using large aperture with fairly thick antenna substrate. By using stacked antenna, bandwidth in excess of 50% can be achieved [12].

In 1999, C. L. Lee et al showed a rectangular air- filled stacked patch antenna with an offset L-shaped probe. The top patch and lower U-slot patch are all supported by thin basswoods at the four corners and was capable of providing an impedance bandwidth of 44.4% and average gain of -15 dB [13].

In 1999, R. B. Waterhouse et al proposed the design strategy to achieve bandwidths in excess of 25% for probe-fed stacked patches and concluded that choice of appropriate dielectric materials for such bandwidths and the selection of the substrate below the lower patch play a major role in producing broad-band responses [14].

In 2002, P. V. Bijumon et al designed a conventional rectangular microstrip antenna and then its bandwidth was improved by placing a cylindrical DR (dielectric resonator) over the patch or on the feed line. A bandwidth of more than 10% was achieved by loading a dielectric resonator of permittivity ε_r=4.8 over the patch and 14% by loading the same dielectric resonator on the feed line. Thus enhancement in bandwidth of the antenna was noticed without any significant affect on its gain and the other radiation characteristics [15].

In 2003, R. B. Waterhouse et al proposed that with the use of reflector patch element in a CPW (coplanar waveguide) fed ACP (aperture coupled patch) antenna which was mounted on a finite sized ground plane backward radiated fields could be decreased. Because with the addition of reflector patch element total power radiated in the rear hemisphere was reduced. Also with the variation of parameters of the reflector element the backward radiated field pattern could be adjusted to provide the field cancellation in random directions [16].

In 2004, S. Mestdagh et al proposed the aperture-coupled stacked patch antenna fed by CPW (coplanar waveguide) to be used at millimeter-wave frequencies in the 30-GHz range. By tuning the dimensions of the excitation slot and with the addition of a small tuning stub impedance-matching of the antenna could be done easily. So an antenna element with a -10 dB impedance bandwidth of 36.8% had been designed this way [17].

In 2005, N. Amiri et al proposed a simple compact design of a dual-polarized aperture-coupled patch antenna suitable for use in base station antennas in GSM900 (890-960 MHz) band. It had a stacked square radiating patch with four slits cut at the corners of the patches which was about 0.74 times that of the conventional design using simple stacked patch on the same substrate. The bandwidth for return loss < −14 dB (SWR<1.5) was 80 MHz or 8.65% which covered the whole operational bandwidth for GSM900 band and port decoupling was < −30dB. An antenna gain of 8.7l dBi had been achieved [18].

In 2006, Y. Lu et al proposed a novel wideband aperture-coupled circularly polarized stacked patch antenna that used one three-stub hybrid coupler, a stacked parasitic patch element and aperture-coupled feeding technique to excite the patch. Both the impedance bandwidth and the 3 dB AR (axial ratio) bandwidth had been improved. The antenna exhibited a simulated −10 dB return loss bandwidth of 37% and AR < 3dB bandwidth of 40.3% in the X band. The maximum gain is 8.4 dBi [19].

In 2007, S. Raje et al proposed that by stacking Koch fractal antenna with aperture coupled feeding technique the impedance bandwidth could be enhanced up to 32% at the resonance frequency of 980 MHz which was much greater than the 3% impedance bandwidth offered by a conventional Koch fractal antenna. Also it had 14% lesser surface area than conventional Koch fractal antenna. This antenna had an 8 dBi flat gain over the bandwidth [20].

In 2008, R. Duan et al proposed that using aperture-coupled feeding technique to excite arrayed of twelve rectangular microstrip patches with a multilayer flexible substrate structure would be designed to develop portable/foldable GSM antenna array for band 935-960MHz, which found applications in passive radar and other wireless systems. When it was compared with traditional design the foldable property made it a suitable choice for portable wireless systems. Moreover the antenna array showed excellent stability and tolerability for different bending angles [21].

Historical Development of Stacked MPA

In 2008, M. A. Alayesh et al proposed that for achieving frequency reconfigurability a stacked MPA (Microstrip Patch Antenna) was designed which was operable in the frequency range of 2-5GHz. The antenna consisted of two layers. The lower substrate layer had a patch

with two slots on each side which could be controlled through switches. The resonant frequencies could be varied with the status of the switches. Thus the frequency re-configurability was achieved. When another patch without slots was placed on the upper substrate layer of the antenna an increase in the number of resonant frequencies and bandwidth was achieved. Also a shift in the resonant frequencies and an increase in their bandwidths was observed with stacking the top patch over bottom patch [22].

In 2009, M. T. Islam et al proposed that the UWB (Ultra wideband has frequency band ranging from 3.1 to 10.6 GHz) antenna was obtained by E-H shaped stacked over H shaped patch, excited with a folded patch feed. The folded patch feeding technique helped in widening the impedance bandwidth of the antenna. The size reduction was realized through the shorting wall of the radiating patch. An impedance bandwidth of approximately 100% (from 3.46 to 10.36 GHz) at −10 dB return loss was achieved. Also, the antenna was able to achieve the radiation characteristics with gain greater than 4 dBi across the UWB band [23].

In 2010, F. Zhang et al worked with a microstrip patch antenna fed with aperture coupled technique and stacked technology. The antenna consisted of four patches on the upper substrate layer electromagnetically coupled to the rectangular patch on the lower substrate layer. The particular antenna had a VSWR (Voltage Standing Wave Ratio) value less than 2 and it achieved an impedance bandwidth of approximately 27% for the frequency range from 8.8 GHz to 11.6 GHz. The maximum gain of the antenna was 10.2 dBi at the resonance frequency of 10 GHz. This particular antenna was the building block of the antenna array which had 8×8 number of such kind of elements. The antenna array exhibited the impedance bandwidth of 18% for frequency range from 9 GHz to 10.8 GHz. Also the gain of the antenna array was over 22 dBi across the frequency range from 9 GHz to 10.5 GHz. Thus the antenna array was more efficient than its building block in terms of achieved gain [24].

Historical Study of Slotted Patch Antennas

In 2010, Z. N. Chen et al proposed a S-shaped slotted patch antenna with a small frequency ratio for GPS applications. It was concluded that frequency ratio can be controlled by adjusting the S-shaped slot arm lengths [25].

In 2010, O. H. Izadi et al presented a microstrip antenna with novel E- shaped coupling aperture. Different parameters of antenna were explored .It was shown that by varying the

dimensions of E- shaped slot and length of matching stub, the antenna could be designed for high gain, dual band or quad band characteristics [26].

In 2011, H. C. Chiung et al designed a broadband microstrip antenna whose impedance bandwidth was enhanced from 8.5% (11.22GHz to 12.21 GHz) to 15.7% (11.58GHz to 13.55 GHz) when the antenna was fed by a coupling aperture offset from the patch center. This generated an open circuit along the radiating edges of the patch which produced an additional resonance and therefore a wide impedance bandwidth of the antenna was obtained [27].

In 2011, H. Zhang et al made an antenna composed of two patches (one patch stacked over the other), feed network with aperture coupled technique & stacking technology was used to obtain dual-band operation. The antenna achieved a −10 dB return loss bandwidth of 100MHz with VSWR < 2.0 for high frequency band as well as for low frequency band. The antenna gain was observed greater than 5 dBi, so the antenna met well the conditions for use of it in WiMAX & WLAN systems. Also, the nominal antenna showed dual band behavior only when the low frequency patch was placed on the top of the antenna [28].

In 2011, S. G. Chang et al proposed a microstrip antenna with an H-shaped coupling aperture which can achieve a wide bandwidth, low cross polarization levels and low backward radiation levels. To achieve a wide bandwidth, stacked patches with an air layer in between is used and H-shaped aperture is used to reduce backward radiation levels [29].

In 2012, N. Ramli et al proposed the FRSPMA (frequency reconfigurable stacked patches microstrip antenna), fed by aperture coupled technique. The RMA (reconfigurable microstrip antenna) is an advanced technique by virtue of which a single antenna structure can be made to operate for different varieties of wireless applications. The antenna used C-Foam as a dielectric substrate material for different stacked patches and FR-4 for feed line substrate material. One RF switch (PIN diode, MEMs switch, varactor diode) was incorporated at the feed line to control and configure the activated patches and aperture slots cut in the ground during on and off states. When the switch was in the on state, the antenna was operable at two resonance frequencies namely 2.169 GHz and 7.552 GHz which comes under S-band and X-band of the electromagnetic spectrum respectively. The antenna resonated at frequency of 6.53 GHz during off state of the switch. The numerical value of the gain was 3.892 dBi at 2.169 GHz and 6.553 dBi at 7.552 GHz during the on state, whereas during the off state of the RF switch, the gain value was increased to 8.28 dBi at 6.53 GHz [31]

In 2012, M. Gujral et al designed a dual patch microstrip patch antenna whose bandwidth was improved by etching dummy EBG (electromagnetic band gap material) pattern on the feed line. A 48.8% increase in bandwidth was obtained. The bandwidth with EBG material etched on the feed line was found to be 0.381 GHz while the reference bandwidth without EBG material on the feed line was 0.256 GHz [32].

In 2012, S. C. Gupta et al designed stacked microstrip antenna incorporating E-shape and modified half E shape patches. The ground plane had a U-slot cut in it. This configuration achieved an impedance bandwidth of 60.2% using stacked structure of modified half E shaped patch [33].

In 2013, N. Ramli et al proposed that with a combination of an aperture coupled feeding technique and stacked patch technology, a FRSPMA (frequency reconfigurable stacked patch microstrip antenna) would be designed. It could be used in wireless communication systems for LTE (long term evolution) and WiMAX (worldwide interoperability for microwave access) applications. The RF switch configured at the feedline controlled the activation of different patches at different substrate layers (either the top patch or the bottom patch) and the aperture slots cut in the ground plane. During the on state of the switch, both radiating patches and aperture slots had become activated and operated at frequency of 2.6 GHz with the return loss value of −25.58 dB. When the switch was in the off state, only bottom patch and aperture slot 1 were activated and now the antenna could be made to operate at frequency of 3.5 GHz with return loss value of −45.37 dB [34].

In 2013, M. Kaur et al presented the design of microstrip patch antenna with aperture coupling. The design has a rectangular patch over the upper substrate supported by the ground plane. The patch is excited by the electromagnetic waves through the aperture cut in the ground. The gain and directivity of the antenna obtained was 6.935 dB and 5.838 dBi respectively. The VSWR obtained was 1.048 [35].

2.2 Research Gaps

- As the variations in antenna thickness yield improved results in terms of return loss but we can use dielectric substrates with different permittivity's. Since the upper substrate in aperture coupled antenna prefers low permittivity and lower substrate prefers high permittivity for appropriate functionality, the asymmetric variations in

dielectric constant of the whole antenna body need to be worked up on to bring out more distinctive and improved results.

- Two different slot configurations proposed are transverse slot and longitudinal slot. Although the first configuration is simpler and does not need impedance matching as compared to the second one, the longitudinal slot antenna provides wider bandwidth. The defected ground structures can be used in the longitudinal slot configurations to improve the bandwidth and increase the gain.
- Among the various available techniques of bandwidth enhancement for microstrip antennas, the one is by the use of a non-resonant aperture with the thick antenna substrate but this results in large radiation produced by the aperture which lead to a radiation pattern with poor front to back ratio. There has not much work been reported in reducing the back radiation level. So work can be done in regard to improve the front to back ratio.
- The drawback of Microstrip Antennas to limit their use in various wireless applications is their narrow bandwidth. So work can be done to improve the bandwidth of microstrip antennas. It can involve increasing the thickness of the dielectric substrates, decreasing the dielectric constant, using parasitic patches, cutting slots like U-slot, using air substrate, E-shaped and H-shaped patch antennas and also by the use of stacking technology.
- By increasing the thickness of the antenna to improve the bandwidth, the unwanted power loss occurs by surface waves. So work can be done to minimize these surface waves and the surface waves can be minimized by the use of photonic bandgap structures.
- The use of parasitic elements, stacked patches, using thick substrates of low permittivity etc have proved to improve the bandwidth of the antenna. However, the broad banding design in microstrip antenna results in high volume in spite of its efficient results. The work regarding the reduction of the profile can be done.
- Stacked aperture coupled microstrip antenna was presented to increase the bandwidth of about one octave which will result in surface waves and increased antenna height. So work can be done regarding reducing antenna size by introducing slots in the patch

cleverly which will result in increased bandwidth without increasing number of stages.

2.3 Thesis Objective

- To Design, Simulate and make a parametric analysis of Single Band Aperture Coupled Microstrip Patch Antenna at 5.8 GHz for WLAN applications.
- To Design and Simulate Dual Band Aperture Coupled Microstrip Antenna with slits cut in the patch for WLAN and WiMAX applications and its bandwidth improvement by placing stubs with the feedline.
- To Design and Simulate Wide Band Aperture Coupled Microstrip Antenna for DBS applications.
- To Design and Simulate Dual Band Aperture Coupled Stacked Microstrip Antenna for WLAN applications and improvement of its bandwidth by introducing an air gap between the ground plane and the upper layer substrate.
- To Fabricate the antennas using PCB Technology and testing the antennas using VNA.
- To publish research papers related to work done.

2.4 Conclusion

In this chapter the literature survey of microstrip patch antennas and techniques to enhance their bandwidths has been studied. The research gaps has also been found in this chapter.

CHAPTER-3

ANALYSIS OF APERTURE COUPLED MICROSTRIP ANTENNA

This chapter represents the analysis of Aperture Coupled Microstrip Patch Antenna using transmission line model to determine the patch admittance, aperture admittance and input impedance. Later on a single band aperture coupled microstrip patch antenna has been designed for WLAN applications using transmission line model and its parametric analysis has been done for various antenna parameters like with length of the antenna, the length of the slot and the length of the stub etc.

3.1 Geometry and Equivalent Structure of ACMPA

A number of theoretical and experimental studies have been performed to analyze the aperture-coupled microstrip patch antenna. Full-wave approaches based on the method of moments, spectral domain analysis, and the finite-difference time-domain method have been used to determine various antenna parameters [37], [38]. For providing the rapid and accurate design, it is effect to use the method of transmission line model, especially thin substrate aperture-coupled antennas.

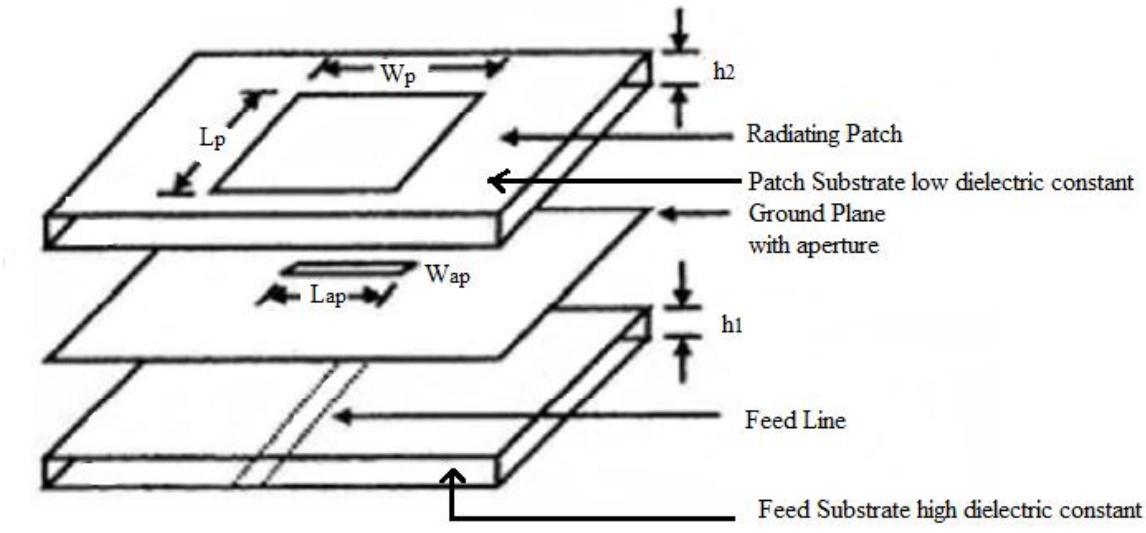

Figure 3.1 Schematic of Aperture Coupled Microstrip Antenna [42]

Figure 3.2(a) show the equivalent network of aperture-coupled microstrip antennas. The equivalent circuit consists of two ideal transformers. n1 is the turn ratio of energy between aperture and patch, it can be calculated by corresponding current distribute equation, can be approximated as the ratio of slot length L_{ap} and patch width W. n1 can be written as [37]:

$$n_1 = \frac{L_{ap}}{W} \tag{3.1}$$

The turn ratio of energy between feed line and aperture is n2, which can be expressed as:

$$n_2 = \frac{\Delta V}{V_o} \tag{3.2}$$

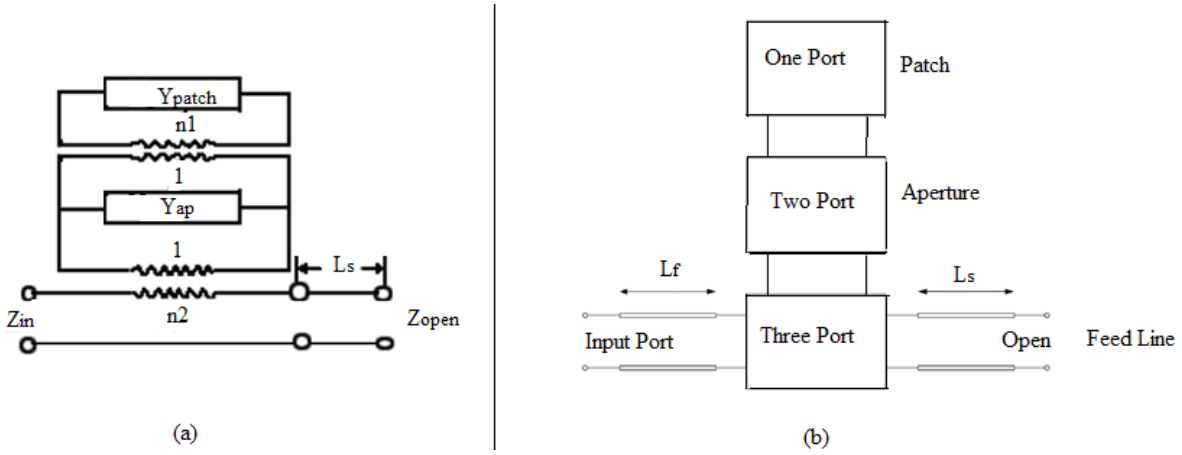

Figure 3.2 (a) Equivalent Circuit of ACMPA, (b) Block Diagram of ACMPA as Three Port Network [37]

Where V_o is the voltage of the aperture, ΔV defines a voltage discontinuity of the microstrip due to the slot and is given by

$$\Delta V = \int_{S_{ap}} e_a \times h_s \, ds \tag{3.3}$$

Where e_a is the electric field of aperture and h_s is normalized magnetic field. If the size of aperture is small, then n_2 also can be written as :

$$n_2 = \frac{L_{ap}}{\sqrt{Dh}} \tag{3.4}$$

Where D is the effective width of feed line, and h is the thickness of substrate. Y_{ap} is the admittance of aperture, Y_{pat} is the admittance of microstrip patch, and they can be calculated as described in [41]. So the input impedance of antenna can be calculated as:

$$Z_{in} = \frac{n_2^2}{n_1^2 Y_{pat} + Y_{ap}} - \mathrm{j} Z_o \cot(\beta_m L_s)$$

Where Z_0 is the open circuit impedance of feed line, Ls is the length of between the center of aperture and open circuit port of feed line.

3.1.1 Patch Admittance

To get an approximation for the admittance Y_p , the patch is also modeled by electric lines in the transmission line model. Figure 3.3 shows the resulting equivalent circuit for the patch. Two lines are positioned behind the transformer, one with length $L_1 = x_o$ and the other with length L_2 = L− L_1. Together they have the total length (L) of the patch, which is split into two lines at the position x_o by the transformer. If input impedances, Z_1 and Z_2 are the impedances looking into left and right side of the aperture, then total impedance of the patch is given by:

$$Z_p = Z_1 + Z_2 = 1/Y_1 + 1/Y_2 \quad (3.5)$$

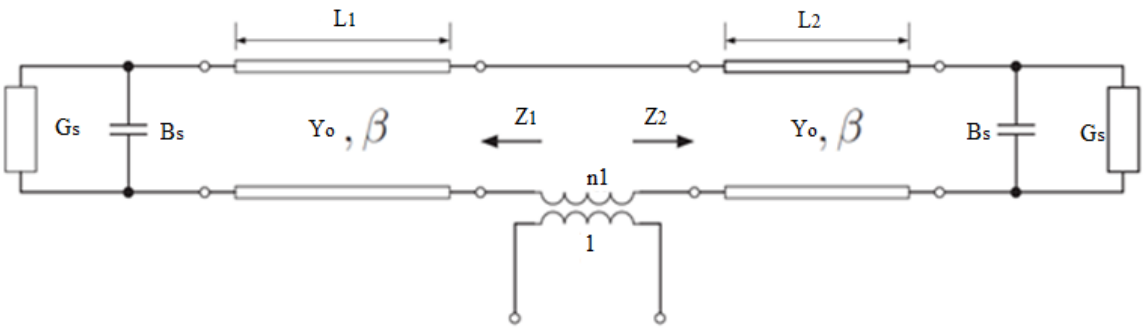

Figure 3.3 Equivalent Circuit of Patch [39]

The equivalent circuit allows the single input impedance to be determined to and is given by:

$$Y_i = Y_o \frac{G_s + jB_s + jY_o \tan(\beta L_i)}{Y_o + j(G_s + B_s)\tan(\beta L_i)}, \text{ with i = 1, 2} \quad (3.6)$$

Within the equivalent circuit, Y_o and β are the transmission line admittance and phase constant of transmission line with the width W on a substrate with a relative permittivity of ε_{r1}. The load admittances $Y_s = G_s + jB_s$ consider the two radiating sides of the patch. Here, G_s depicts the radiated power and B_s depicts the stored energy save in the field near the slot.

3.1.2 Aperture Admittance

The admittance of the coupling aperture Y_a is also determined by the transmission line theory, as the coupling aperture is modeled as a short ended slot line at both ends. Hence, the admittance of aperture is given by:

$$Y_a = -j2Y_{ao} \cot\left(\frac{\beta L_a}{2}\right) = jB_a \quad (3.7)$$

With Y_{ao} being the characteristic impedance of a slot line, placed on the substrate with the relative permittivity ε_r^2.

3.1.3 Input Impedance

Based on these transmission line models, an expression for the input impedance Z_{in} of the aperture coupled patch antenna in the equivalent circuit of Figure 3.2(a) can be derived to

$$Z_{in} = \frac{n_2^2}{n_1^2 Y_p + Y_a} - \mathrm{j}Z_{mo} \cot(\beta_m \Delta L) \quad (3.8)$$

Here, Z_{mo} is the transmission line impedance of the feeding line and β_m is the corresponding phase constant. Setting $n_1^2 B_p + B_a = 0$ results in:

$$B_p = \frac{-B_a}{n_1^2} \quad (3.9)$$

Substitute equation 1 and 5 in equation 6 and consider cot(x) = 1/x for smaller x, yields the following condition for resonance given by:

$$B_p \approx \frac{4Y_{ao} W^2}{\beta_s L_a^3} \quad (3.10)$$

Here, β_s describes the phase constant of the slot line. Above equation shows that increasing length L_a results in a decreasing susceptance B_p resulting in decreasing resonance frequency [40]. An increasing length L_a not only results in a decreasing resonance frequency f_{res}, but also in an increasing resonance R_{res} , due to the increasing coupling between the patch and microstrip line. Hence, the influence of the admittance Y_p is increased, too. In general, an increased coupling yields an increasing resonance resistance and a decreasing resonance frequency.

Due to the fact, both resonances – the one of the patch and other of the aperture – results in two loops different sides within the smith chart, a greater bandwidth can be achieved. An increased coupling can also be achieved by decreasing height, so the patch and the coupling aperture are closer together [40].

3.2 Single Band Aperture Coupled Microstrip Antenna Design and its Parametric Analysis

3.2.1 Antenna Design

A single band antenna consists of rectangular shape patch, rectangular shape aperture and feed line is designed at frequency of 5.794 GHz for WLAN applications. The dimensions of the patch, ground plane and the substrates are calculated as per the design equations from 1.1 to 1.8 given in CHAPTER 1. The various design specifications of the nominal antenna has been shown in Table 3.1. Also the optimized design parameters has been shown in Table 3.2.

Resonant Frequency (f_r)	5.794 GHz
Patch Substrate Material, Feed Substrate Material	FR-4
Patch Substrate Thickness, Feed Substrate Thickness	1.6 mm
Dielectric Constant of the material used	4.7
Thickness of PEC Material	0.02 mm

Table 3.1 Single Band Antenna Design Specifications

Parameters	L_p	W_p	L_g	W_g	L_f	W_f
Description	Length of the Patch	Width of the Patch	Length of the Ground	Width of the Ground	Length of the Feedline	Width of the Feedline
Values	8.1 mm	14 mm	20.96 mm	24.91 mm	13.48 mm	1 mm

Table 3.2 Optimized Dimensions of the Single Band Antenna

3.2.2 Simulation Setup and Results

CST MWS (Computer Simulation Technology Microwave Studio) 2010 is used to design and simulate the antenna. CST MWS is a tool for the 3D EM simulation of high frequency devices such as antennas, couplers, planar and multilayer structures. It is exceptionally user friendly and enables the fast and accurate analysis. Figure 3.4 shows the front and back view of the antenna with dimensions labeled. The various simulation results are

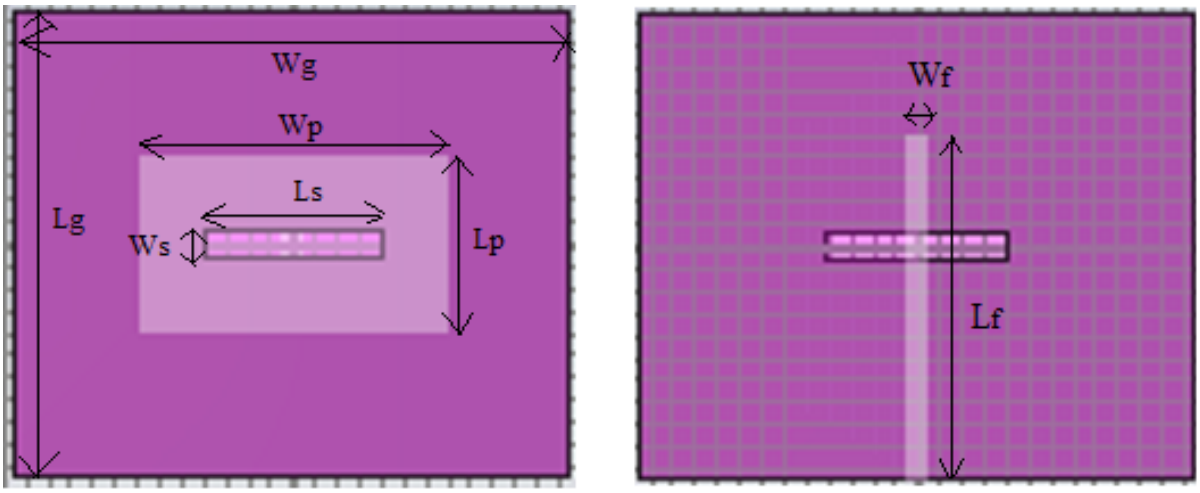

Figure 3.4 Front and Back View of the Single Band Antenna

3.2.2.1 Return Loss and Antenna Bandwidth

Figure 3.5 shows the S-parameter as a function of frequency. The antenna resonated at 5.794 GHz with S_{11} parameter (return loss) value of -32.42 dB. The bandwidth of antenna is also calculated from this return loss vs. frequency plot. The bandwidth of the antenna is the range of frequencies over which the return loss is larger than -10 dB and it corresponds to a VSWR (Voltage Standing Wave Ratio) value of 2. For this particular design the measured -10 dB bandwidth is 223 MHz. The higher value of the return loss indicates better coupling which leads to higher value of the directivity and more gain for the antenna designed.

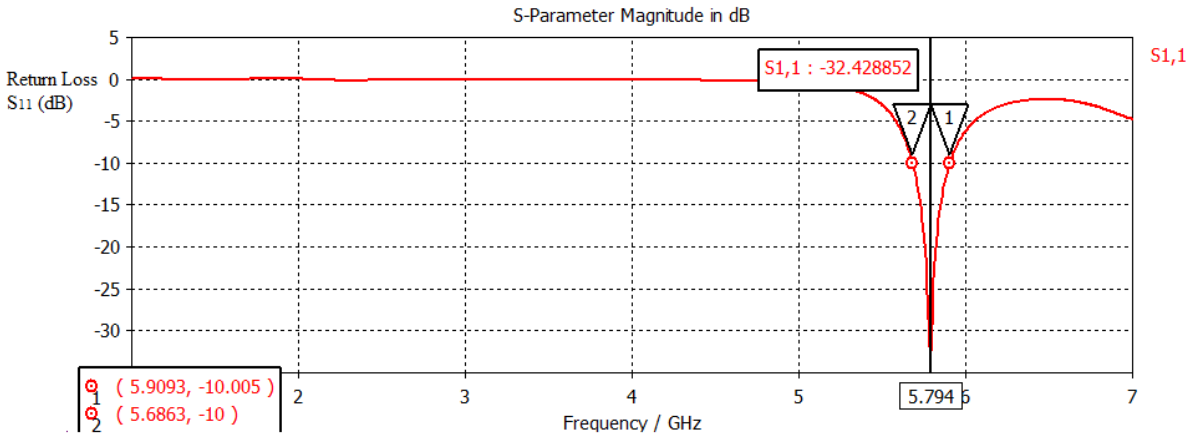

Figure 3.5 Return Loss $S_{11}(dB)$ Versus Frequency Plot of the Single Band Antenna

3.2.2.2 Smith Chart and Antenna Impedance

Figure 3.6 shows the smith chart of the nominal single band antenna. It depicts the variation of antenna impedance with frequency. The size of the locus of the smith chart is controlled by the slot length and it increases with increasing the slot length. The locus must be large enough to pass the center of the smith chart for properly matched antenna.

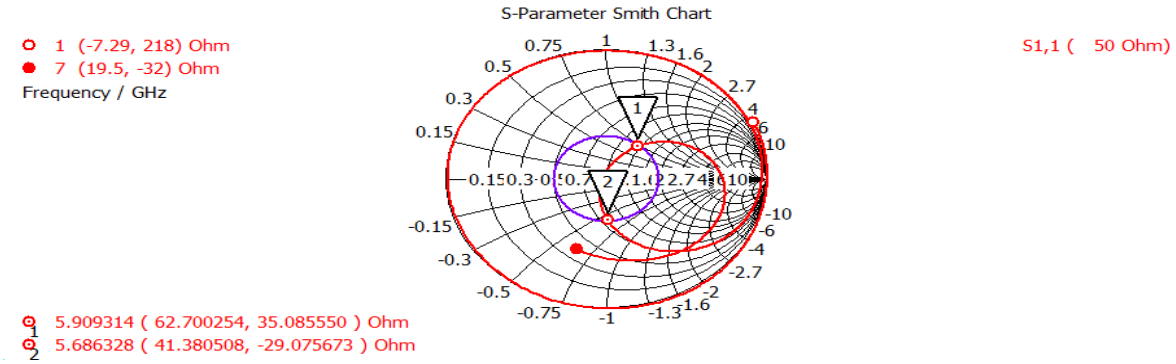

Figure 3.6 Smith Chart showing the Characteristics Impedance of the Single Band Antenna

3.2.2.3 Directivity

Figure 3.7 shows the 3D directivity plot of the antenna. It represents the antenna resonating at 5.794 GHz provides a directivity value of 5.838 dBi which means the designed antenna radiates more by an amount of 5.838 dBi in a particular direction when compared with an isotropic antenna which radiates equally in all directions. Figure 3.8 shows the polar plot of the directivity indicating the main lobe is at an angle of 2 degree, having angular width of 89.7 degree. The magnitude of the main lobe is 5.8 dBi.

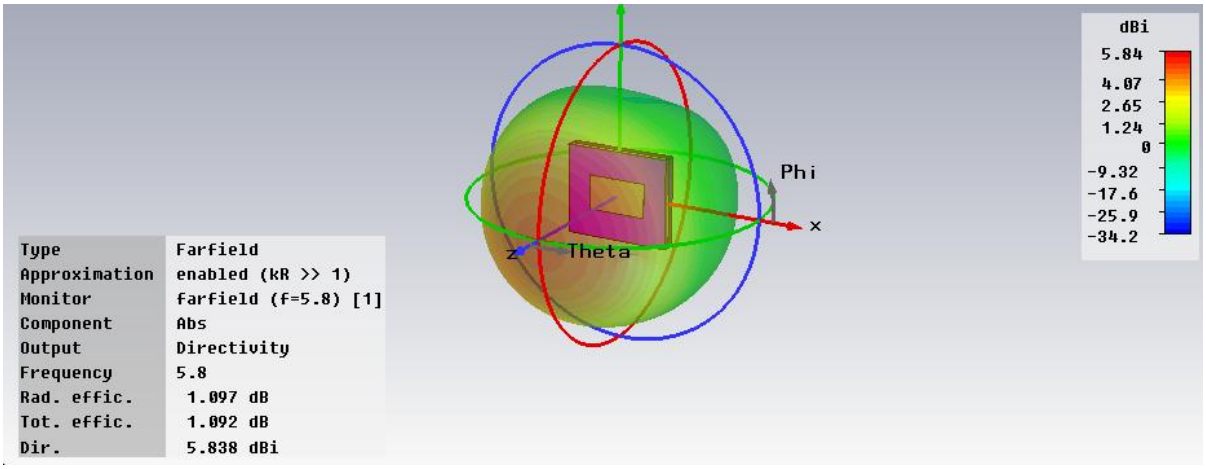

Figure 3.7 3D Radiation Pattern of the Directivity of the Single Band Antenna at 5.8 GHz

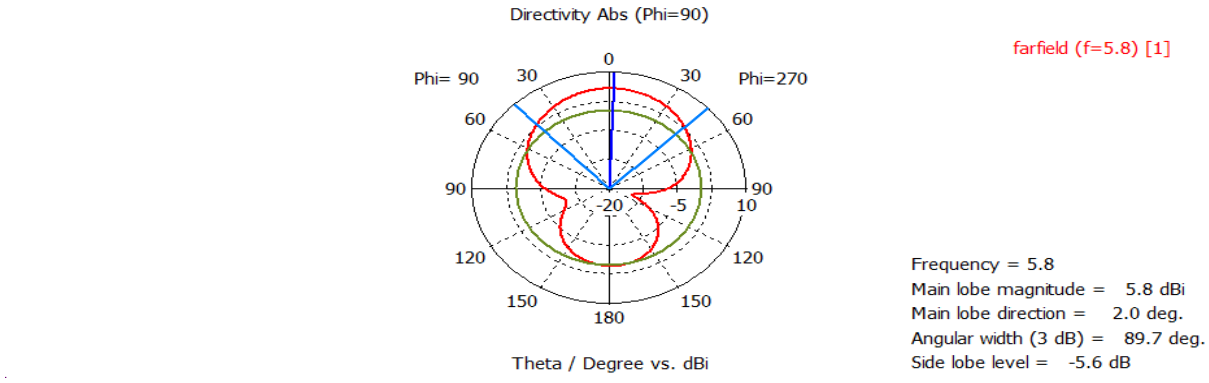

Figure 3.8 Polar Plot of the Directivity of the Single Band Antenna at 5.8 GHz

3.2.2.4 Gain

The gain of the nominal antenna in a particular direction is more when compared with an isotropic antenna which radiates equally in all directions making it very useful for WLAN applications providing a better performance. The proposed single band antenna provides the gain of 6.935 dB at 5.8GHz. The 3D radiation pattern of the gain of the antenna at 5.8 GHz has been shown in figure 3.9. Figure 3.10 shows the polar plot of the gain of the antenna at 5.8 GHz.

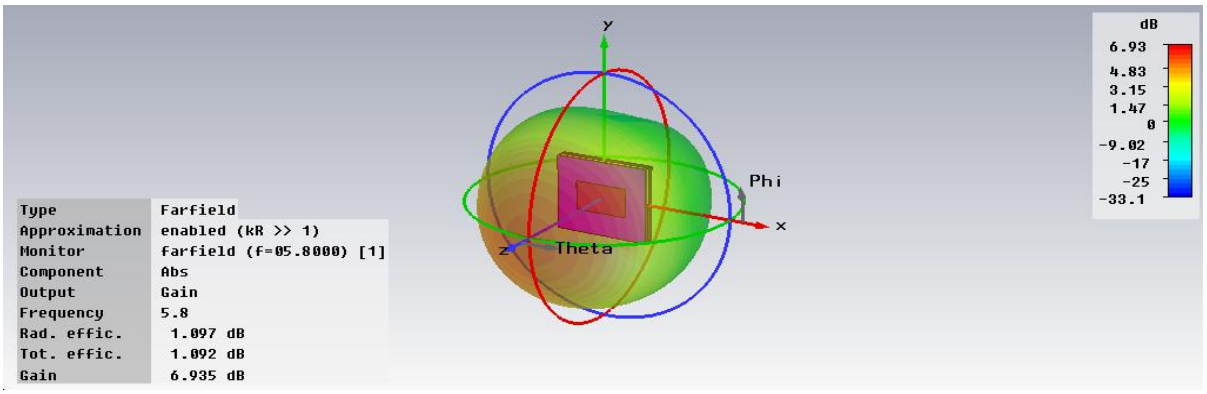

Figure 3.9 3D Radiation Pattern of the Gain of the Single Band Antenna at 5.8 GHz

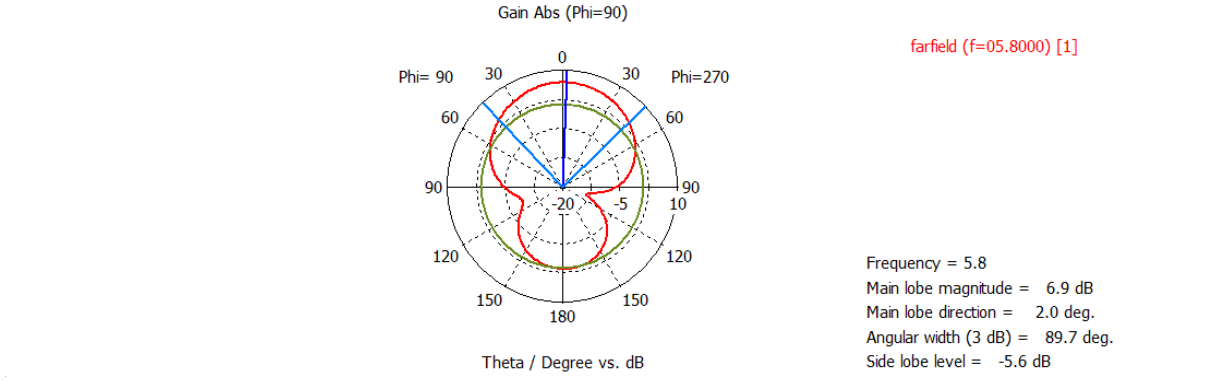

Figure 3.10 Polar Plot of the Gain of the Single Band Antenna at 5.8 GHz

3.2.3 Effect of Patch Length

The patch length affects the resonance frequency of the antenna. Figure 3.11 and Table 3.3 represents with the variation of patch length from 10mm to 18mm, the resonating frequency changes from 5.698 GHz to 5.842 GHz.

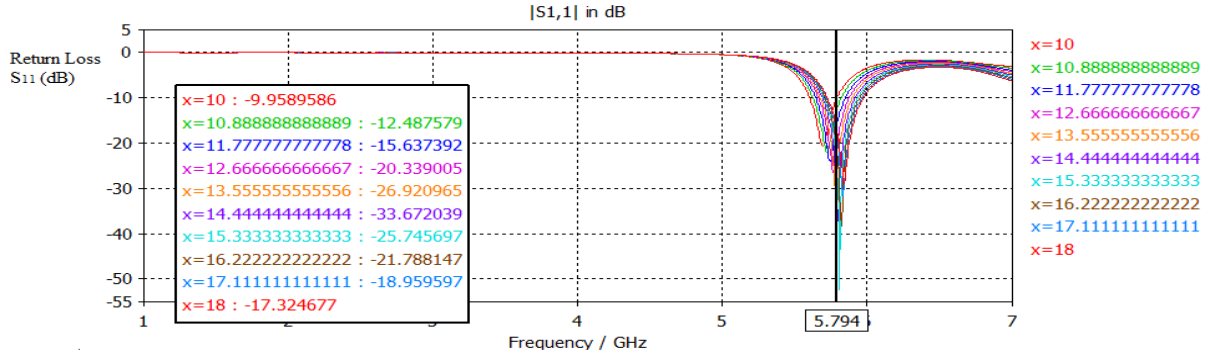

Figure 3.11 Variation of Return Loss (S_{11}) with Change in Patch Length

Length of Patch(mm)	10	10.89	11.78	12.67	13.56	14.44	15.33	16.22	17.11	18
Resonating Freq(GHz)	5.698	5.722	5.746	5.764	5.782	5.8	5.812	5.824	5.836	5.842

Table 3.3 Resonating Frequencies of the Single Band Antenna for Various Patch Lengths

For this particular design the optimized value of the length of the patch is chosen to be 14 mm, because it provides resonance at the desired frequency value.

3.2.4 Effect of Slot Length

The coupling level is determined by the length of the slot cut in the ground plane to feed the patch electromagnetically from the energy provided by the feed line. For efficient coupling the ratio of width to length of the slot is made to $1/10$. Figure 3.12 and Table 3.4 shows the variation of resonating frequency and return loss with the variation of slot length keeping all other parameters constant. The size of the locus of the smith chart increases with increase in the slot length as shown in Figure 3.13. The locus must be large enough to pass through the center of the smith chart for proper matching condition.

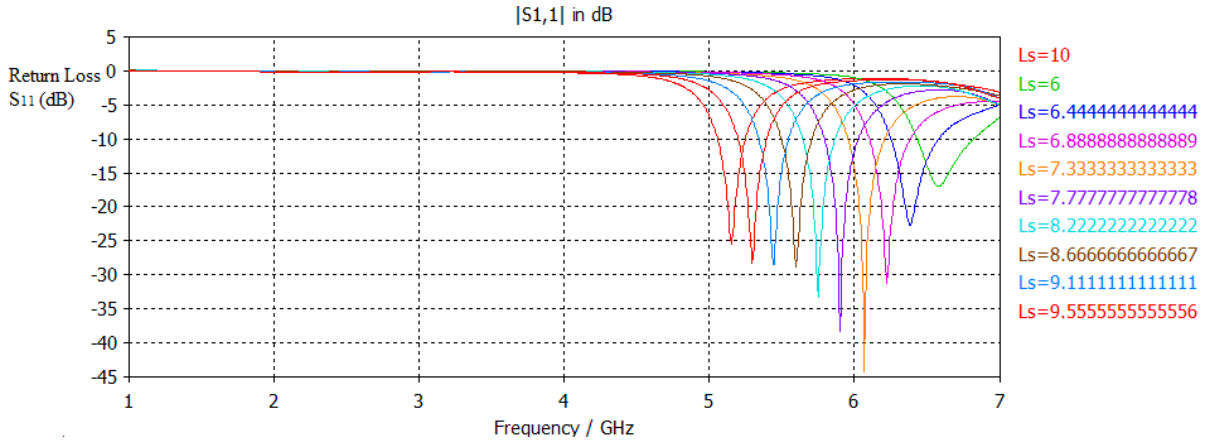

Figure 3.12 Variation of Return Loss (S_{11}) with Change in Slot Length

Slot Length(mm)	6	6.44	6.89	7.33	7.78	8.22	8.67	9.11	9.55	10
Resonating Freq(GHz)	6.58	6.382	6.226	6.07	5.902	5.752	5.602	5.446	5.296	5.152
S_{11} (dB)	-16.95	-22.67	-31.31	-44.24	-38.24	-33.32	-28.92	-28.42	-28.28	-28.50

Table 3.4 Resonating Frequencies and S_{11} Values of the Single Band Antenna for Various Slot Lengths

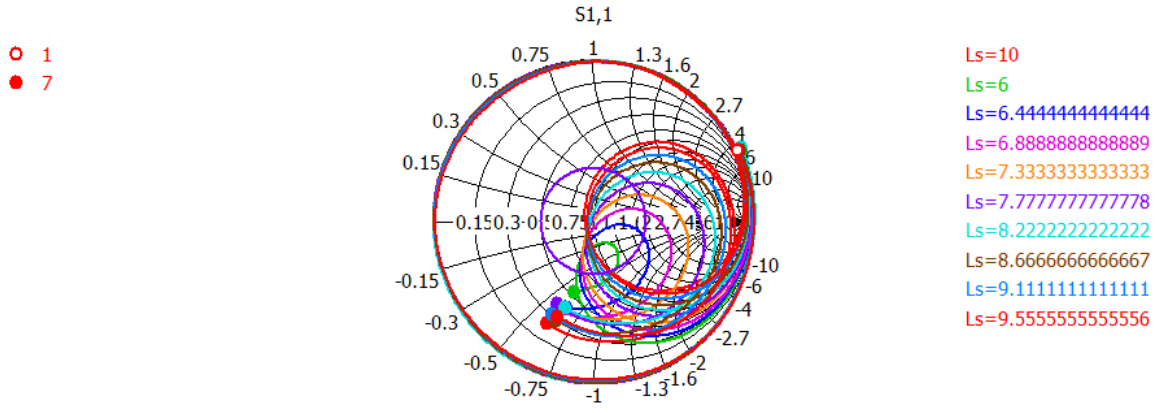

Figure 3.13 Smith Chart Variations of the Single Band Antenna with Change in Slot Length

For this particular design the optimized value of the length of the slot is chosen to be 8.1 mm, because it provides the sufficient coupling for the antenna to resonate at the desired frequency value.

3.2.5 Effect of stub length (L_{stub})

The length of the stub also affects the coupling level. It should be placed perpendicular to the slot for maximum coupling. Figure 3.14 and Table 3.5 shows the variation of resonating frequency and return loss with the variation of the stub length. From Figure 3.14 it can be seen that as the stub length increases from 2 mm to 4.66 mm return loss changes from -4.57 dB to -28.77 dB and afterwards for stub length from 4.66 mm to 6 mm the return loss changes from -28.77 dB to -12.82 dB. The stub length is used to rotate the locus of the smith chart up (inductive) or down (capacitive). Figure 3.15 depicts as the stub length increase from 2 mm to 6 mm the locus of the smith chart rotates towards capacitive side. For an optimal matching the size of the locus of the smith chart should be large enough to pass through its center and it could be achieved by adjusting the slot length and stub length.

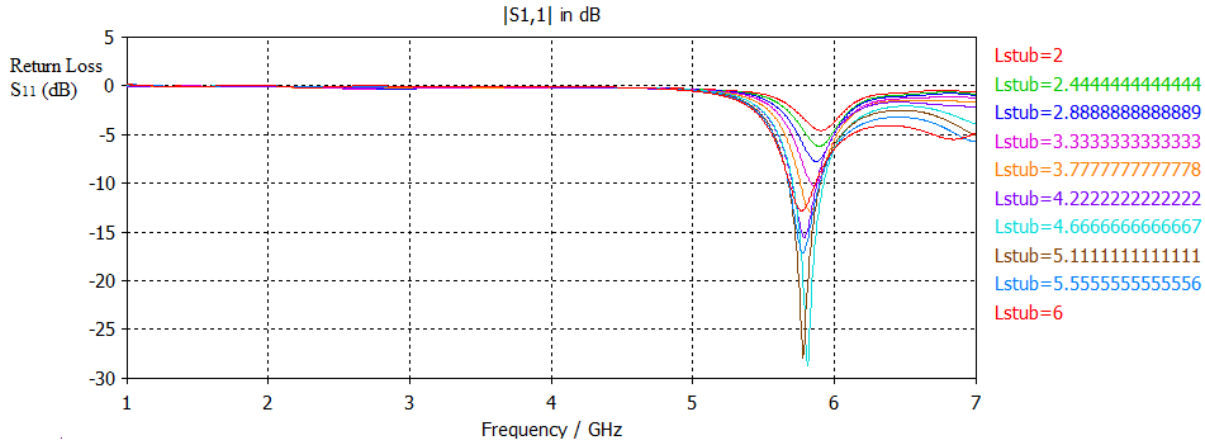

Figure 3.14 Variation of Return Loss (S_{11}) with Change in Stub Length

L_{stub}(mm)	2	2.44	2.89	3.33	3.78	4.22	4.67	5.11	5.56	6
S_{11}	-4.57	-6.189	-7.761	-10.27	-12.92	-15.57	-28.77	-27.93	-17.17	-12.82

Table 3.5 Return Loss (S_{11}) Values of the Single Band Antenna for Various Stub Lengths

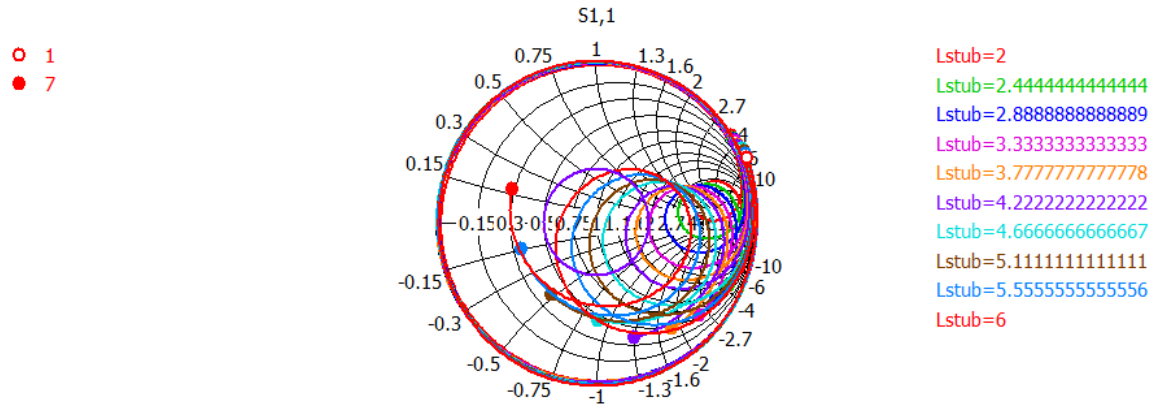

Figure 3.15 Smith Chart Variations of the Single Band Antenna with Change in Stub Length

For this particular design the optimized value of the length of the stub is chosen to be 5 mm, because it provides the less return loss value for the designed antenna.

3.2.6 Effect of Antenna and Feed Substrates

For the nominal antenna design FR-4 is chosen as the antenna and the feed substrate material. From Figure 3.16 and Table 3.6 it can be seen that resonating frequency of the antenna depends up on the dielectric constant (relative permittivity) of the substrate material. As the dielectric constant of the substrate material is changed from 3.2 to 5 keeping all other design parameters as constant the resonating frequency of the antenna is decreased from 6.91 GHz to 5.626 GHz.

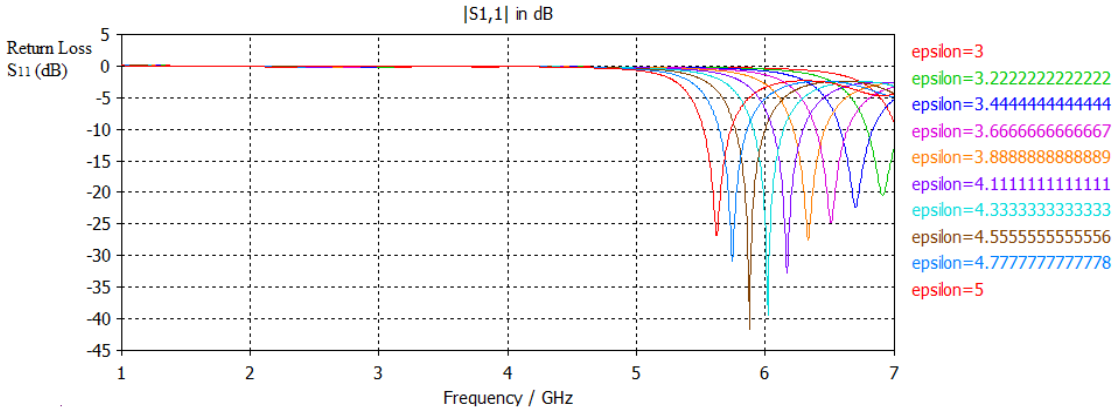

Figure 3.16 Variation of Return Loss (S_{11}) with Change in Dielectric Constant of the Substrate

Dielectric Constant(ε_r)	3	3.22	3.44	3.67	3.89	4.11	4.33	4.56	4.78	5
Resonating Freq(GHz)	-	6.91	6.706	6.52	6.346	6.172	6.028	5.878	5.746	5.626

Table 3.6 Resonating Frequencies of the Single Band Antenna for Various Values of Epsilon

3.3 Conclusion

In this chapter Aperture Coupled Microstrip Antenna using transmission line model has been analyzed. Also the designing of the single band antenna along with its parametric study for WLAN 802.11a applications has been done. The bandwidth of designed antenna is found to be 223 MHz.

CHAPTER 4

DUAL BAND APERTURE COUPLED PATCH ANTENNA

This chapter covers the designing of Dual Band Aperture Coupled Microstrip Antenna and improvement of its bandwidth by using the stubs along the sides of the feedline. Then the designs are simulated and various simulation results are obtained. The designed antennas finds applications in WLAN frequency bands.

4.1 Antenna Design

For this particular antenna design the slits have been cut at the boundaries of the rectangular shaped patch, so E-shaped configuration is achieved for the patch as shown in Figure 4.1. The slit loaded patch antenna excites at more than one adjacent modes. The dimensions and the position of the slits controls the width of the frequency bands. The slits divide the patch in three or more parts and each part corresponds to an equivalent circuit of resonance as shown in Figure 4.1. The nominal dual band antenna resonate at frequencies of 3.692 GHz and 5.2 GHz. The various design specifications of the designed dual band antenna has been shown in Table 4.1. The nominal dual band antenna is designed using FR-4 as substrate material both for the antenna substrate and the feed substrate. The FR-4 material has the dielectric permittivity ε_r of 4.4 with tangent loss component as 0.0009. Also the various design parameters has been shown in Table 4.2.

Resonance Frequencies (f_r)	3.692 GHz, 5.2 GHz
Patch Substrate Material, Feed Substrate Material	FR-4
Patch Substrate Thickness, Feed Substrate Thickness	1.57 mm
Dielectric Constant of the material used	4.4
Thickness of PEC material	0.02 mm

Table 4.1 Dual Band Antenna Design Specifications

The dimensions of the Dual Band Aperture Coupled Microstrip Antenna has been calculated by the design equations from 1.1 to 1.8 given in CHAPTER 1. The dimensions of the patch, the ground plane, the substrate layers, the feedline, the slits and the stubs of the antenna are given in Table 4.2.

Parameter	Description	Value
L	Length of the Patch	23.41 mm
W	Width of the Patch	23.35 mm
L_g	Length of the Ground Plane	29.01 mm
W_g	Width of the Ground Plane	34.95 mm
L_f	Length of the Feedline	23.655 mm
W_f	Width of the Feedline	3.2 mm
L_{slit}	Length of slit 1 and slit 2	19.675 mm
W_{slit}	Width of slit 1 and slit 2	1 mm
L_{stub}	Length of the Stub (For Improved Dual Band Antenna only)	14.7 mm
W_{stub}	Width of the Stub (For Improved Dual Band Antenna only)	1.2 mm

Table 4.2 Various Dimensions of the Dual Band Antenna

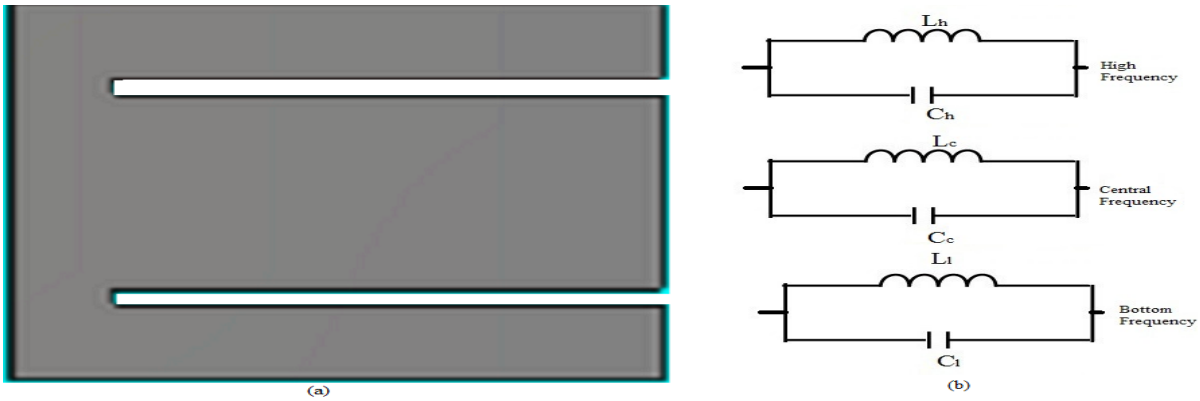

Figure 4.1 (a) E-shaped Patch Configuration, (b) its Electrical Equivalent Model

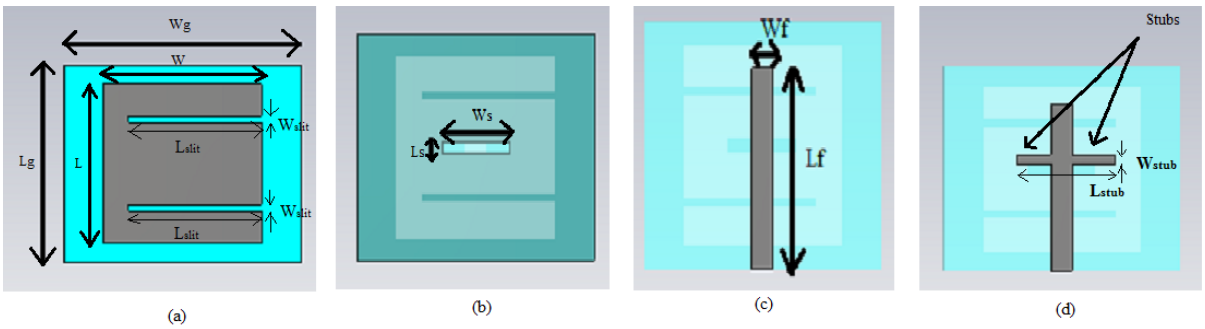

Figure 4.2 (a)Top View, (b)Ground Plane with Rectangular Slot, (c)Back View Showing Feedline for Dual Band Antenna; (d)Back View Showing Feedline with Stubs for Improved Dual Band Antenna

4.2 CST Simulation Results

CST 2010 has been used to simulate the proposed dual band antennas and various simulation results like return loss, smith chart, VSWR, surface current, farfield patterns of the gain and the directivity are observed.

4.2.1 Return Loss and Antenna Bandwidth

When the antenna is excited by the Gaussian pulse at the waveguide port the return loss of the antenna is obtained as shown in Figure 4.3. This curve is basically the variation of magnitude of S-parameter (S_{11}) in logarithmic scale with the frequency range. The lower frequency band resonates at 3.692 GHz with a return loss value of -20.94 dB and the upper frequency band resonates at 5.172 GHz with a return loss of -41.10 dB. The bandwidth of the dual band antenna can be calculated from the return loss versus frequency plot. The bandwidth of the antenna is the range of frequencies over which the return loss is larger than -10 dB and it corresponds to a VSWR value of 2. The measured -10 dB bandwidth of the designed antenna is 50.2 MHz and 139 MHz at resonant frequencies of 3.692 GHz and 5.172 GHz respectively. Thus bandwidth of the designed antenna is not as good enough. So bandwidth has been enhanced by placing the stubs along the sides of the feedline as shown in Figure 4.2(d). The -10 dB bandwidth of the improved dual band antenna is 48.6 MHz with return loss of -30.40 dB at lower band resonant frequency and 224.8 MHz with return loss value of -26.99 dB at upper band resonant frequency as shown in Figure 4.4.

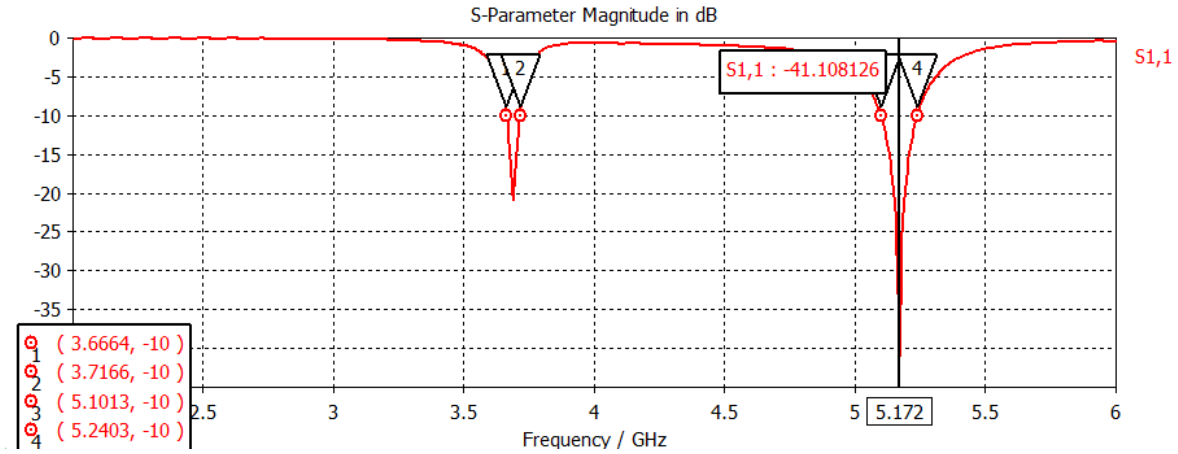

Figure 4.3 Return Loss (S_{11}) Versus Frequency Plot of the Dual Band Antenna

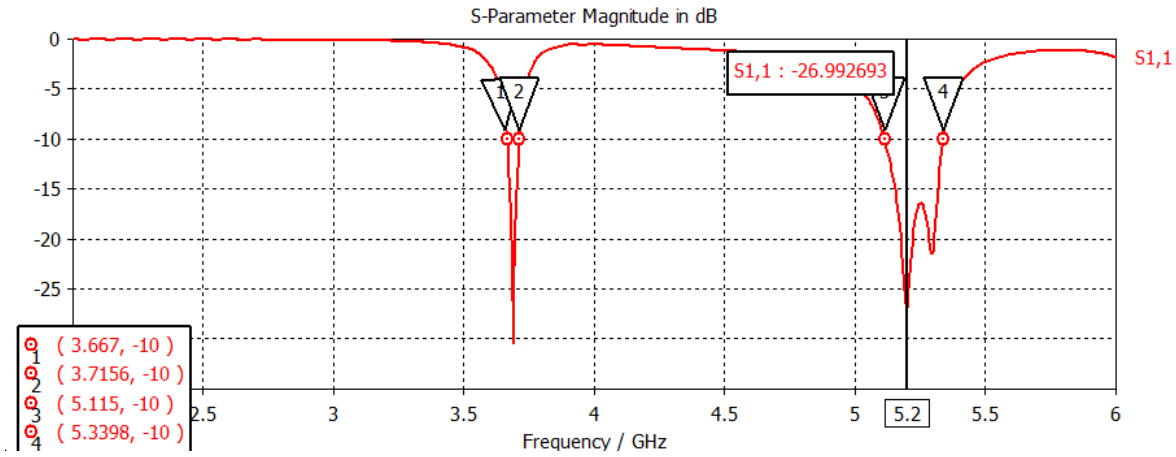

Figure 4.4 Return Loss (S_{11}) Versus Frequency Plot of the Improved Dual Band Antenna with the Introduction of Stubs

4.2.2 Smith Chart and Antenna Impedance

The smith chart represents variation of the antenna impedance with the frequency. It shows the complex impedance of the reflected S-parameter (S_{11}) within a specified frequency range. It is also possible to estimate the bandwidth of the antenna from the smith chart by reading the frequencies at the points where the VSWR=2 circle and input impedance curve intersects. The size of the locus of the smith chart increases with increase in slot length and stub length. For proper matching conditions the locus of the smith chart must pass through its center. The smith chart for the dual band antenna and improved dual band antenna has been shown in Figure 4.5 and 4.6 respectively.

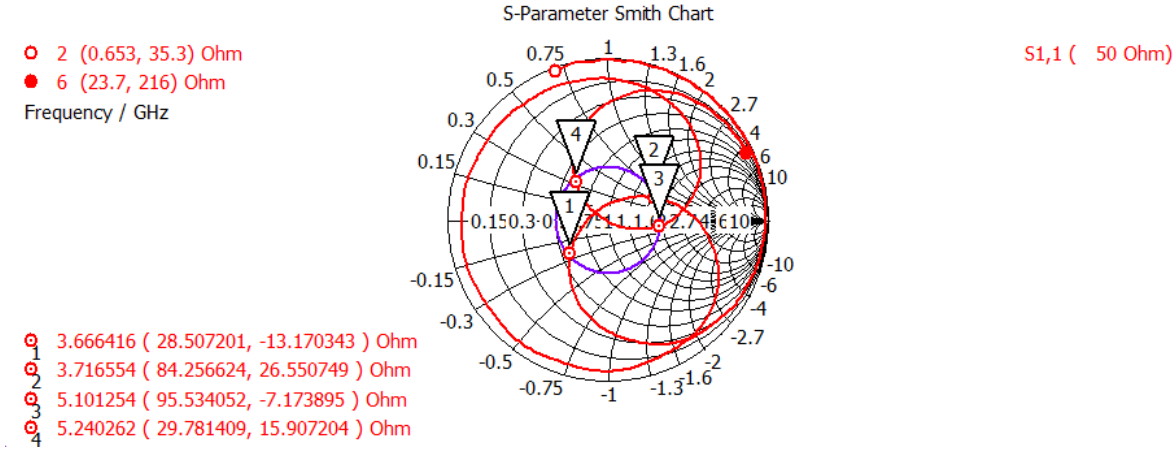

Figure 4.5 Smith Chart Showing the Characteristics Impedance of the Dual Band Antenna

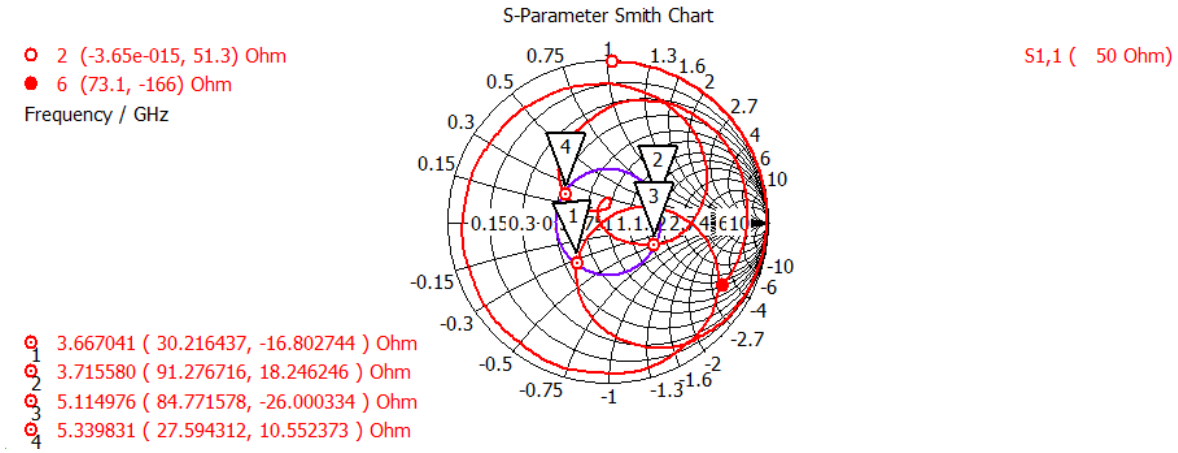

Figure 4.6 Smith Chart of the Improved Dual Band Antenna with the Introduction of Stubs

4.2.3 VSWR

The VSWR (Voltage Standing Wave Ratio) is related to the reflection parameter. It is the quotient between the maximum and minimum voltage that can be measured along a waveguide. Its value lies between 1 to ∞ theoretically depending upon the reflection coefficient lies from 0 to 1. The VSWR value should be less than 2 to have considerable performance with the best matching. The designed dual band antenna has a VSWR of 1.1971 and 1.0179 at the operating frequencies of 3.692 GHz and 5.172 GHz respectively as shown in VSWR versus frequency plot in Figure 4.7. The improved dual band antenna obtains the VSWR value of 1.0623 and 1.0936 at the operating frequencies of 3.692 GHz and 5.2 GHz respectively as shown in Figure 4.8.

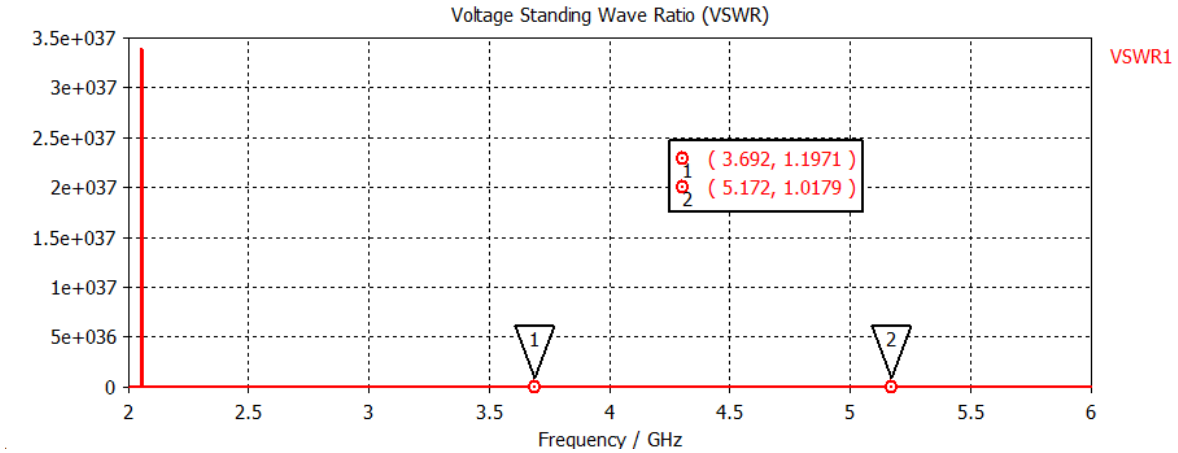

Figure 4.7 VSWR Plot of the Dual Band Antenna

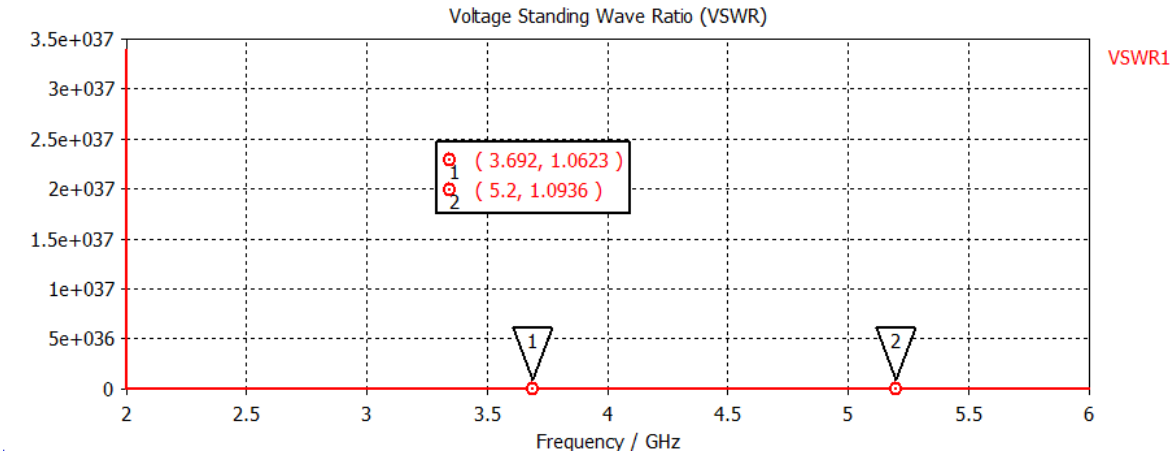

Figure 4.8 VSWR Plot of the Improved Dual Band Antenna with the Introduction of Stubs

4.2.4 Surface Current

According to the current distributions the slits of different dimensions are cut in the patch to achieve dual band characteristics. Basically the position of the slits in the patch describes the current distribution at both the resonance frequencies. Figure 4.9(a), reveals the surface current of the dual band antenna is highest in the arms of E-shaped patch at the frequency of 3.692 GHz. The maximum surface current at the slit of the patch is 79.12 A/m. Figure 4.9(b) reveals the surface current of the dual band antenna is highest in the middle of E-shaped patch at the frequency of 5.172 GHz. The maximum surface current at the center of the patch is 58.37 A/m.

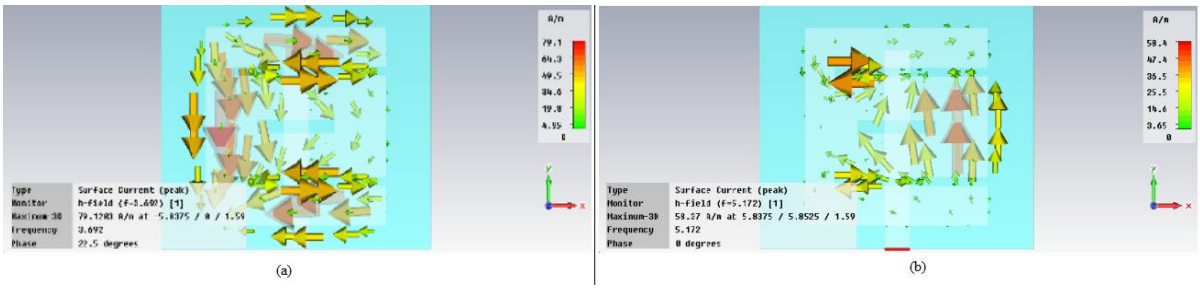

Figure 4.9 Surface Current Distribution of the Patch of Dual Band Antenna (a) at 3.692 GHz, (b) at 5.172 GHz

Similarly the surface current distribution for the improved dual band antenna is shown in Figure 4.10(a), (b) at both the operating frequencies.

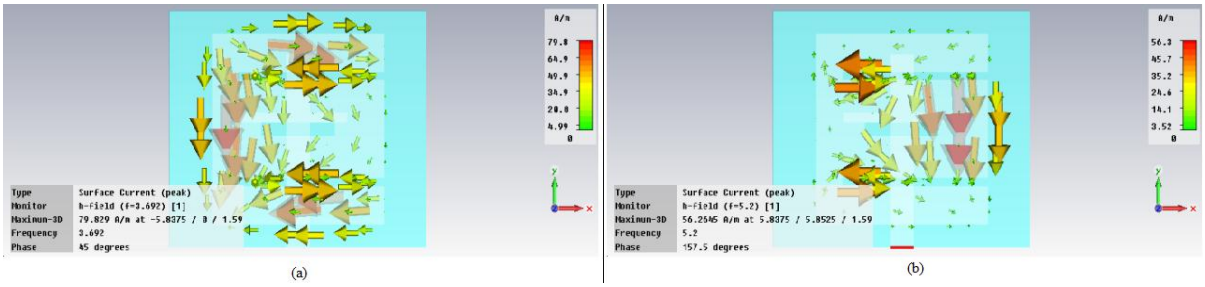

Figure 4.10 Surface Current Distribution of Patch of Improved Dual Band Antenna with Stubs (a) at 3.692 GHz, (b) at 5.2 GHz

4.2.5 Directivity

The designed dual band antenna has a directivity of 5.576 dBi and 5.440 dBi at the resonance frequencies of 3.692 GHz and 5.172 GHz respectively as shown in 2D and 3D directivity plot of the antenna in Figure 4.11(a), (b), (c), (d). The nominal antenna radiates more in a particular direction by an amount of 5.576 dBi and 5.440 dBi when it is compared to an isotropic antenna which radiates equally in all directions.

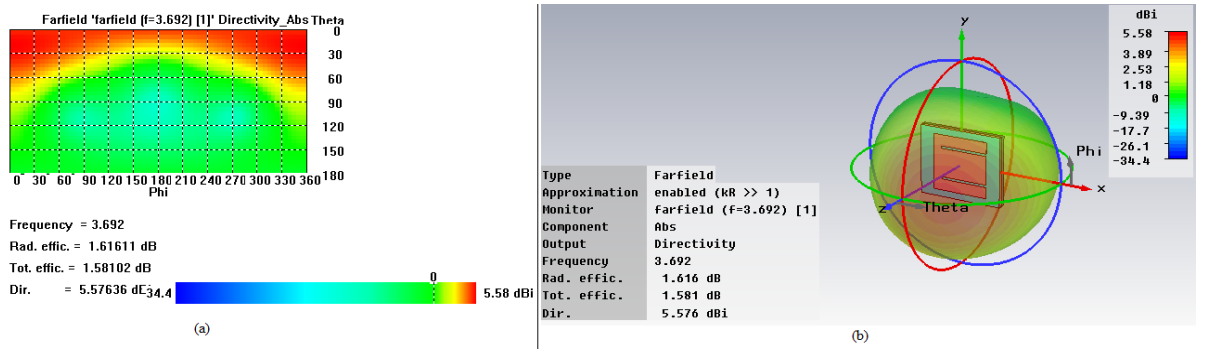

Figure 4.11 Radiation Pattern of Directivity of the Dual Band Antenna at Frequency 3.692 GHz (a) 2D plot, (b) 3D plot

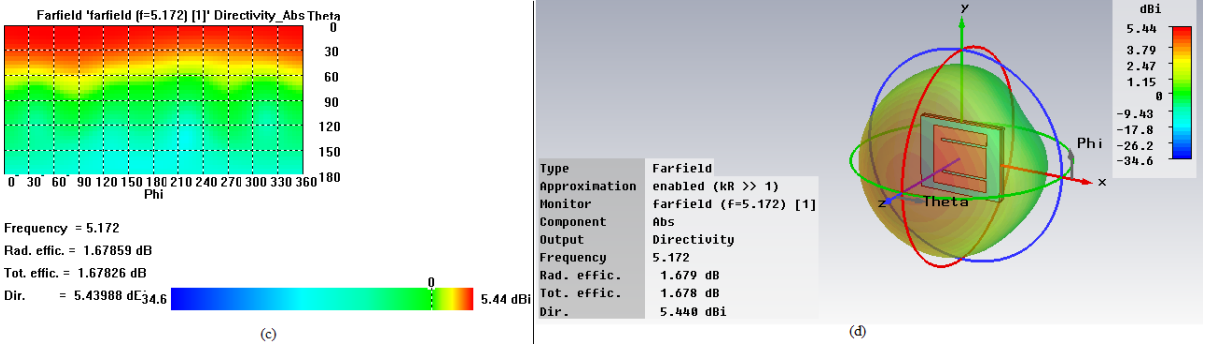

Figure 4.11 Radiation Pattern of Directivity of the Dual Band Antenna at Frequency 5.172 GHz (c) 2D plot, (d) 3D plot

Similarly the improved dual band antenna with stubs has a directivity of 5.586 dBi and 5.309 dBi at the resonance frequencies of 3.692 GHz and 5.2 GHz respectively as shown in 2 D and 3D directivity plot of the improved antenna in Figure 4.12(a), (b), (c), (d). The improved dual band antenna radiates more in a particular direction by an amount of 5.586 dBi and 5.309 dBi when it is compared to an isotropic antenna which radiates equally in all directions.

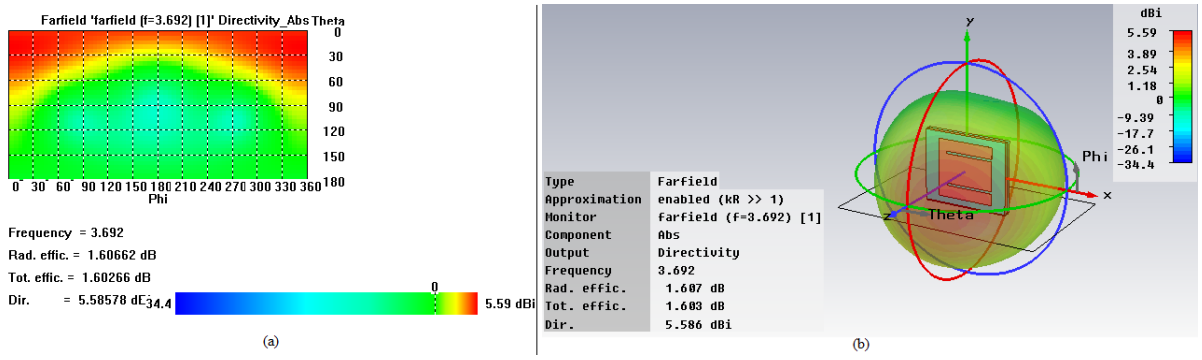

Figure 4.12 Radiation Pattern of Directivity of the Improved Dual Band Antenna with the Introduction of Stubs at Frequency 3.692 GHz (a) 2D plot, (b) 3D plot

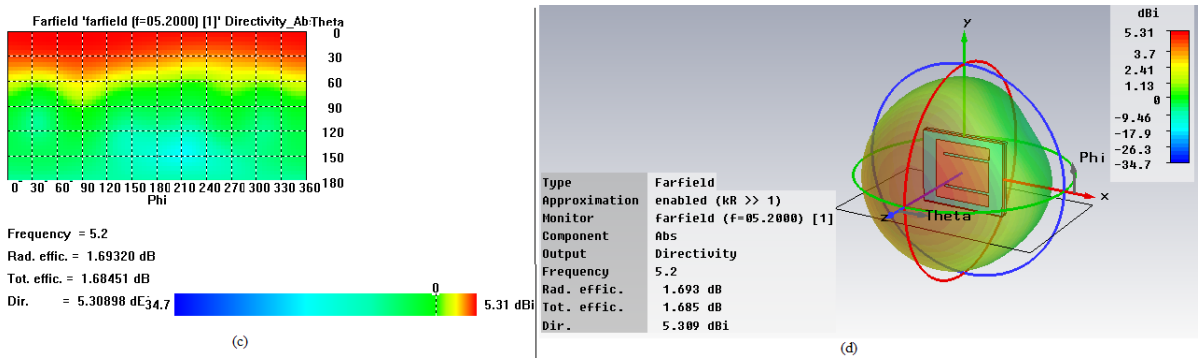

Figure 4.12 Radiation Pattern of Directivity of the Improved Dual Band Antenna with the Introduction of Stubs at Frequency 5.2 GHz (c) 2D plot, (d) 3D plot

4.2.6 Gain

The polar plot of the realized gain of the dual band antenna is shown in Figure 4.13(a), (b) for both the operating frequencies. The Figure 4.13(a), (b) depicts the main lobe magnitude, direction of main lobe and the angular width (half power beam width) for the corresponding frequencies of 3.692 GHz and 5.172 GHz

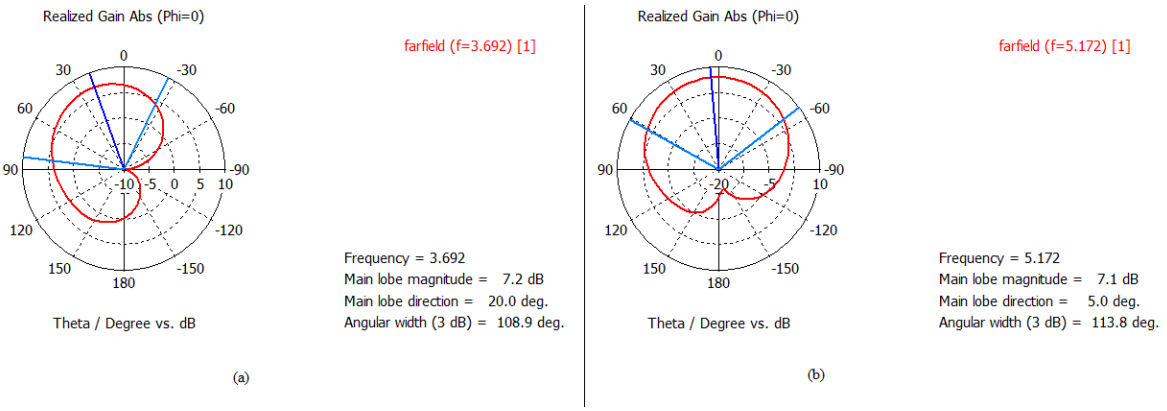

Figure 4.13 Polar Plot of Gain of the Dual Band Antenna at Frequency (a) 3.692 GHz, (b) 5.172 GHz

Similarly the polar plot of the realized gain of the improved dual band antenna is shown in Figure 4.14(a), (b) for both the operating frequencies. The Figure 4.14(a), (b) depicts the main lobe magnitude, direction of main lobe and the angular width (half power beam width) for the corresponding frequencies of 3.692 GHz and 5.2 GHz

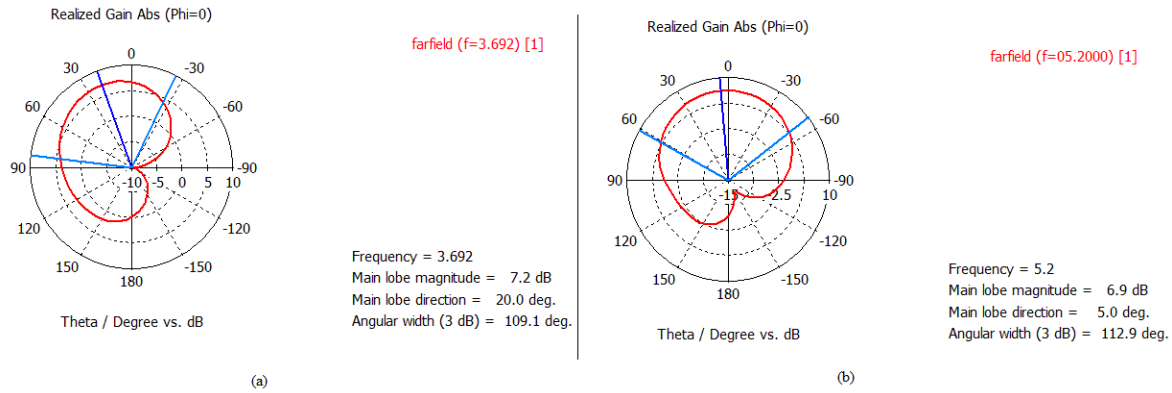

Figure 4.14 Polar Plot of Gain of the Improved Dual Band Antenna with the Stubs at Frequency (a) 3.692 GHz, (b) 5.2 GHz

A comparison is made on basis of various simulation results obtained (like return loss, bandwidth, VSWR, gain and directivity) between the dual band antenna and the improved dual band antenna with the introduction of stubs with the feedline has been given in Table 4.3 and it is seen from the table return loss has increased to −30.40 dB at frequency of 3.692 GHz and the bandwidth of the antenna has increased to 224.8 MHz at frequency of 5.2 GHz.

	Frequency (GHz)	Return Loss (dB)	Bandwidth (MHz)	VSWR	Gain (dB)	Directivity (dBi)
Dual Band Antenna	3.692	−20.94	50.2	1.197	7.2	5.576
	5.172	−41.10	139	1.017	7.1	5.440
Dual Band Antenna with Stubs	3.692	−30.40	48.6	1.062	7.2	5.586
	5.2	−26.99	224.8	1.093	6.9	5.309

Table 4.3 Comparison between Dual Band Antenna and Improved Dual Band Antenna with Stubs

4.3 Conclusion

In this chapter dual band aperture coupled microstrip patch antenna is designed for WLAN applications. But the bandwidth of the designed antenna is not good enough, so to improve the bandwidth stubs are placed with the feedline and the bandwidth is enhanced for the improved dual band aperture coupled microstrip patch antenna with the stubs.

CHAPTER 5

BROADBAND MICROSTRIP PATCH ANTENNA

This chapter covers the designing and simulation of broadband aperture coupled microstrip patch antenna. The designed antenna resonates at frequency 12.5 GHz with upper -10 dB frequency and lower -10 dB frequency of 12.202 GHz and 13.339 GHz respectively. The frequency range of the designed broadband antenna comes under ITU Region 3 which has frequency allocations from 12.2 GHz to 12.7 GHz. The designed antenna finds application in Direct Broadcast Satellite Television for home reception purposes.

5.1 Antenna Design

A broadband aperture coupled microstrip patch antenna is designed for home reception of DBS (Direct Broadcast Satellite) Television in this chapter. The antenna is excited by a coupling aperture which is generating a fictitious open circuit along the radiating edges of the patch producing an additional resonating frequency which results a wide impedance bandwidth for the antenna. Figure 5.1 represents the geometrical dimensioning of the each layer of the designed antenna. The various design specifications of the wide band antenna has been shown in Table 5.1. Also the various design parameters has been shown in Table 5.2 are calculated from the design equations from 1.1 to 1.8 given in CHAPTER 1.

Resonant Frequency (f_r)	12.5 GHz
Patch Substrate Material, Feed Substrate Material	FR-4
Patch Substrate Thickness, Feed Substrate Thickness	1.57 mm
Dielectric Constant of the material used	4.4
Thickness of PEC Material	0.02 mm

Table 5.1 Broadband Antenna Design Specifications

Parameters	**L**	**W**	L_g	W_g	L_f	W_f
Description	Length of the Patch	Width of the Patch	Length of the Ground	Width of the Ground	Length of the Feedline	Width of the Feedline
Values	16 mm	16 mm	40 mm	40 mm	24.1 mm	1.8 mm

Table 5.2 Various Dimensions of the Broadband Antenna

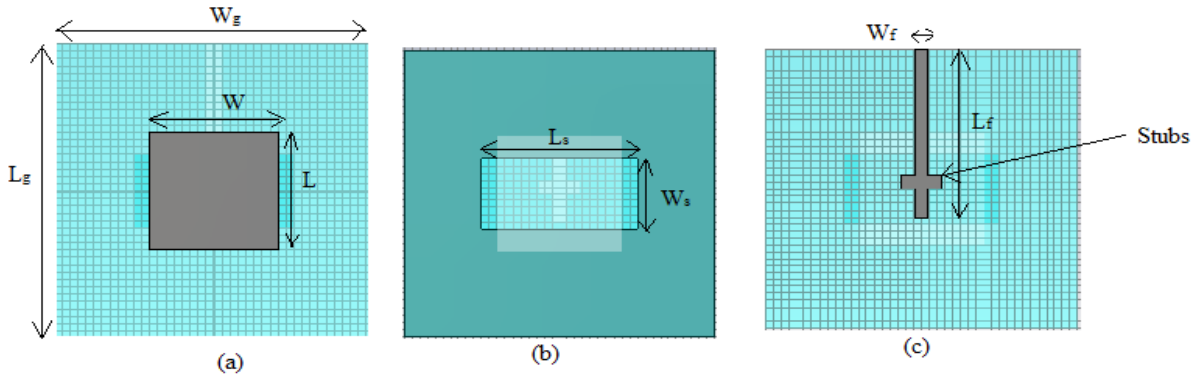

Figure 5.1 Broadband Antenna (a)Top View, (b)Ground Plane with Slot, (c)Back View

5.2 CST Simulation Results

CST Microwave Studio 2010 has been used to simulate the broadband aperture coupled microstrip antenna and various simulation results like return loss, smith chart, VSWR plot, impedance plot, surface current, farfield patterns of the gain and directivity of the antenna are observed.

5.2.1 Return Loss and Antenna Bandwidth

Figure 5.2 shows the return loss versus frequency plot of the designed antenna. It is a wide band covering the frequency range from 12.202 GHz to 13.339 GHz having a bandwidth of 1.137 GHz or 1137 MHz with the return loss value of −35.459 dB at resonant frequency of 12.5 GHz.

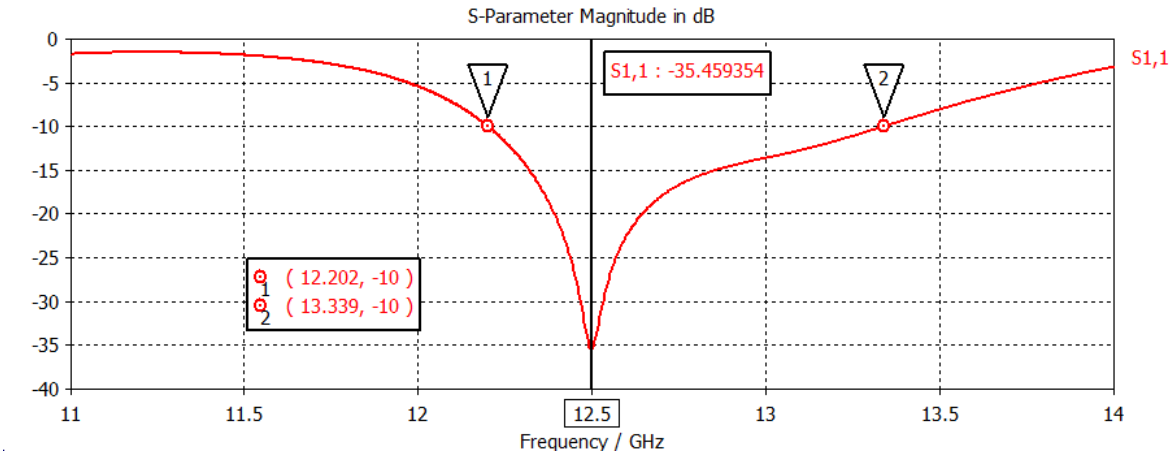

Figure 5.2 Return Loss (S_{11}) Versus Frequency Plot of the Broadband Antenna

5.2.2 Smith Chart and Antenna Impedance

The smith chart represents variation of the antenna impedance with the frequency. It shows the complex impedance of the reflected S-parameter (S_{11}) within a specified frequency range. It plots the complex reflection coefficient in two dimensional plane. It has been scaled in normalized impedance. Normalized scaling allows the smith chart to be used for the problems which involves the characteristics impedance. The most commonly used characteristics impedance is 50 ohms. It is also possible to estimate the bandwidth of the antenna from the smith chart by reading the frequencies at the points where the VSWR=2 circle and input impedance curve intersects. The size of the locus of the smith chart increases with increase in slot length and stub length. For proper matching conditions the locus of the smith chart must pass through its center. The smith chart for the broadband antenna has been shown in Figure 5.3.

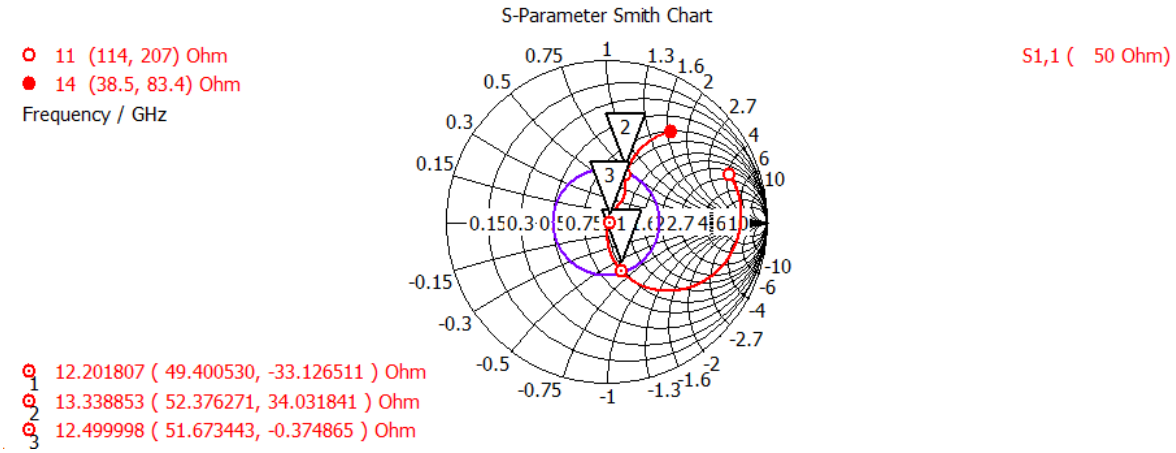

Figure 5.3 Smith Chart Showing the Characteristics Impedance of the Broadband Antenna

5.2.3 VSWR

The VSWR (Voltage Standing Wave Ratio) is related to the reflection parameter. It is the quotient between the maximum and minimum voltage that can be measured along a waveguide. Its value lies between 1 to ∞ theoretically depending upon the reflection coefficient lies from 0 to 1. The VSWR value should be less than 2 to have considerable performance with the best matching. The designed broadband antenna has a VSWR of 1.034 at the operating frequencies of 12.5 GHz as shown in VSWR versus frequency plot in Figure 5.4.

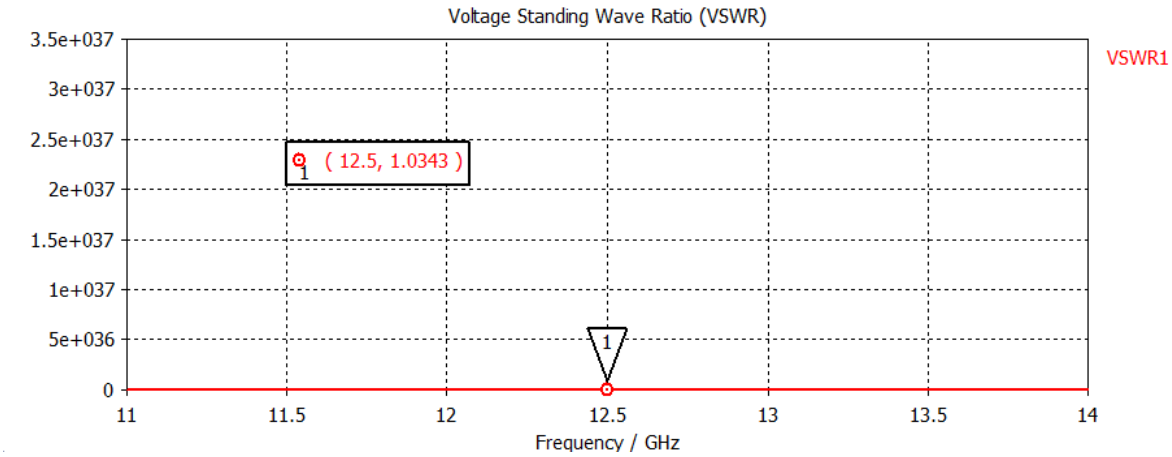

Figure 5.4 VSWR Plot of the Broadband Antenna

5.2.4 Impedance

The impedance versus frequency plot of the broadband antenna has been shown in Figure 5.5 which depicts the impedance (resistance as well as reactance) of the antenna at the resonating frequency of 12.5 GHz.

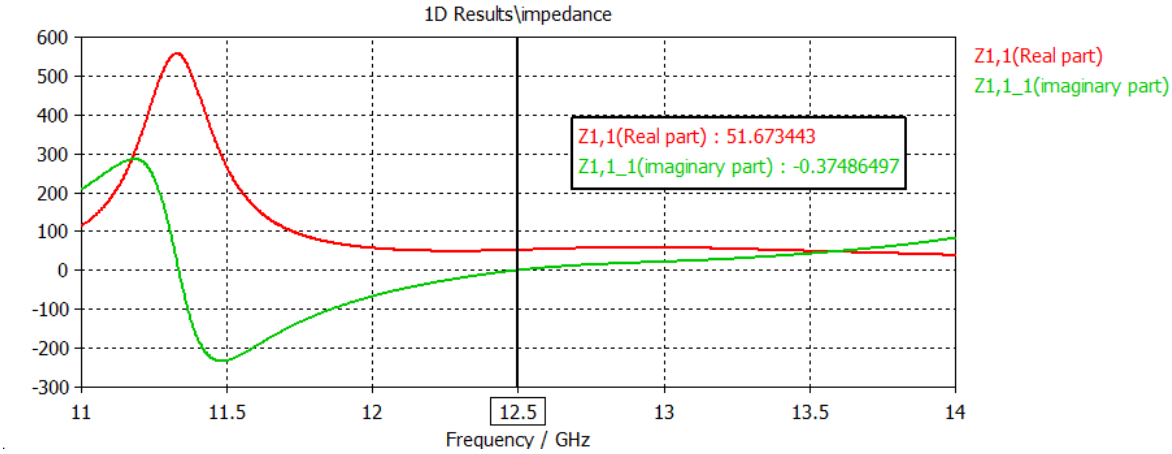

Figure 5.5 Impedance Versus Frequency Plot

5.2.5 Surface Current

The surface current distribution at the patch, ground and the feedline for the broadband microstrip patch antenna resonating at frequency of 12.5 GHz is shown in Figure 5.6(a), (b), (c) respectively. Figure 5.6(a) depicts the current is flowing in almost the entire patch, but it has more magnitude in the lower portion of the patch. The magnitude of the current is more around the boundaries of the slot in the ground plane as shown in Figure 5.6(b). And for the feedline the current density is more in the center as shown in Figure 5.6(c). The arrows are

pointed in the direction of the field and the color of the arrows are related to the field strength.

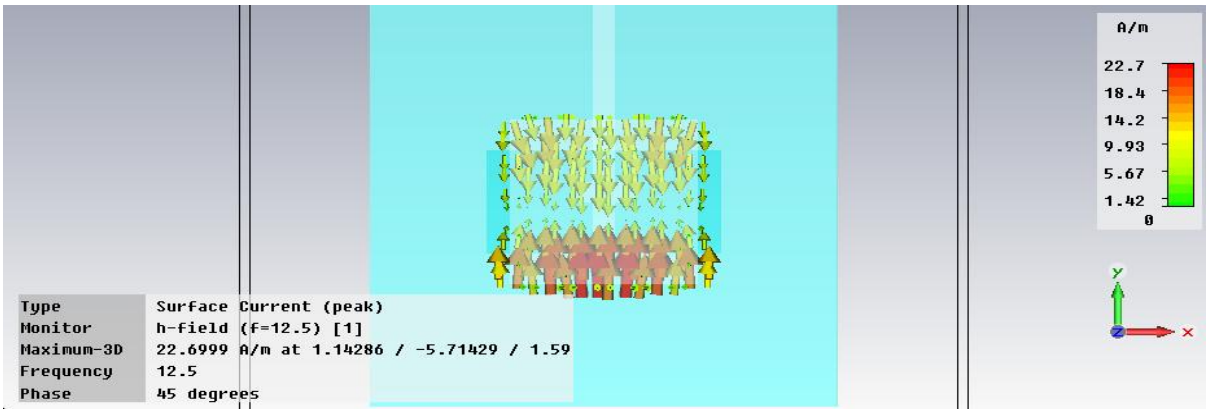

Figure 5.6(a) Surface Current Distribution of the Patch of the Antenna at 12.5 GHz

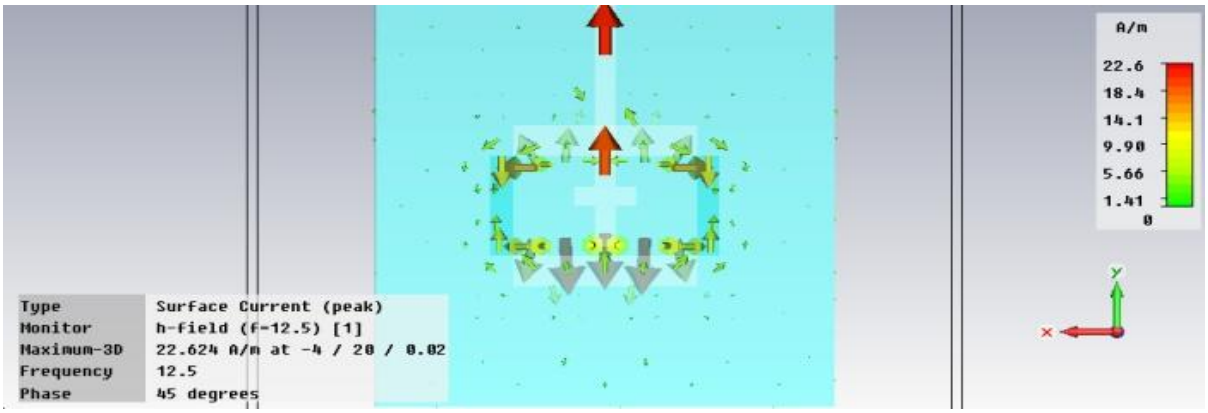

Figure 5.6(b) Surface Current Distribution of the Slot in the Ground at 12.5 GHz

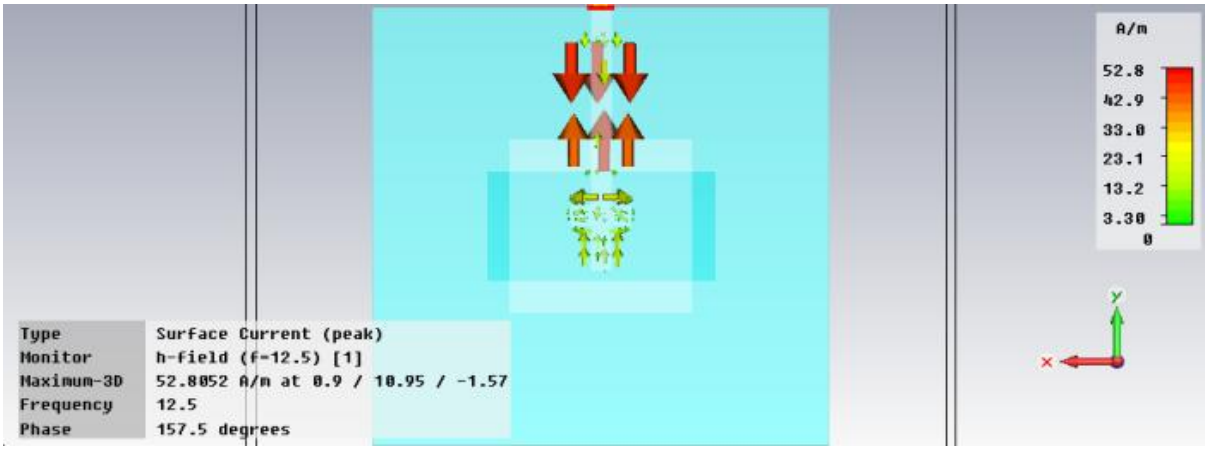

Figure 5.6(c) Surface Current Distribution of the Feedline of the Antenna at 12.5 GHz

5.2.6 Directivity

The 2D and 3D directivity plot of the broadband antenna operating at 12.5 GHz represents the amount of radiation intensity i.e. 6.573 dBi. The nominated antenna radiates more in a particular direction by an amount of 6.573 dBi when compared to an isotropic antenna which radiates equally in all directions.

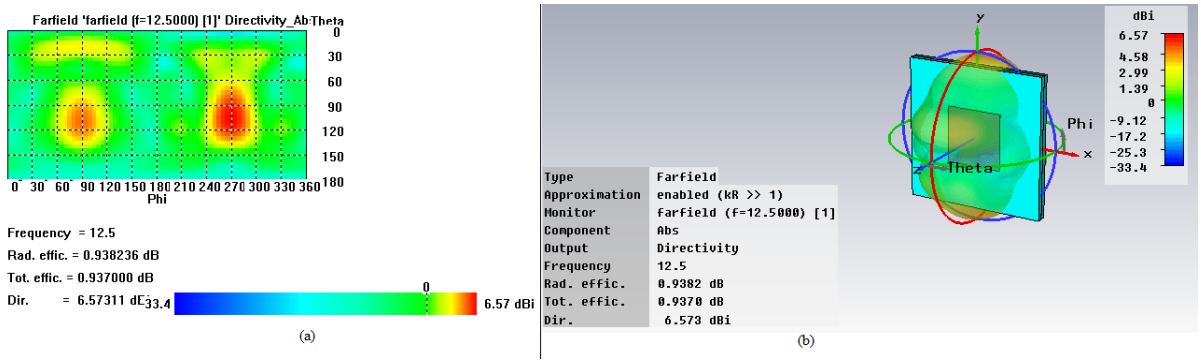

Figure 5.7 Radiation Pattern of Directivity of the Broadband Antenna at Frequency 12.5 GHz (a) 2D plot, (b) 3D plot

5.2.7 Gain

Figure 5.8 shows the polar plot view of the gain for broadband antenna at the resonant frequency of 12.5 GHz. The main lobe is directed at an angle of 105.0 degree and has a magnitude of 7.5 dB. The angular width (3 dB) or HPBW (Half Power Beam width) or simply beam width of the antenna designed is 70.4 degree.

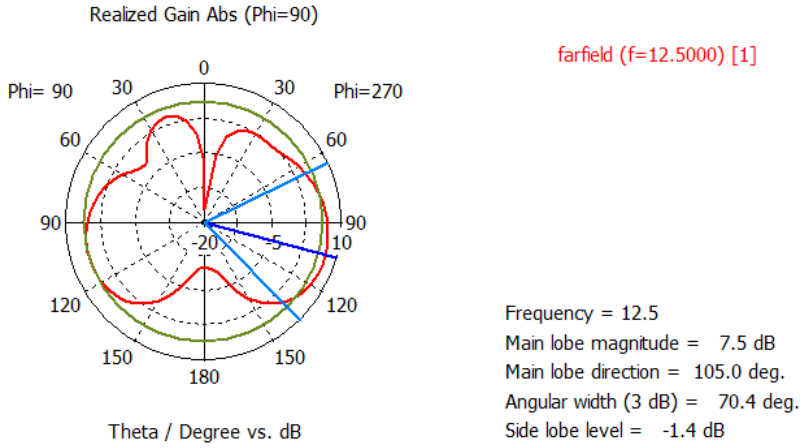

Figure 5.8 Polar Plot of the Gain of the Broadband Antenna at 12.5 GHz

5.3 Conclusion

In this chapter a broadband microstrip antenna is designed and simulated to resonate at 12.5 GHz and the frequency of operation of the designed antenna lies in ITU Region 3 for DBS applications. The performance of the antenna is analyzed in terms of return loss, bandwidth, VSWR, impedance matching, gain and directivity and satisfactory results are obtained for covered frequency band of operation.

CHAPTER 6

DUAL BAND STACKED MICROSTRIP PATCH ANTENNA

This chapter deals with two antenna designs, one is dual band aperture coupled stacked microstrip patch antenna and the other is dual band aperture coupled stacked microstrip patch antenna with an air gap between the ground plane and the upper layer substrate. The later design is the sequel of the former which increases its bandwidth for WLAN applications.

6.1 Antenna Design

An aperture coupled microstrip patch antenna resonating at two frequencies is designed using stacking. Stacking is a technique to achieve the dual band behavior and to increase the impedance bandwidth of the antenna. It involves a multilayered structure consisting of number of dielectric substrates and patches. In it parasitic elements (or stacked patches) are placed over the driven element (or the main patch). The electromagnetic coupling between the parasitic element and the driven element increases the impedance bandwidth. FR-4 is the material used for antenna substrate (for both the upper substrate layers) and feed substrate (the lower substrate layer). The material has a thickness (h) of 1.6 mm and dielectric permittivity (ε_r) of 4.4 with tangent loss component ($\tan\delta$) as 0.0009. The antenna structure has a bottom patch of rectangular shape over the substrate material supported by the ground plane. The top patch of the antenna is of a rectangular shape having a rectangular slot of dimensions exactly same as the dimensions of the bottom patch. The dual band antenna is fed through an aperture cut in the ground plane coupled to a 50 Ω microstrip line under the feed substrate. The side view of the antenna showing various layers organizations with placement of waveguide port is shown in Figure 6.1. Figure 6.2 depicts the every layer view of the antenna with labeled dimensions. The front view of the antenna is shown in Figure 6.3. The design specifications of the dual band ACSMPA has been given in Table 6.1. Also the various dimensions of the antenna has been calculated by the design equations from 1.1 to 1.8 given in CHAPTER 1. The dimensions of the top patch, bottom patch, ground plane, substrate layers, slot and the feedline of the designed dual band antenna has been given in Table 6.2.

Resonance Frequencies (f_r)	3.455 GHz, 5.225 GHz
Patch (top as well as bottom patch) Substrate Material, Feed Substrate Material	FR-4
Patch (top as well as bottom patch) Substrate Thickness, Feed Substrate Thickness (h)	1.6 mm
Dielectric Constant of the material used (ε_r)	4.4
Thickness of PEC Material (t)	0.02 mm

Table 6.1 Design Specifications of the Dual Band ACSMPA

Parameters	Description	Values
L	Length of the Top Patch	19.72 mm
W	Width of the Top Patch	25.75 mm
L_b	Length of the Bottom Patch	9.7 mm
W_b	Width of the Bottom Patch	16.44 mm
L_g	Length of the Ground Plane	29.32 mm
W_g	Width of the Ground Plane	35.35 mm
L_s	Length of the Aperture in the ground plane	18 mm
W_s	Width of the Aperture in the ground plane	1.6 mm
L_f	Length of the Feedline	22.36 mm
W_f	Width of the Feedline	3 mm

Table 6.2 Various Dimensions of the Dual Band ACSMPA

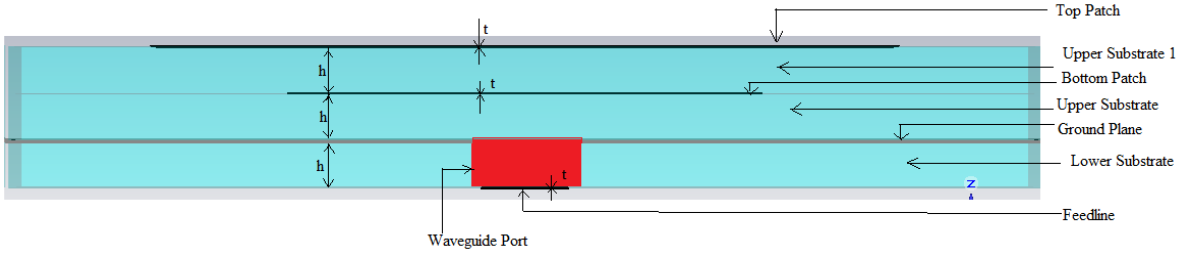

Figure 6.1 Side View of the Dual Band ACSMPA

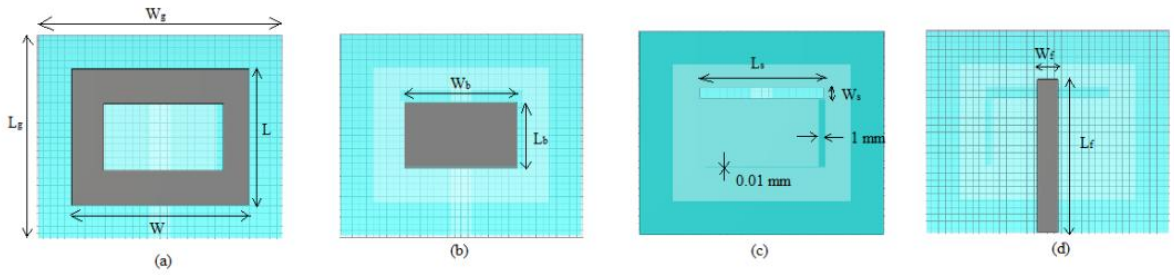

Figure 6.2 Dual Band ACSMPA (a)Front View Showing Top Patch, (b)Bottom Patch, (c)Slot in the Ground Plane, (d)Back View Showing Feedline

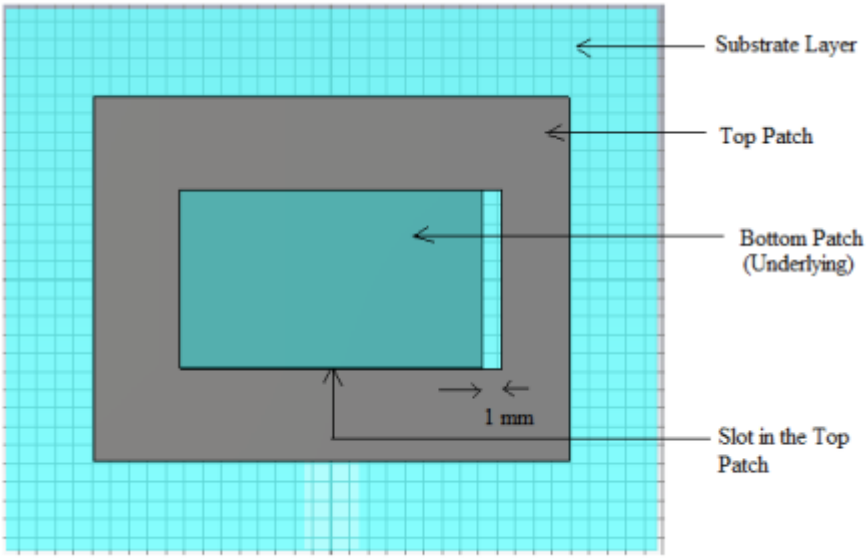

Figure 6.3 Front View of the Antenna Showing Position of the Bottom Patch below the Slot Cut in the Top Patch

6.2 CST Simulation Results

CST Microwave Studio 2010 has been used to simulate the proposed dual band aperture coupled microstrip patch antenna and various simulation results like return loss, smith chart, VSWR, impedance versus frequency plot, surface current and farfield patterns of the gain and directivity of the antenna has been observed.

6.2.1 Return Loss and Antenna Bandwidth

The (S_{11}) versus frequency plot of the antenna shows two dips indicating dual frequency operation of the antenna at the resonance frequencies of 3.455 GHz and 5.225 GHz. The value of reflection coefficients (Γ) are 0.0473 and 0.0560 at the corresponding resonance

frequencies. The return loss ($20\log_{10}\Gamma$) values are -26.488 dB and -25.034 dB at the corresponding resonance frequencies. The S_{11} parameter represents the power reflected from the antenna. The whole power is reflected from the antenna and nothing is radiated for $S_{11} = 0$ dB. $S_{11} = -10$ dB indicates 10% of the power is reflected. The bandwidth of the dual band antenna can be calculated from the return loss versus frequency plot. The bandwidth of the antenna is the range of frequencies over which the return loss is larger than -10 dB and it corresponds to a VSWR value of 2. The measured -10 dB bandwidth of the designed antenna is 86.5 MHz and 172.6 MHz at the lower resonant frequency of 3.455 GHz and the upper resonant frequency of 5.225 GHz respectively.

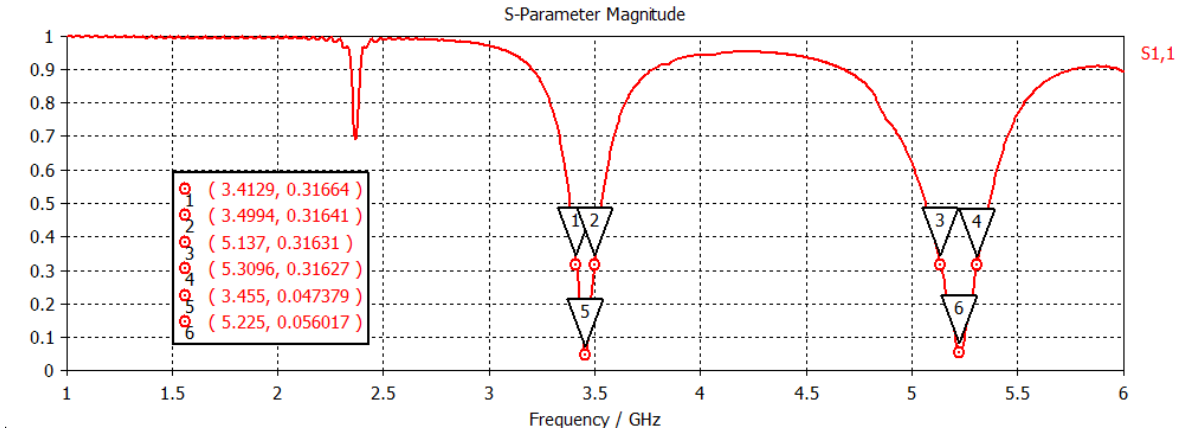

Figure 6.4 S-parameter (Γ or Reflection Coefficient) Versus Frequency Plot of the Dual Band ACSMPA

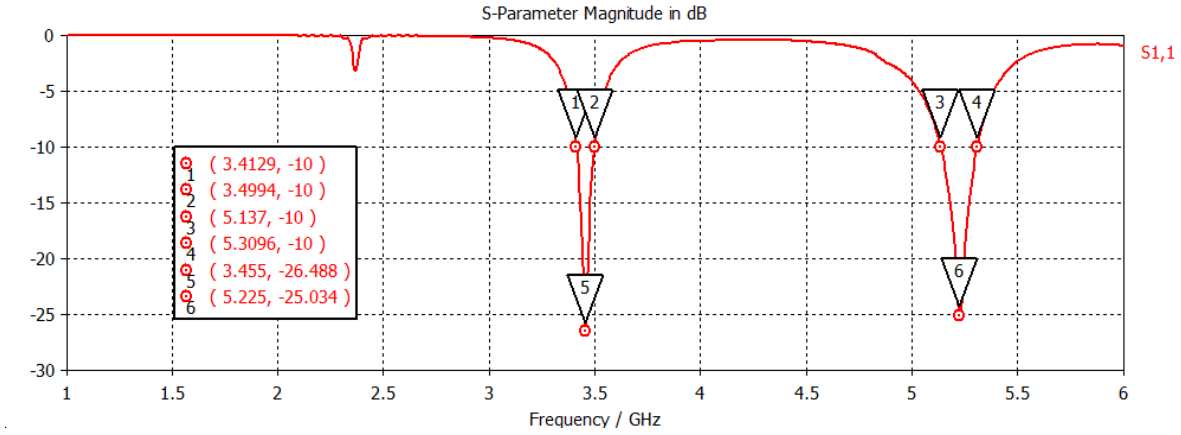

Figure 6.5 Return Loss (S_{11}) Versus Frequency Plot of the Dual Band ACSMPA

6.2.2 Smith Chart and Antenna Impedance

Smith chart is plot of complex reflection coefficient of the antenna in polar form. Since reflection coefficient corresponds directly to the impedance of the antenna. So the smith chart is a tool for plotting the impedance of the antenna as the function of the frequency. At the center of the polar form of smith chart the value of reflection coefficient is zero and only at this point no power is reflected by the antenna. The outermost circle of the smith chart where the magnitude of the reflection coefficient is one, all the power is reflected by the antenna. The smith chart has been scaled in normalized impedance. Normalized scaling allows the smith chart to be used for the problems which involves the characteristics impedance. The most commonly used characteristics impedance is 50 ohms. It is also possible to estimate the bandwidth of the antenna from the smith chart by reading the frequencies at the points where the VSWR=2 circle and input impedance curve intersects. The size of the locus of the smith chart increases with increase in slot length and stub length. For proper matching conditions the locus of the smith chart must pass through its center. The smith chart for the dual band antenna has been shown in Figure 6.6 which depicts the impedance values (resistance as well as reactance) at the marked frequency values.

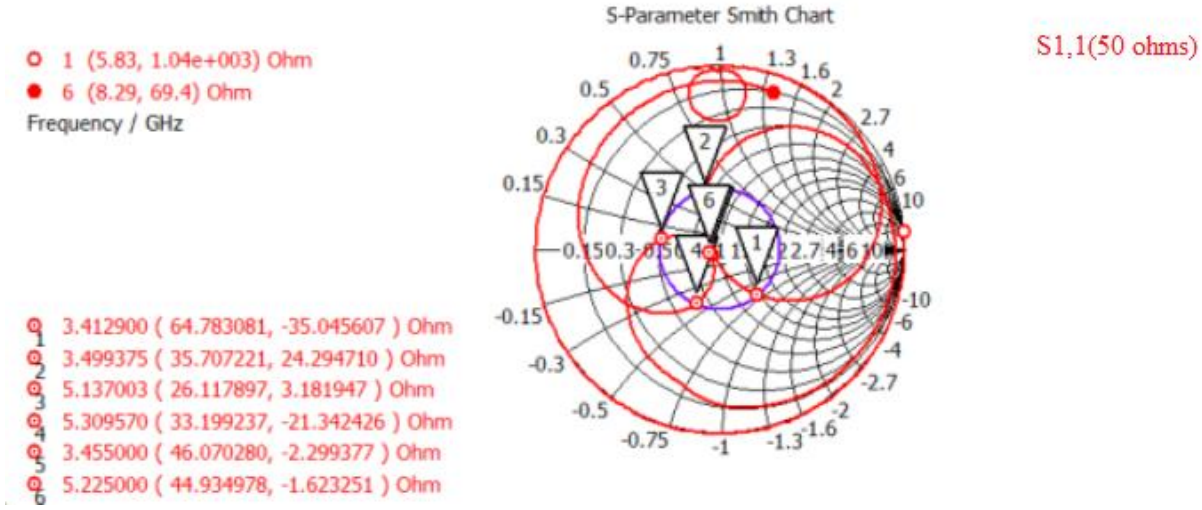

Figure 6.6 Smith Chart of the Dual Band ACSMPA

6.2.3 VSWR

VSWR (Voltage Standing Wave Ratio) is a parameter which describes how well the antenna is matched to the transmission line. It is directly related to the reflection coefficient (S_{11}) in linear scale. The value of VSWR lies between 1 and ∞ depending on the value of reflection

coefficient from 0 to 1. The smaller value of the VSWR indicates the better matching of the antenna to the transmission line. Hence lesser power is reflected from the antenna and more power is delivered to the antenna. For the minimum possible value of VSWR equal to one no power is reflected from the antenna. The VSWR plot of the dual band antenna designed with stacking is shown in Figure 6.7. The VSWR value at the lower resonant frequency of 3.455 GHz is 1.0995 and at the upper resonant frequency of 5.225 GHz is 1.1187.

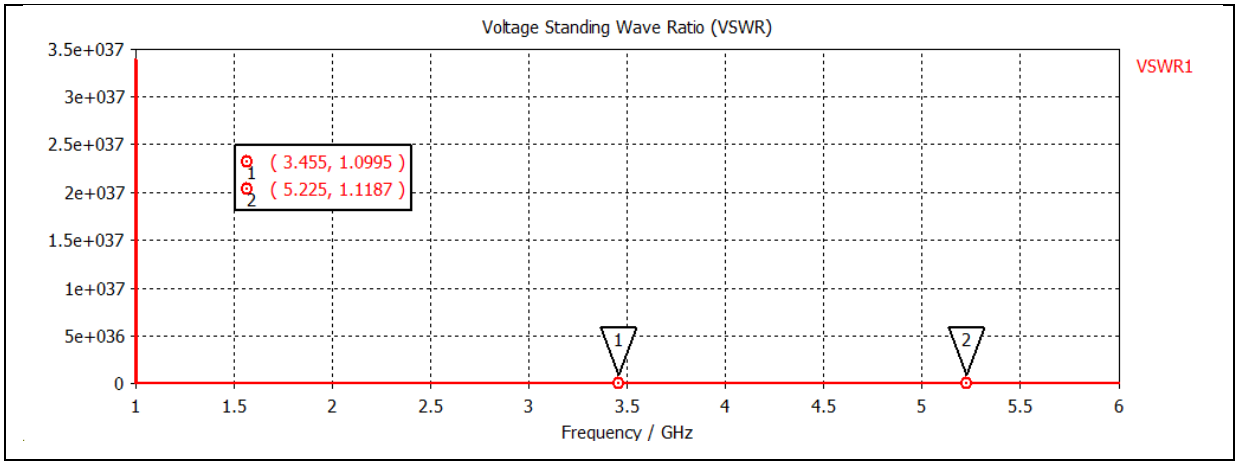

Figure 6.7 VSWR Plot of the Dual Band ACSMPA

The following Table 6.3 shows the relationship between the reflection coefficient (S_{11}or Γ), VSWR, reflected power and the return loss of the dual band stacked antenna at the resonant frequencies

Parameters / **Frequency**	S_{11} **or** Γ	**VSWR=** $\frac{1+\lvert\Gamma\rvert}{1-\lvert\Gamma\rvert}$	**Reflected Power /** Γ^2 **(%)**	**Return Loss(dB)** $20\log_{10}\lvert\Gamma\rvert$
3.455 GHz	0.047379	1.0995	0.22	−26.488 dB
5.225 GHz	0.056017	1.1187	0.31	−25.034 dB

Table 6.3 Relation between Various Parameters of the Dual Band ACSMPA

6.2.4 Impedance

The input impedance of the antenna is almost real at the resonance frequencies of 3.455 GHz and 5.225 GHz as shown in Figure 6.8. The real values of impedances are 46.067 Ω and 44.933 Ω and their reactance as −2.3123 Ω and −1.6194 Ω at the corresponding resonance frequencies. The voltage and the current are in phase at the terminals of the antenna. This

makes the good impedance matching of the antenna to the microstrip transmission line as the imaginary part of the impedance does not need to be tuned out. The return loss versus frequency plot of the antenna shows a large decrease in the magnitude of S_{11} around the resonance frequencies which indicates the power is radiated well around the resonance frequencies.

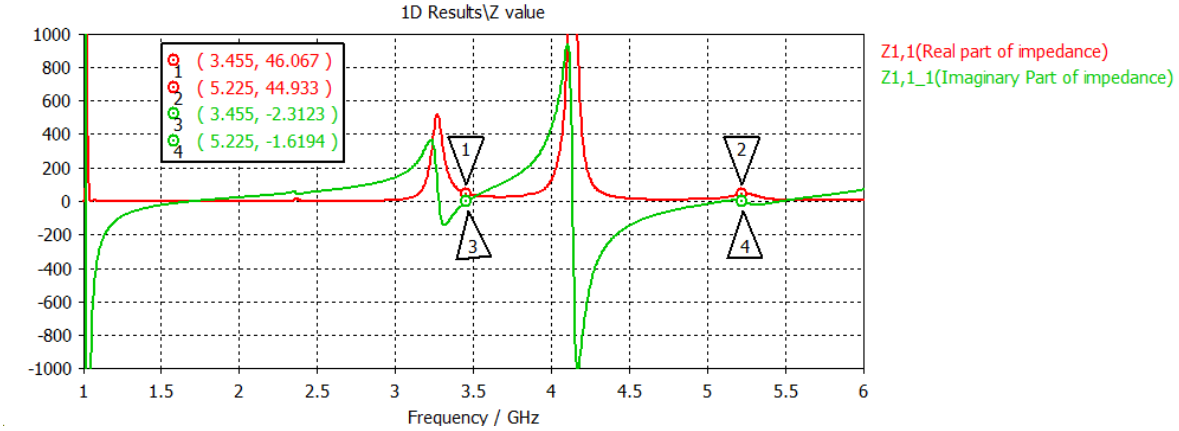

Figure 6.8 Impedance Versus Frequency plot of the Dual Band ACSMPA

6.2.5 Surface Current

The surface current distribution at the top patch, bottom patch, ground and the feedline for the dual band microstrip patch antenna resonating at lower band frequency of 3.455 GHz is shown in Figure 6.9(a), (b), (c), (d) respectively. Figure 6.9(a) depicts the current is flowing in almost the entire patch, but it has more magnitude near the rightmost boundary of the slot cut in the patch. The bottom patch has more current density in the upper section of the patch as seen from the Figure 6.9(b). The magnitude of the current is more around the boundaries of the slot in the ground plane as shown in Figure 6.9(c). And for the feedline the current density is more in the center as shown in Figure 6.9(d). The arrows are pointed in the direction of the field and the color of the arrows are related to the field strength.

The surface current distribution at the top patch, bottom patch, ground and the feedline for the dual band microstrip patch antenna resonating at upper band frequency of 5.225 GHz is shown in Figure 6.9(e), (f), (g), (h) respectively. Figure 6.9(e) depicts the current is flowing in almost the entire patch, but it has more magnitude near the lowermost boundary of the slot cut in the patch. The bottom patch has more current density in the middle of the patch as seen from the Figure 6.9(f). The magnitude of the current is higher in the central section of the

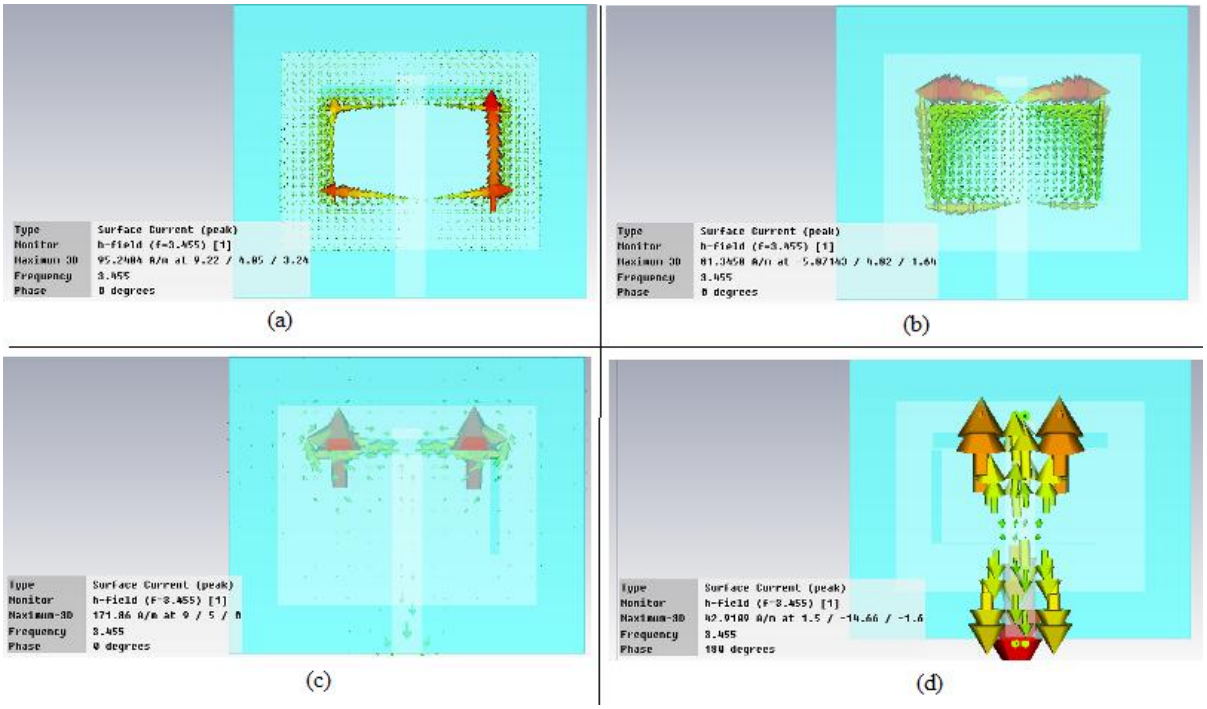

Figure 6.9 Surface Current Distribution of the Dual Band ACSMPA at 3.455 GHz (a) Top Patch, (b) Bottom Patch, (c) Ground Plane, (d) Feedline

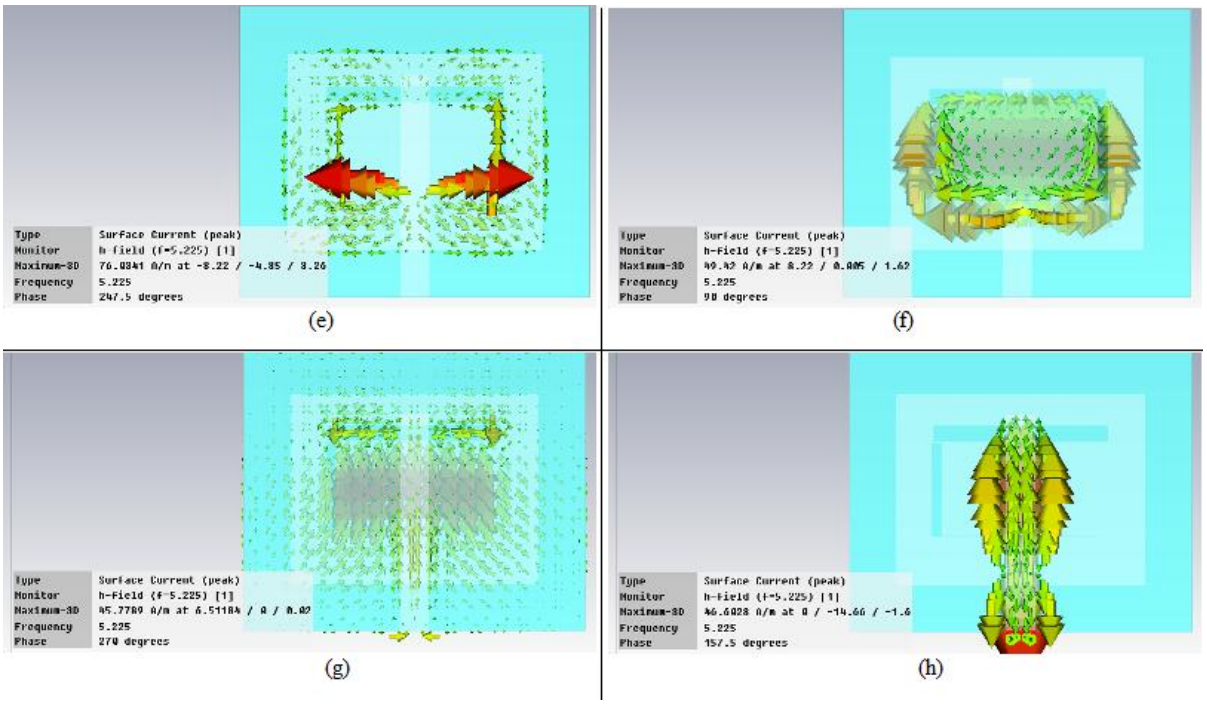

Figure 6.9 Surface Current Distribution of the Dual Band ACSMPA at 5.225 GHz (e) Top Patch, (f) Bottom Patch, (g) Ground Plane, (h) Feedline

ground plane as shown in Figure 6.9(g). And for the feedline the current density is more in the center as shown in Figure 6.9(h).

6.2.6 Directivity

The directivity of the antenna is the measure of directional property of the antenna's radiation pattern. For the antenna which radiates equally in all the directions the directionality would be zero and the directivity would be 1 (or 0 dBi). The polar plot of the directivity with the elevation angle (θ degrees) at the azimuth angle (ϕ) phi equal to 90 degrees of the designed dual band antenna with stacked technology at both the resonance frequencies of 3.455 GHz and 5.225 GHz is shown in Figure 6.10(a), (b).

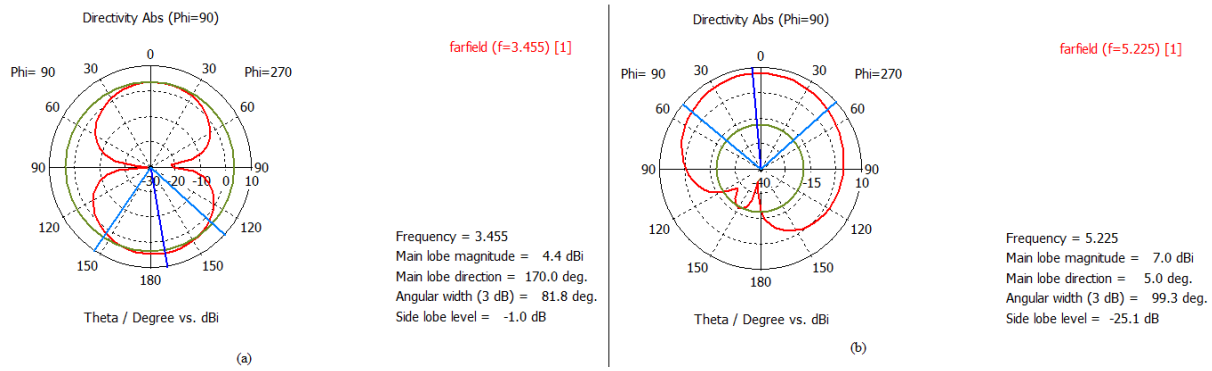

Figure 6.10 Polar Plot of the Directivity of the Dual Band ACSMPA at Frequency (a) 3.455 GHz, (b) 5.225 GHz

Also the 2 D and 3D radiation pattern of the directivity of the dual band ACSMPA at frequency 3.455 GHz has been shown in Figure 6.10 (c), (d). The 2 D and 3D radiation pattern of the directivity of the dual band ACSMPA at frequency 5.255 GHz has been shown in Figure 6.10 (e), (f).

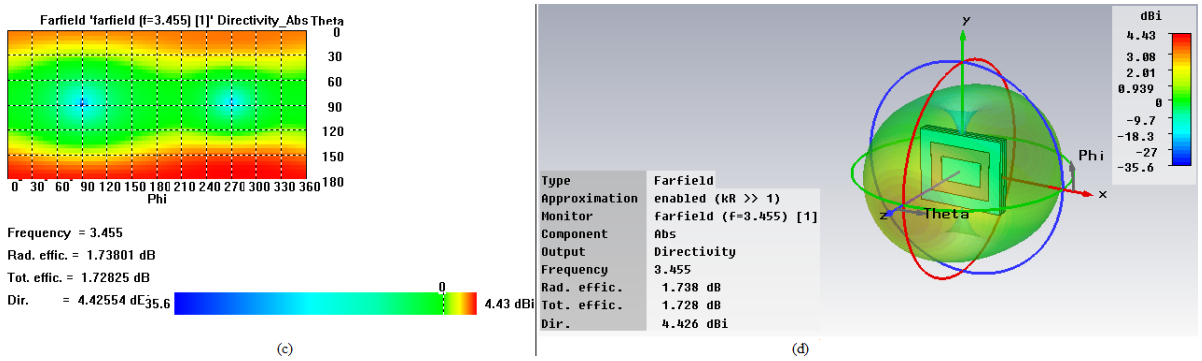

Figure 6.10 Radiation Pattern of the Directivity of the Dual Band ACSMPA at Frequency 3.455 GHz (c) 2D plot, (d) 3D plot

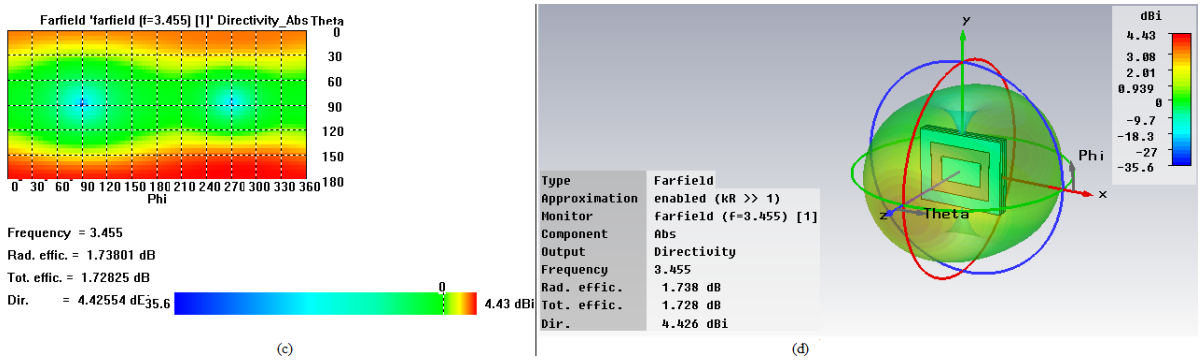

Figure 6.10 Radiation Pattern of the Directivity of the Dual Band ACSMPA at Frequency 3.455 GHz (c) 2D plot, (d) 3D plot

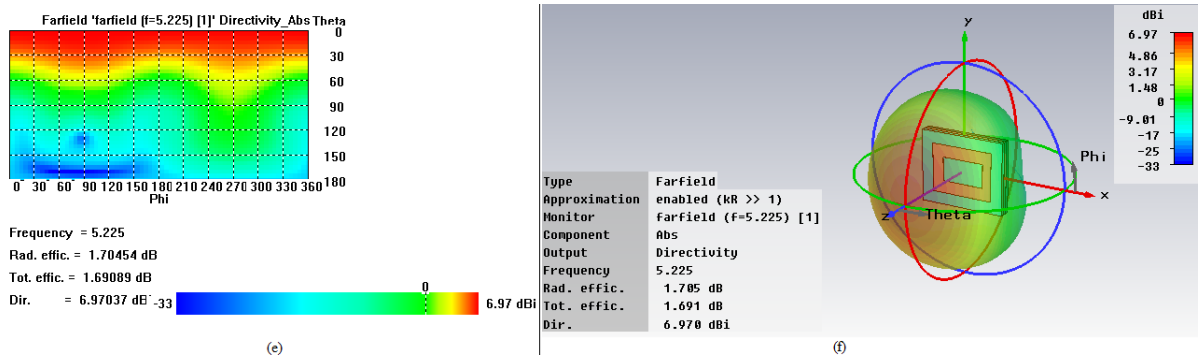

Figure 6.10 Radiation Pattern of the Directivity of the Dual Band ACSMPA at Frequency 5.225 GHz (e) 2D plot, (f) 3D plot

6.2.7 Gain

The gain of an antenna describes the power transmitted in the direction of peak radiation to that of an isotropic antenna. The polar plot of the gain with the elevation angle (θ degrees) at the azimuth angle (ϕ) phi equal to 90 degrees of the designed dual band antenna with stacked technology at both the resonance frequencies of 3.455 GHz and 5.225 GHz is shown in Figure 6.11(a), (b). The dual band antenna has a gain of 6.2 dB at frequency 3.455 GHz which means the power received far from the antenna would be 6.2 dB higher than that would be received from an isotropic antenna. The antenna has a gain of 8.7 dB at frequency 5.225 GHz which means the power received far from the antenna would be 8.7 dB higher than that would be received from an isotropic antenna.

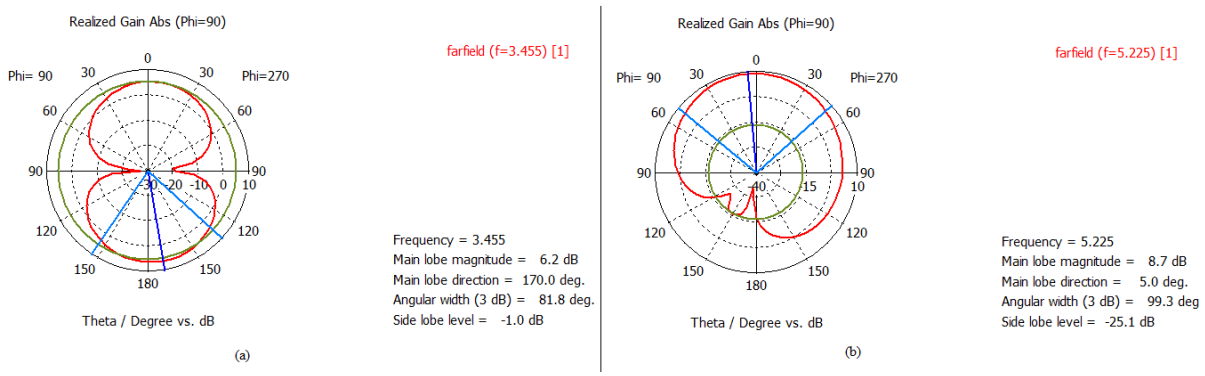

Figure 6.11 Polar Plot of the Gain of the Dual Band ACSMPA at Frequency (a) 3.455 GHz, (b) 5.225 GHz

Also the 2 D and 3D radiation pattern of the gain of the dual band ACSMPA at frequency 3.455 GHz has been shown in Figure 6.11 (c), (d) and the 2 D and 3D radiation pattern of the gain of the dual band ACSMPA at frequency 5.255 GHz has been shown in Figure 6.11 (e), (f).

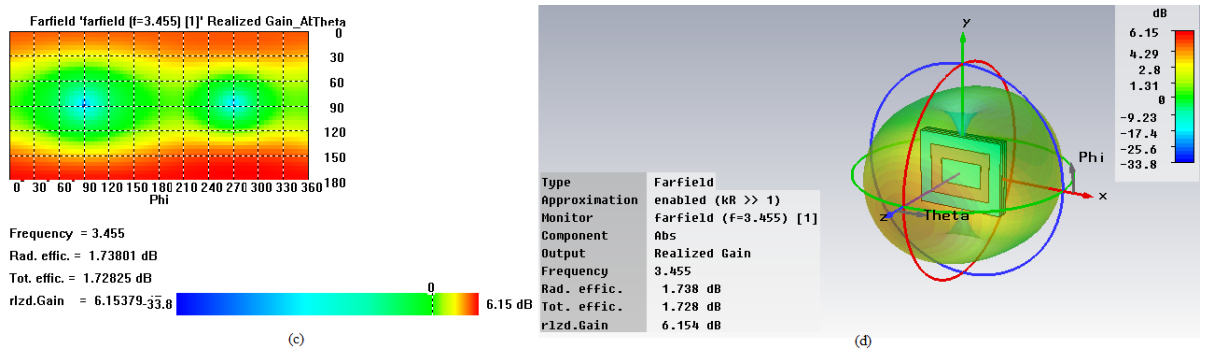

Figure 6.11 Radiation Pattern of the Gain of the Dual Band ACSMPA at Frequency 3.455 GHz (c) 2D plot, (d) 3D plot

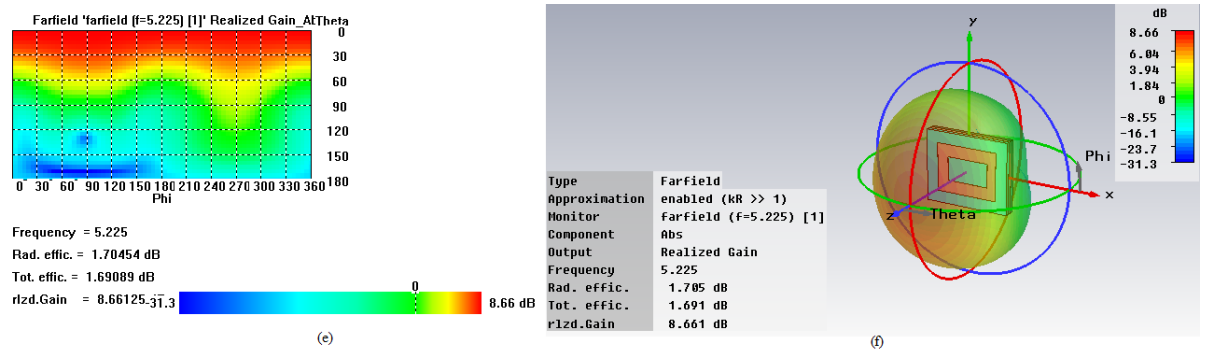

Figure 6.11 Radiation Pattern of the Gain of the Dual Band ACSMPA at Frequency 3.455 GHz (e) 2D plot, (f) 3D plot

6.3 Improved Dual Band Aperture Coupled Stacked Microstrip Patch Antenna with an Air Gap between the Ground Plane and the Upper Layer Substrate

In order to enhance the bandwidth of antenna designed in section 6.1 an air gap of 3 mm has been introduced between the ground plane and the upper layer substrate in this section and the result is a new antenna with improved bandwidth.

6.3.1 Antenna Design

An aperture coupled dual band stacked microstrip patch antenna has been designed in the previous section. The antenna achieved an impedance bandwidth of 86.5 MHz and 172.6 MHz at the frequency of 3.455 GHz and 5.225 GHz respectively. The bandwidth of the antenna is a major concern in the wireless applications of the antenna. Thus the design of the antenna has been modified slightly by placing an air gap of exactly 3 mm between the ground plane and the upper layer substrate to enhance the bandwidth of the antenna keeping all other parameters of the antenna same. Air gap increases the overall height of the antenna. Also the bandwidth of the antenna is proportional to the height of the antenna structure, that is why the bandwidth gets increased. The resulting antenna is simulated by CST Microwave Studio 2010 and the various simulation results are discussed as under.

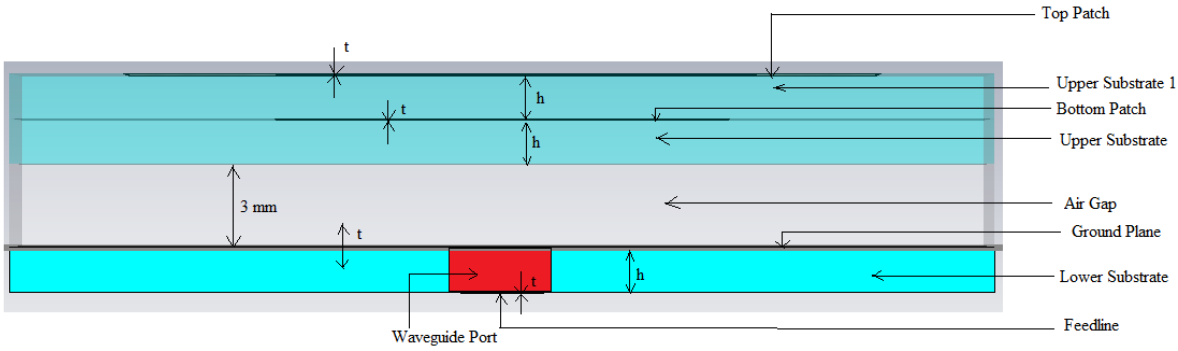

Figure 6.12 Side View of the Improved Dual Band ACSMPA

Resonance Frequencies (f_r)	3.905 GHz, 5.36 GHz
Patch (top as well as bottom patch) Substrate Material, Feed Substrate Material	FR-4
Patch (top as well as bottom patch) Substrate Thickness, Feed Substrate Thickness (h)	1.6 mm

Dielectric Constant of the material used (ε_r)	4.4
Thickness of PEC Material (t)	0.02 mm
Height of Air Gap	3 mm

Table 6.4 Design Specifications of the Improved Dual Band ACSMPA

Parameters	Description	Values
L	Length of the Top Patch	19.72 mm
W	Width of the Top Patch	25.75 mm
L_b	Length of the Bottom Patch	9.7 mm
W_b	Width of the Bottom Patch	16.44 mm
L_g	Length of the Ground Plane	29.32 mm
W_g	Width of the Ground Plane	35.35 mm
L_s	Length of the Aperture in the ground plane	18 mm
W_s	Width of the Aperture in the ground plane	1.6 mm
L_f	Length of the Feedline	22.36 mm
W_f	Width of the Feedline	3 mm

Table 6.5 Various Dimensions of the Improved Dual Band ACSMPA

6.3.2 CST Simulation Results

CST Microwave Studio 2010 has been used to simulate the proposed dual band aperture coupled microstrip patch antenna with an air gap and various simulation results like return loss, smith chart, VSWR, impedance versus frequency plot, surface current and farfield patterns of the gain and directivity of the antenna has been observed.

6.3.2.1 Return Loss and Antenna Bandwidth

The (S_{11}) versus frequency plot of the modified antenna also shows two dips indicating dual frequency operation of the antenna at the resonance frequencies of 3.905 GHz and 5.36 GHz. The value of reflection coefficients (Γ) are 0.10301 and 0.054688 at the corresponding resonance frequencies as seen from the Figure 6.13. The return loss $(20\log_{10}|\Gamma|)$ values are -25.242 dB and -19.742 dB at the corresponding resonance frequencies. The S_{11} parameter represents the power reflected from the antenna. The whole power is reflected from the

antenna and nothing is radiated for $S_{11} = 0$ dB. $S_{11} = -10$ dB indicates 10% of the power is reflected. The bandwidth of the dual band antenna can be calculated from the return loss versus frequency plot. The bandwidth of the antenna is the range of frequencies over which the return loss is larger than -10 dB and it corresponds to a VSWR value of 2. The measured -10 dB bandwidth of the designed antenna is 134.8 MHz and 384.9 MHz at the lower resonant frequency of 3.905 GHz and the upper resonant frequency of 5.36 GHz respectively.

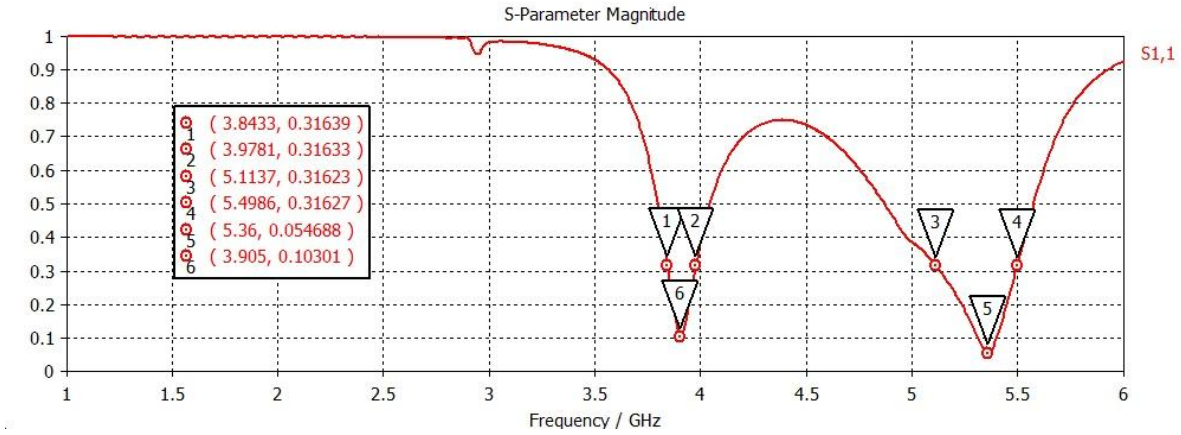

Figure 6.13 S-parameter (Ţ or Reflection Coefficient) Versus Frequency Plot of the Improved Dual Band ACSMPA

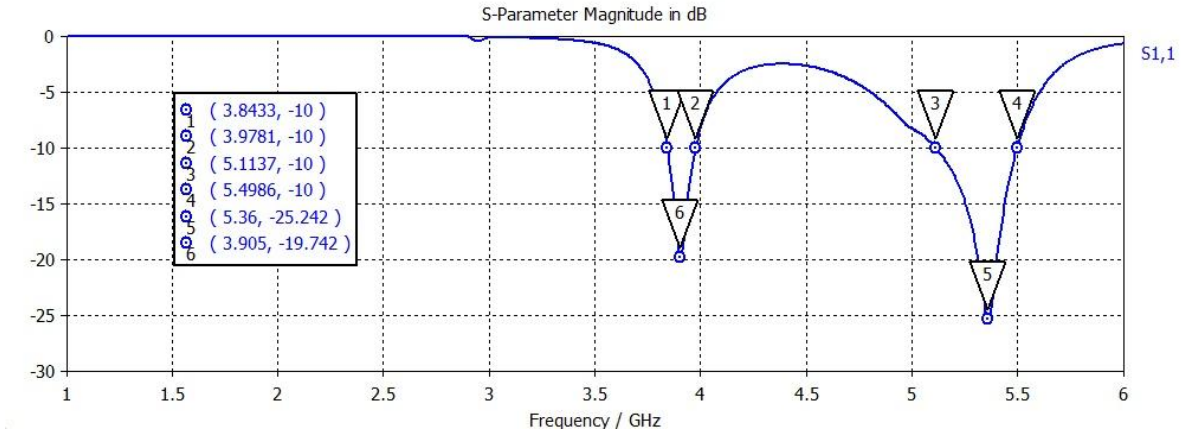

Figure 6.14 Return Loss (S_{11}) Versus Frequency Plot of the Improved Dual Band ACSMPA

A comparison of the return loss versus frequency plot between the dual band antenna and the modified dual band antenna with an air gap is shown in Figure 6.15. By introducing an air

gap of 3 mm the resonance frequencies has been shifted from 3.455 GHz and 5.225 GHz to 3.905 GHz and 5.36 GHz respectively but still they lie in the wireless bands with enhanced bandwidths. The similar results are observed for the foam material instead of air gap is also shown in same Figure 6.15.

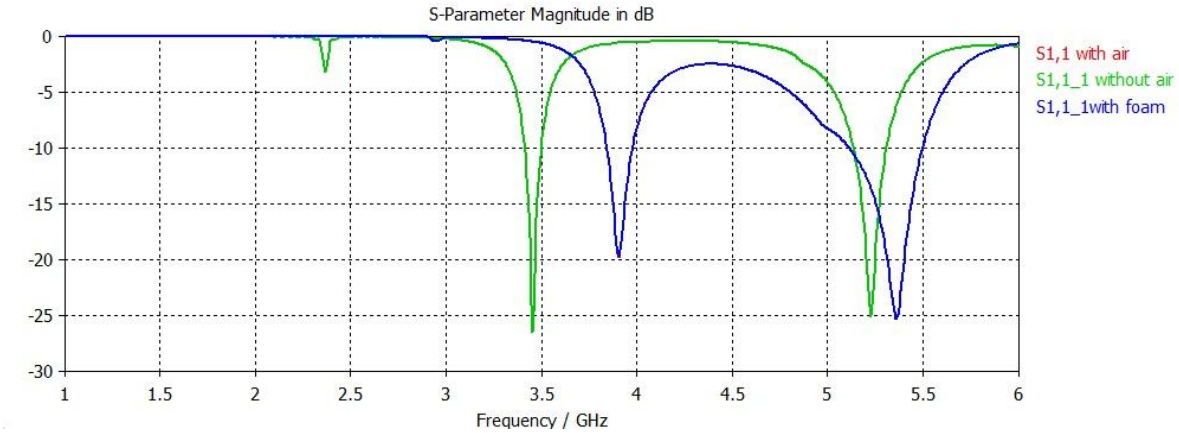

Figure 6.15 Comparison of Return Loss Plot of the Dual Band and Improved Dual Band ACSMPA

6.3.2.2 Smith Chart and Antenna Impedance

The smith chart of the modified dual band antenna has been shown in Figure 6.16 which depicts the impedance values (resistance as well as reactance) of the antenna at the marked frequency values. The almost real value of the impedance (with a very small reactance) at the resonance frequencies indicates the antenna requires lesser tuning to be done to match the antenna's impedance with the transmission line.

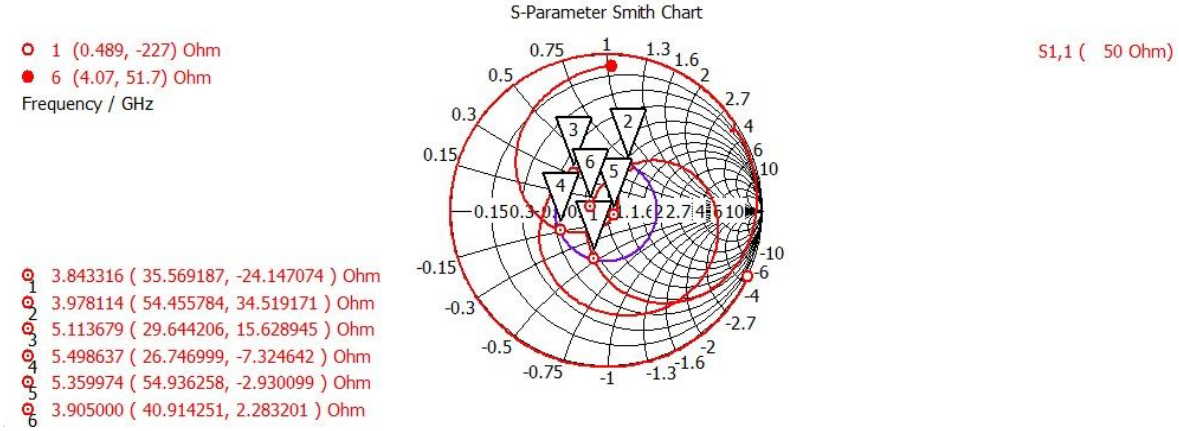

Figure 6.16 Smith Chart of the Improved Dual Band ACSMPA

6.3.2.3 VSWR

The VSWR versus frequency plot of the modified dual band antenna has been shown in Figure 6.17 which depicts the VSWR values at both the resonance frequencies. The antenna achieves a VSWR value of 1.2297 at the lower band frequency of 3.905 GHz and 1.1157 at the upper band frequency of 5.36 GHz.

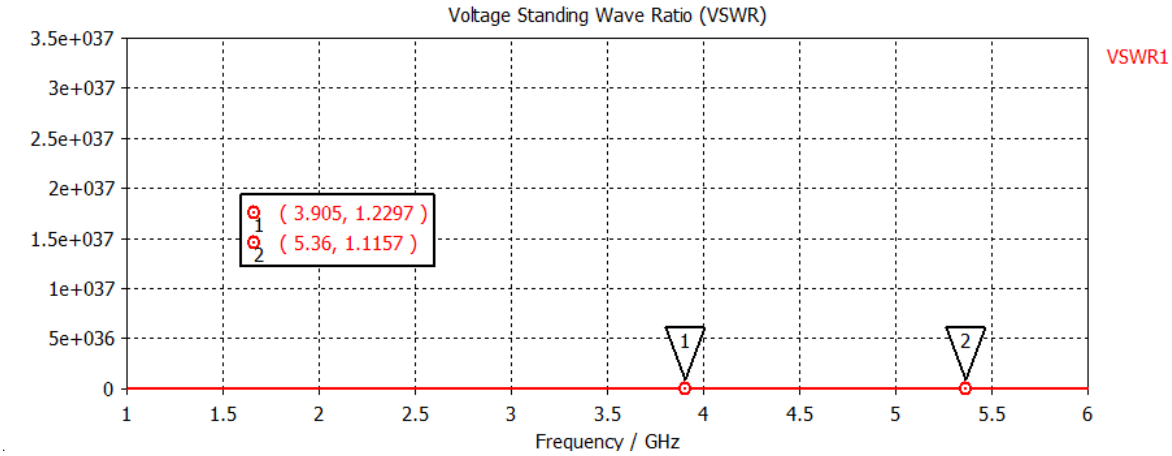

Figure 6.17 VSWR Plot of the Improved Dual Band ACSMPA

6.3.2.4 Impedance

The real and imaginary part of antenna's impedance at both the resonance frequencies has been shown in Figure 6.18. The very small value of reactance (imaginary part of the complex impedance) provides good matching of the antenna's impedance to the transmission line, because it gives the lesser reflection from the antenna and a more negative value of the return loss.

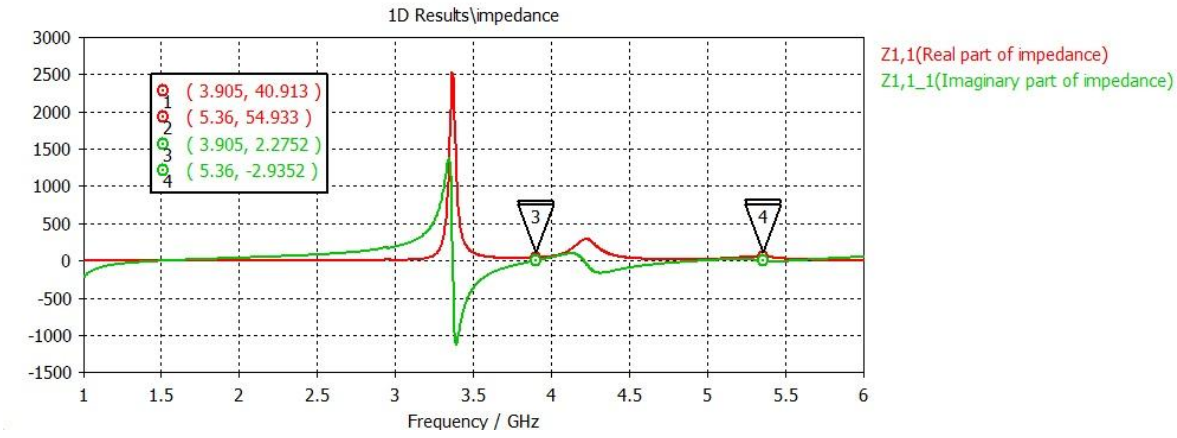

Figure 6.18 Impedance Versus Frequency Plot of the Improved Dual Band ACSMPA

6.3.2.5 Surface Current

The surface current distribution at the top patch, bottom patch, ground and the feedline for the improved dual band microstrip patch antenna resonating at lower band frequency of 3.905 GHz is shown in Figure 6.19(a), (b), (c), (d) respectively. Figure 6.19(a) depicts the current is flowing in almost the entire patch, but it has more magnitude near the leftmost and rightmost boundary of the slot cut in the patch. The bottom patch has more current density near the left and right edge of the patch as seen from the Figure 6.19(b). The magnitude of the current is more around the boundaries of the slot in the ground plane as shown in Figure 6.19(c). And for the feedline the current density is more in the center as shown in Figure 6.19(d). The arrows are pointed in the direction of the field and the color of the arrows are related to the field strength.

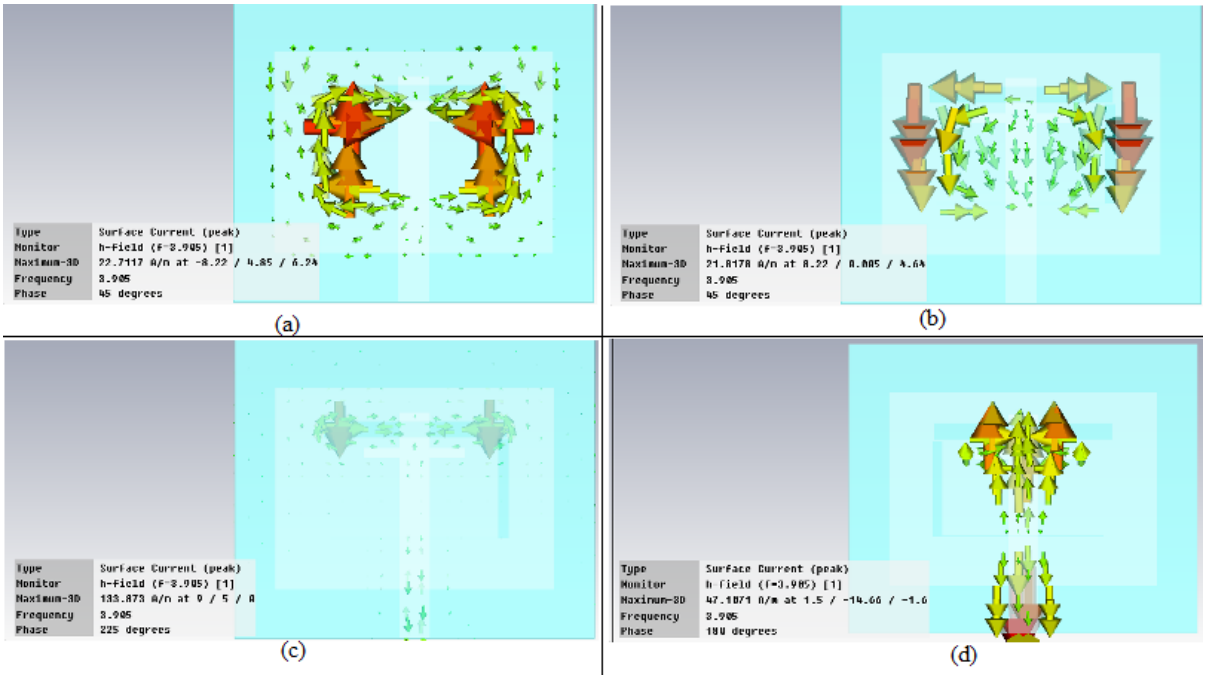

Figure 6.19 Surface Current Distribution of the Improved Dual Band ACSMPA at 3.905 GHz (a) Top Patch, (b) Bottom Patch, (c) Ground Plane, (d) Feedline

The surface current distribution at the top patch, bottom patch, ground and the feedline for the dual band microstrip patch antenna resonating at upper band frequency of 5.36 GHz is shown in Figure 6.19(e), (f), (g), (h) respectively. Figure 6.19(e) depicts the current is flowing in almost the entire patch, but it has more magnitude in the arms of the patch. The

bottom patch has more current density near the leftmost and rightmost edge of the patch as seen from the Figure 6.19(f). The magnitude of the current is more around the boundaries of the slot in the ground plane as shown in Figure 6.19(g). And for the feedline the current density is more in the center as shown in Figure 6.19(h)**.**

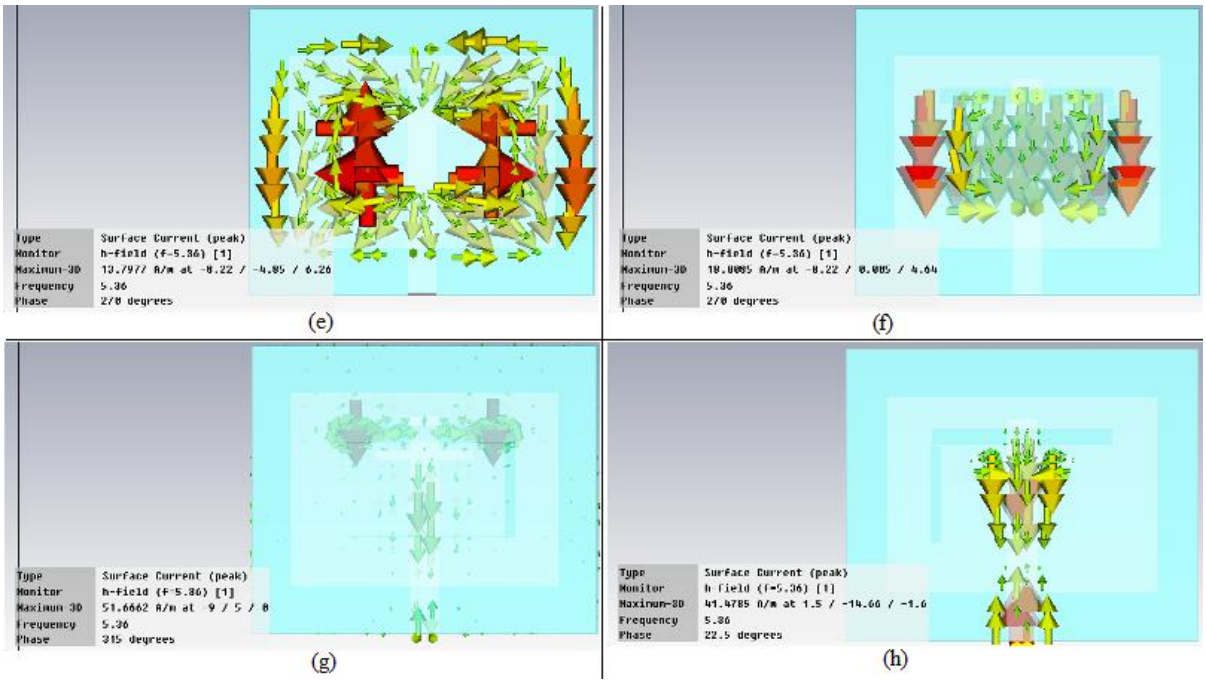

Figure 6.19 Surface Current Distribution of the Improved Dual Band ACSMPA at 5.36 GHz (e) Top Patch, (f) Bottom Patch, (g) Ground Plane, (h) Feedline

6.3.2.6 Directivity

The polar plot of the directivity with the elevation angle (θ degrees) at the azimuth angle (ϕ) phi equal to 90 degrees of the improved dual band antenna with stacked technology at both the resonance frequencies of 3.905 GHz and 5.36 GHz is shown in Figure 6.20(a), (b)

Also the 2 D and 3D radiation pattern of the directivity of the improved dual band ACSMPA with air gap between the ground plane and the upper layer substrate at frequency 3.905 GHz has been shown in Figure 6.20 (c), (d). The 2 D and 3D radiation pattern of the directivity of the improved dual band ACSMPA with air gap between the ground plane and the upper layer substrate at frequency 5.36 GHz has been shown in Figure 6.20 (e), (f).

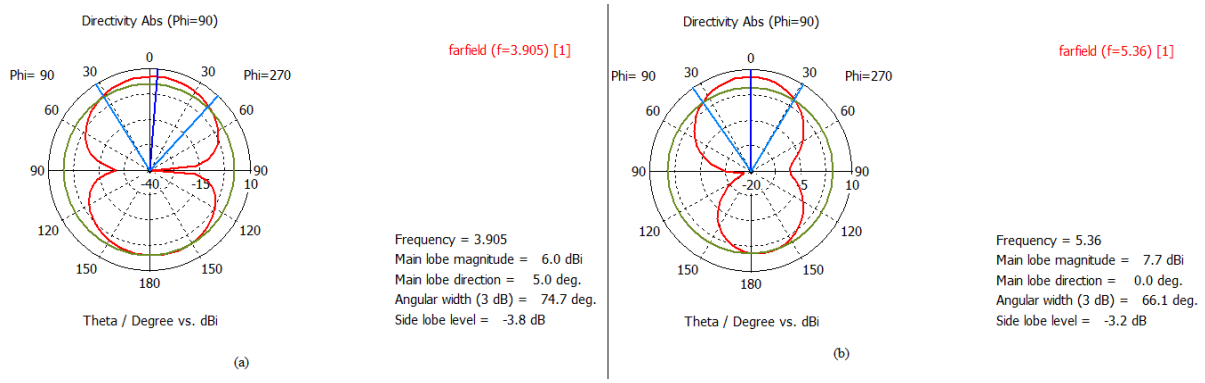

Figure 6.20 Polar Plot of the Directivity of the Improved Dual Band ACSMPA with Air Gap at Frequency (a) 3.905 GHz, (b) 5.36 GHz

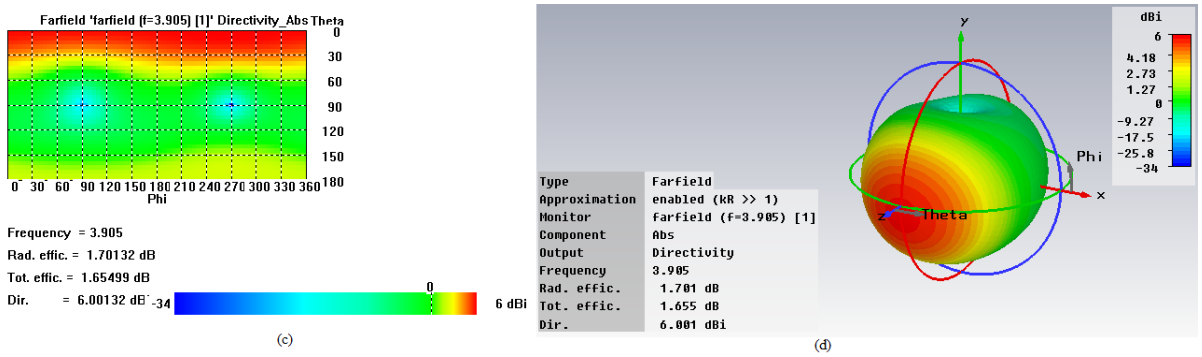

Figure 6.20 Radiation Pattern of the Directivity of the Improved Dual Band ACSMPA with Air Gap at Frequency 3.905 GHz (c) 2D plot, (d) 3D plot

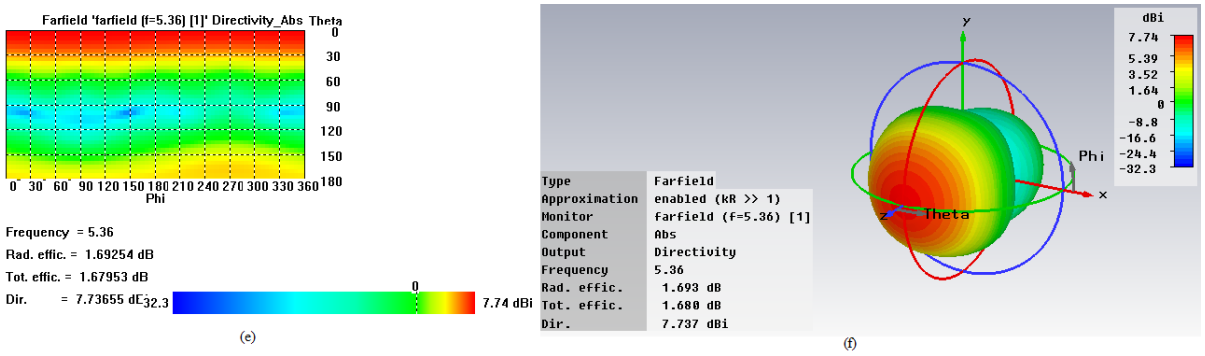

Figure 6.20 Radiation Pattern of the Directivity of the Improved Dual Band ACSMPA with Air Gap at Frequency 5.36 GHz (e) 2D plot, (f) 3D plot

6.3.2.7 Gain

The polar plot of the gain with the elevation angle (θ degrees) at the azimuth angle (ϕ) phi equal to 90 degrees of the improved dual band antenna with stacked technology at both the resonance frequencies of 3.905 GHz and 5.36 GHz is shown in Figure 6.21(a), (b).

Also the 2 D and 3D radiation pattern of the gain of the improved dual band ACSMPA with air gap between the ground plane and the upper layer substrate at frequency 3.905 GHz has been shown in Figure 6.21 (c), (d). The 2 D and 3D radiation pattern of the gain of the improved dual band ACSMPA with air gap between the ground plane and the upper layer substrate at frequency 5.36 GHz has been shown in Figure 6.21 (e), (f).

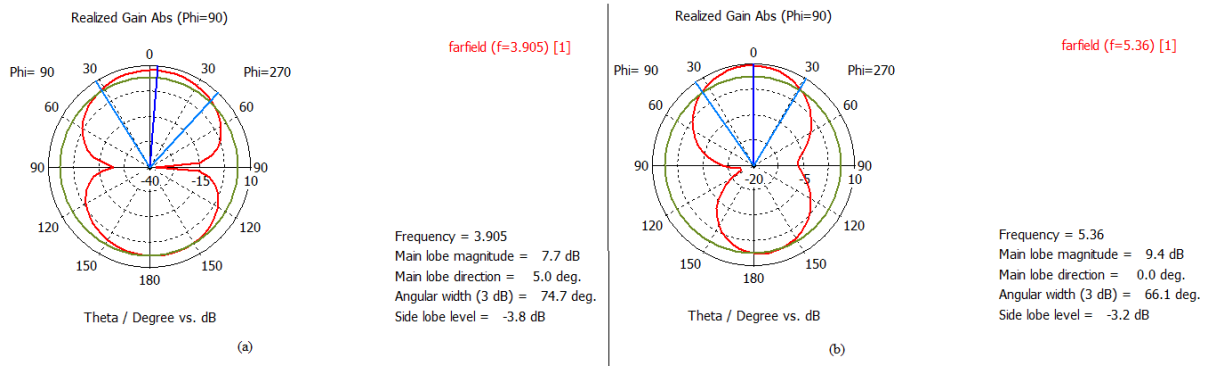

Figure 6.21 Polar Plot of the Gain of the Improved Dual Band ACSMPA with Air Gap at Frequency (a) 3.905 GHz, (b) 5.36 GHz

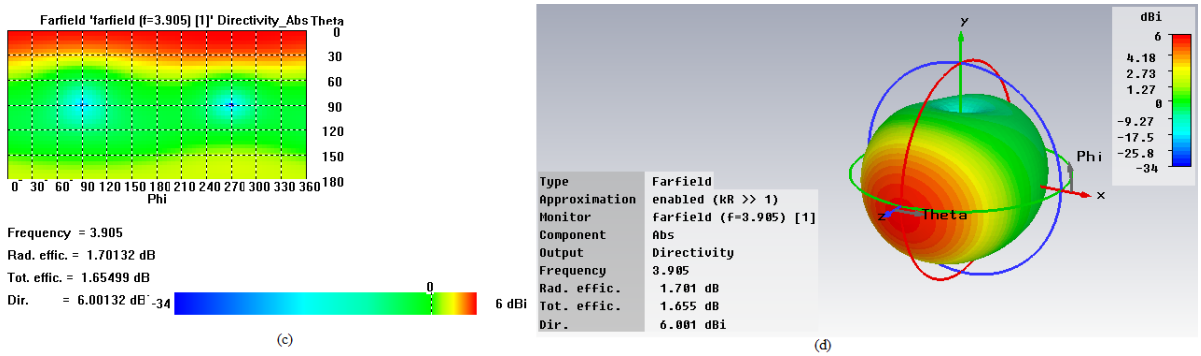

Figure 6.21 Radiation Pattern of the Gain of the Improved Dual Band ACSMPA with Air Gap at Frequency 3.905 GHz (c) 2D plot, (d) 3D plot

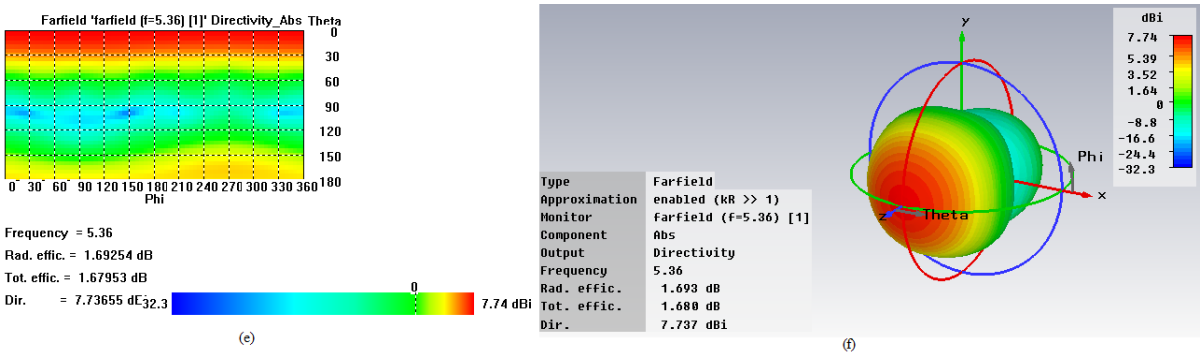

Figure 6.21 Radiation Pattern of the Gain of the Improved Dual Band ACSMPA with Air Gap at Frequency 5.36 GHz (e) 2D plot, (f) 3D plot

6.4 Conclusion

The two antenna designs have been discussed in this chapter for WLAN applications. One is dual band aperture coupled stacked microstrip patch antenna and the other is dual band aperture coupled stacked microstrip patch antenna with an air gap between the ground plane the upper layer substrate.

CHAPTER 7

FABRICATION AND TESTING OF BROADBAND ACMPA

The whole fabrication process of the broadband aperture coupled microstrip patch antenna simulated in CHAPTER 5 is covered in this chapter.

7.1 Fabrication Procedure

The process of fabrication of nominal antenna is done in few steps and is discussed in the flow chart below. The flow chart makes the fabrication procedure easy to understand.

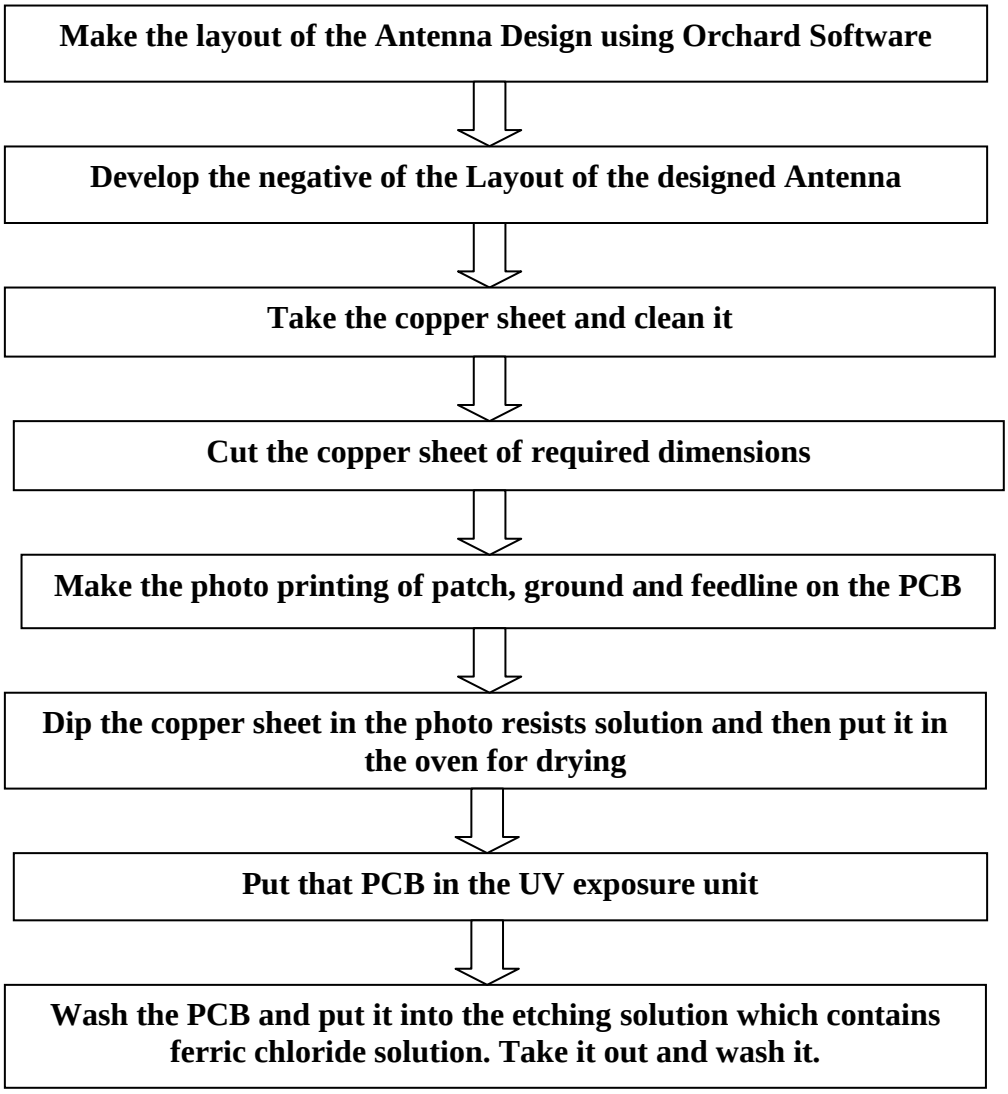

Figure 7.1 Flow Chart of Antenna Fabrication Process

7.2 Fabricated Antenna Design

The fabrication of the antenna involves the development of the negative of the antenna design and it done by using orchard software. Thus the layout is printed out and it is dipped in a photo resist developer further. Then it is dried in an oven unit at 140-150 degree temperature properly. After drying the antenna design, it is dipped into the nitric acid solution for etching out the painted part out of the design.

The negative of the fabricated design of the broadband microstrip patch antenna is as shown in the figure below:

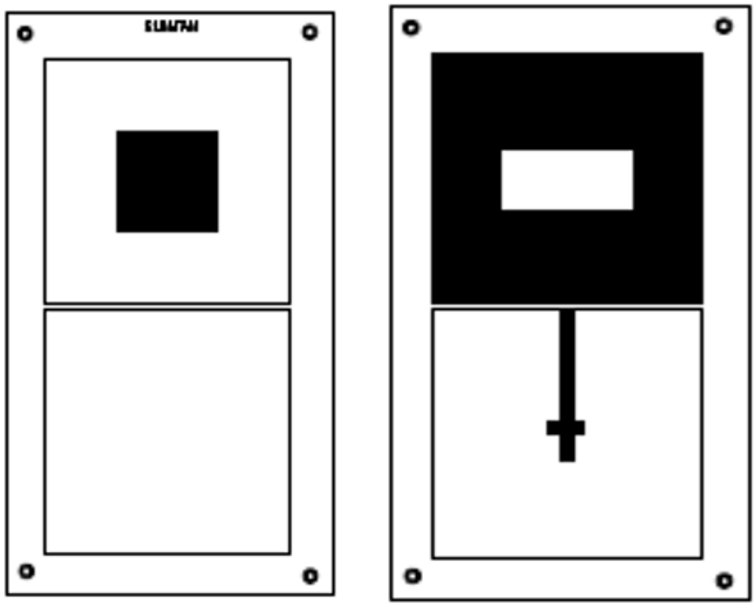

Figure 7.2 Negative of the Antenna (a) Top View, (b) Back view

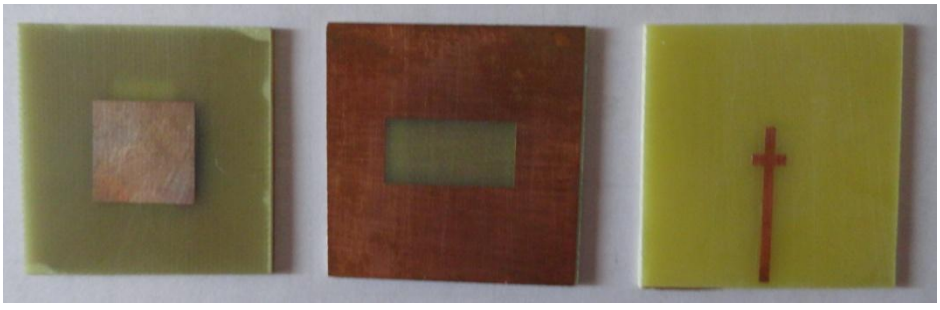

Figure 7.3 Fabricated Antenna at 12.5 GHz (a) Top View, (b) Ground Plane, (b) Back View

7.3 Testing of Antenna

The testing of the fabricated antenna has been done by using VNA model no N5222A of Agilent Technologies, whose frequency range is from 10 MHz to 26.5 GHz and it is shown in Figure 7.4 below:

Figure 7.4 Network Analyzer for Testing

7.4 Comparison of Simulated and Fabricated Antenna

Figure 7.5 shows the return loss versus frequency plot of the broadband antenna designed in CHAPTER 5. It is a wide band covering the frequency range from 12.202 GHz to 13.339 GHz having a bandwidth of 1.137 GHz or 1137 MHz with the return loss value of −35.459 dB at resonant frequency of 12.5 GHz.

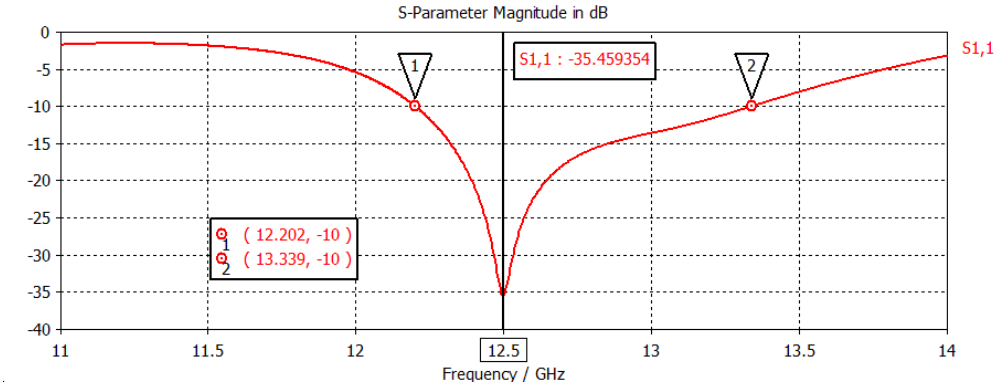

Figure 7.5 Return Loss (S_{11}) Versus Frequency Plot of the Simulated Broadband Antenna

Figure 7.6 shows the return loss (S_{11}) in dB versus frequency plot of the fabricated broadband antenna on VNA.

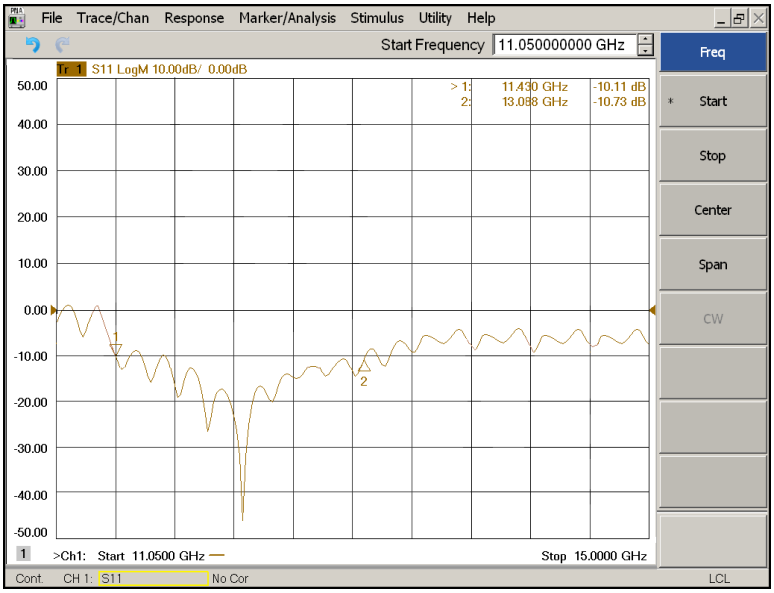

Figure 7.6 Measured Return Loss using Network Analyzer

Parameters	Tested results at 12.5 GHz	Simulated result at 12.5 GHz
Return Loss	−35.45 dB	−45 Db
Resonating frequency	12.5 GHz	12.3 GHz
Bandwidth	1137 MHz	~1258 MHz
Application Covered	DBS	DBS

Table 7.1 Comparison of Simulated and Tested Results

7.5 Conclusion

The simulated broadband aperture coupled microstrip antenna discussed in CHAPTER 5 has been fabricated and tested in this chapter. It is observed that there occurs some shift of frequency approximately 0.2 GHz in the results of simulated and fabricated antenna. Even though the resonance frequency has been shifted, still it is covering ITU region 2 (12.2 GHz - 12.7 GHz) and ITU region 3 (11.7 GHz-12.2 GHz) fulfilling the DBS applications because during simulation ±10% margin has been considered.

CHAPTER 8

CONCLUSION AND FUTURE WORK

8.1 Conclusions

- The thesis work starts with the general discussion on Microstrip Antennas and their applications to the present Wireless Communication scenario, based upon the historical review done in the field of application of Microstrip Antennas to WLAN and DBS (ITU Region 2 and 3), the main objective of the thesis was defined to design and simulate MPAs for these bands.

  One of the antennas was fabricated and tested for operation in the DBS scenario. Below mentioned are the details of the major work coved in the thesis and how it can be implemented in the real world.

- In this report firstly the single band aperture coupled microstrip rectangular patch antenna has been designed to resonate at 5.794 GHz using transmission line model. The nominal antenna can be used for WLAN applications and has −10 dB bandwidth of 223 MHz. The various physical parameters which affect the performance of the antenna are dimensions of the patch, the stub and the slot, dielectric constant of the substrate material used, the height of the dielectric material, the position of the slot relative to patch and the position of the slot relative to the feedline. The antenna characteristics like operating frequency, input impedance, bandwidth, return loss, directivity and gain depends upon the antenna parameters. The antenna design parameters under parametric sweep and their corresponding results has been discussed in CHAPTER 3.

- A dual band aperture coupled microstrip patch antenna has been designed in CHAPTER 4 by cutting the slits at the boundaries of the rectangular shaped patch. The designed antenna resonate at 3.692 GHz and 5.2 GHz, hence can be used for WLAN and WiMAX applications. The simulated −10 dB bandwidth of the dual band antenna is 50.2 MHz and 139 MHz at lower and upper band resonant frequencies respectively. Thereafter the bandwidth of the antenna has been improved by placing

the stubs perpendicular to the feedline and the bandwidth of the upper resonant frequency band has been enhanced to 224.8 MHz. The gain of magnitude 6.6 dB and 7.0 dB has been obtained for the lower and upper band resonant frequencies respectively.

- A broadband aperture coupled microstrip rectangular patch antenna has been designed to resonate at 12.5 GHz frequency which lies in Ku-band (12-18 GHz) for home reception of Direct Broadcast Satellite Television applications in CHAPTER 5. The nominal antenna has simulated −10 dB return loss bandwidth of 1137 MHz. The gain obtained of broadband antenna design is 7.5 dB.
- The dual band aperture coupled microstrip stacked patch antenna has been designed in CHAPTER 6 in which a stacked patch (top patch) residing on upper layer substrate1 is placed over the bottom patch residing on upper layer substrate supported by the ground plane. The designed antenna resonate at 3.455 GHz and 5.225 GHz, hence can be used for WLAN and WiMAX applications. The antenna has −10 dB return loss bandwidth of 86.5 MHz and 172.6 GHz at lower and upper resonant frequency bands respectively. Then the antenna design is modified by introducing an air gap between the ground plane and the upper layer substrate. As a result the lower resonant frequency is changed to 3.905 GHz which lies in the frequency band (3400-4200 MHz) of IMT applications and the upper resonant frequency is changed to 5.36 GHz which lie in the frequency band of WLAN and WiMAX standards. The −10 dB return loss bandwidth of the improved microstrip stacked patch antenna is 134.8 MHz and 384.9 MHz at lower and upper resonant frequency band respectively. The gain of the designed antenna is 7.7 dB and 9.4 dB at the lower and upper band resonant frequencies respectively.

The results of the designed antennas are summarized in the following Table 8.1

Design	**Resonant Freq(GHz)**	**Return Loss(dB)**	**Bandwidth (MHz)**	**Directivity (dBi)**	**Gain (dB)**	**VSWR**
Single Band ACMPA	5.794	−32.42	223	5.838	6.935	1.048
Dual Band ACMPA	3.692	−20.94	50.2	5.576	6.6	1.1971
	5.172	−41.11	139	5.440	7.1	1.0179

Improved Dual Band ACMPA	3.692	−30.40	48.6	5.586	6.6	1.0623
	5.2	−26.99	224.8	5.309	7.0	1.0936
Broadband ACMPA	12.5	−35.46	1137	6.573	7.5	1.0343
Dual Band ACSMPA	3.455	−26.48	86.5	4.4	6.2	1.0995
	5.225	−25.03	172.6	7	8.7	1.1187
Improved Dual Band ACSMPA	3.905	−19.74	134.8	6	7.7	1.2297
	5.36	−25.24	384.9	7.7	9.4	1.1157

Table 8.1 Concluded Results of all the Designs

8.2 Future Scope

Although an extreme research has been done for optimum antenna design used for wireless applications but still there is so much work to be done with microstrip antennas. In this thesis work aperture coupled microstrip patch antennas designed from single band to dual band and up to broadband has been proposed for WLAN, WiMAX and DBS applications. Next, one can work on various techniques listed below to improve antenna performance:

- In this thesis work optimization of the parameters has been done manually. The optimization can be done by inbuilt optimizer in CST Microwave Studio using different optimization techniques like Genetic Algorithm, Neural Network and PSO (Particle Swarm Optimization).
- Antenna array can be designed to enhance the gain.
- DGSs (Defected Ground Structures) can be used for miniaturization of the designed antennas and to improve the performance of the antenna.
- Wideband and ultra-wideband patch antennas can be designed which is helpful in telecommunications and high speed data transmission system.
- Multiband patch antennas can be designed for various wireless applications.
- **Smart Antennas:** Smart Antennas are becoming very popular because of low profile structure and formidable rate thereby creating new and improved services at lower cost. They are extremely compatible embedded antennas in handheld wireless devices

such as cellular phones, pagers etc. These antennas have received enormous interest worldwide due to advancement in powerful low cost digital signal processors, general purpose processors, ASICs (Application Specific Integrated Circuits) as well as innovative software based signal processing technique (Algorithm).

- **Split Ring Resonator Structure (SRS):** A split ring resonator is a component of a negative index metamaterial, also known as double negative metamaterials or left handed medium. Split ring resonators also used for research in Terahertz metamaterials, acoustic metamaterials, and metamaterial antennas. A single cell split ring resonator structure has a pair of enclosed loops with splits in them at opposite ends. The loops are made of nonmagnetic metal like copper and have a small gap between them. The loop can be concentric, or square, and gapped as needed.
- **Electromagnetic Band Gap Structure (EBG):** Electromagnetic Band Gap (EBG) substrates for patch antennas significantly reduce the effect of surface waves as a function of frequency and are able to provide relatively broadband frequency performance. EBG structures are 3-D periodic objectives that prevent the propagation of the EM waves in the specified band frequency for all angles and for all polarization states. In EBG only one out of ε_r and μ_r is negative.
- **Other Feeding Techniques:** The other feeding techniques of microstrip patch antenna like microstrip line, coaxial feeding, proximity coupling and CPW can also be used in future to design microstrip patch antenna.
- **Patch Antennas with Switchable Slots:** The patch antennas with switchable slots can realize various functionalities with an attractive, simple structure, only one layer and a single feed, which is desirable in wireless communication systems. The patch antenna with one switchable slot realizes dual frequency operation with a small and flexible frequency ratio, and similar radiation patterns at the two frequencies. Dual band circularly polarized performance can be achieved by adding two switchable slots to a conventional circularly polarized patch antenna. The PASS concept can also be utilized to design an antenna that has a polarization sense that is switchable between RHCP and LHCP. As a practical example of these PASS applications, the PASS was applied to the antenna design for future Mars rover missions.

LIST OF PUBLICATIONS

PUBLISHED

Gunjan Makkar, Amanpreet Kaur, "Dual Band Aperture Coupled Patch Antenna for WLAN and WiMAX", IJARCCE, Vol. 3, Issue 5, May 2014.

COMMUNICATED

Gunjan Makkar, Amanpreet Kaur, "Dual Band Aperture Coupled Stacked Patch Antenna for WLAN Applications", IJRAT, Vol. 2, Issue 7, July 2014.

REFERENCES

[1] Andrea Goldsmith, "Wireless Communications," Cambridge University Press, 2005.

[2] T. S. Rappaport, "Wireless Communications and Practice," 2nd Edition, 2009.

[3] C. A. Balanis, "Microstrip Antennas," Antenna Theory Analysis and Design, Third Edition, John Wiley & Sons, pp 811-876, 2010.

[4] R. Garg, P. Bhartia and A. Ittipiboon, "Microstrip Antenna Design handbook Boston: Artech House," 2001.

[5] D. M. Pozar and R. Pous, "A Frequency Selective Surface Using Aperture Coupled Microstrip Patches," IEEE Transaction on Antennas and Propagation, vol.49, 12, pp 1763-1769 December 1990.

[6] Y. Kamiya, W. Chujo and M. Fujise, "Design for Dual Frequency Microstrip Antenna using Annular Slot Aperture Coupling," Indian Conference, vol. 7, no. 8, pp 1118-1121, 1991.

[7] K. F. Lee, K. M. Luk, K. M. Mak, and S. L. S. Yang, "Dual and Triple Band Patch Antenna," IEEE Antennas and Propagation Magazine, vol. 53, no. 3, pp 60-74, June 2011.

[8] L. Giauffret, J. M. Laheurte and A. Papiernik, "Experimental and Theoretical Investigations of New Compact Large Bandwidth Aperture Coupled Microstrip Antenna," vol. 31, no. 6, pp 2139-2140, March 1996.

[9] V. R. Girish and K. P. Ray, "Improved Coupling for Aperture Coupled Microstrip Antennas," vol. 44, no. 8, August 1996.

[10] S. Egashira and E. Nishiyama, "Stacked Microstrip Antenna with High Bandwidth and High Gain," IEEE Transaction on Antennas and Propagation, vol. 44, no. 11, pp 1533-1534, November 1996.

[11] W. P. Harokopus, S. Sanzgiri and P. Gilliland, "A Broadband High Gain Antenna using Aperture Coupled Microstrip Patches," Wireless Application Digest, IEEE MIT Symposium on Technologies, pp 89-92, February 1997.

[12] S. D. Targonski and D. M. Pozar, “Aperture Coupled Microstrip Antennas using Reflector Elements for Wireless Communication,” Indian Conference, pp 163-166, 2006.

[13] B. L. Ooi and C. L. Lee, “Broadband Air Filled Stacked U- Slot Patch Antenna,” IEEE Transaction on Antennas and Propagation, vol. 35, no. 7, pp 515-517, April 1999.

[14] Rod B. Waterhouse, “Stacked Patches using High and Low Dielectric Constant Material Combinations,” vol. 47, no. 12, pp 1767-1771, December 1999.

[15] P. V. Bijumon, S. K. Menon, M. T. Sebastian and P. Mohanan, “Enhanced Bandwidth Microstrip Patch Antennas Loaded with High Permittivity Dielectric Resonators,” Microwave and Optical Technology Letters, vol. 35, pp 327-330, 2002.

[16] W. S. T. Rowe and R. B. Waterhouse, “Reduction of Backward Radiation for CPW Fed Aperture Stacked Patch Antennas on Small Ground Planes,” IEEE Transactions on Antennas & Propagation, vol. 51, pp 1411-1413, 2003.

[17] S. Mestdagh, W. D. Raedt and A. E. Vandenbosch, “CPW Fed Stacked Microstrip Antennas,” IEEE Transactions on Antennas & Propagation, vol. 52, pp 74-83, 2004.

[18] N. Amiri, K. Forooraghi, and R. Dehbashi, “A Compact Dual Polarized Aperture Coupled Stacked Patch Antenna for GSM 900 MHz,” Asia Pacific Conference on Applied Electromagnetic, pp 79-81, 2005.

[19] Y. Lu, H. Wang and D. G. Fang, “A Novel Wideband Aperture Coupled Circularly Polarized Stacked patch,” Asia Pacific Conference on Environmental Electromagnetics, pp 904-907, 2006.

[20] S. Raje, S. Kazemi and H. R. Hassani, “Wideband Stacked Koch Fractal with H-Shape Aperture Coupled Feed,” Proceedings of Asia Pacific Microwave Conference, pp 1-4, 2007.

[21] R. Duan, Y. Lu, “Foldable Aperture Coupled Microstrip Antenna Array for Portable Wireless Application,” IEEE Radio and Wireless Symposium, pp 471-474, 2008.

[22] M. A. Alayesh, C. G. Christodoulou, M. Joler and S. E. Barbin, "Reconfigurable Multiband Stacked Microstrip Patch Antenna for Wireless Applications," Antennas and Propagation Conference, pp 329-332, 2008.

[23] M. T. Islam, M. N. Shakib, N. Misran and B. Yatim, "Design of Compact Ultra Wideband Patch Antenna for Wireless Communications," IEEE International Workshop on Antenna Technology, pp 1-4, 2009.

[24] F. Zhang, F. S. Zhang, C. Lin and G. Zhao, "Broadband Microstrip Patch Antenna Array using Stacked Structure," pp 388-391, 2010.

[25] Z. N. Chen and X. Qing, "Dual Band Circularly Polarized S- Shaped Slotted Patch Antenna with Small Frequency Ratio," IEEE Transaction on Antennas and Propagation, vol. 58, no. 6, pp 2112-2115, June 2010.

[26] O. H. Izadi and M. Mehrparvar, "A Compact Microstrip Slot Antenna with Novel E- shaped Coupling Aperture," 5th International Symposium on Telecommunication, pp 110-114, 2010.

[27] H. C. Chiung, S. Y. Chen, "A Novel Broadband Aperture Coupled Microstrip Patch Antenna," Asia Pacific Microwave Conference Proceedings, pp 709-712, 2011.

[28] H. Zhang, B. Shen, "The Study of Aperture Coupled Dual Band Microstrip Patch Antennas," International Conference on Electronics, Communications and Control, pp 1162-1165, 2011.

[29] H. Oraizi, R. Pazoki, "Radiation Bandwidth Enhancement of Aperture Stacked Microstrip Antennas," IEEE Transactions on Antennas & Propagation, vol. 59, pp 4445-4453, 2011.

[30] P. Hazdara, M. Capek, P. Hamouz, M. Mazanek, "Advanced Modal Techniques for Microstrip Patch Antenna Analysis," ICECom Conference Proceedings, pp 1-6, 2012.

[31] N. Ramli, M. T. Ali, A. L. Yusof and S. K. Kayat, H. Alias and M. A. Sulaiman, "A Frequency Reconfigurable Stacked Patch Microstrip Antenna using C-Foam in Stacked Substrate," Asia Pacific Conference on Applied Electromagnetics, pp 322-326, 2012.

[32] M. Gujral, J. L. W. Li, T. Yuan, and C. W. Qiu "Bandwidth Improvement of Microstrip Antenna Array using Dummy EBG Pattern on Feedline," Progress in Electromagnetic Research, vol. 127, pp 79-92, 2012.

[33] S. C. Gupta, A. Singh "Review and Survey of Broadband Microstrip Patch Antennas," International Journal of Computer Applications, vol. 59, pp 49-55, 2012.

[34] N. Ramli, M. T. Ali, A. L. Yusof and N. Ya'acob, "Frequency Reconfigurable Stacked Patch Microstrip Antenna for LTE and WiMAX Applications," International Conference on Computing, Management and Telecommunications, pp 55-59, 2013.

[35] M. Kaur, A. Kaur and R. Khanna, "A Microstrip Patch Antenna with Aperture Coupler Technique at 5.8 GHz," International Journal of Modern Engineering Research, vol. 3, pp 587-597, 2013.

[36] C. Schulz, C. Baer, T. Musch, and I. Rolfes "A Broadband Stacked Patch Antenna with Enhanced Antenna Gain by an Optimized Ellipsoidal Reflector for X-Band Applications," pp 1-7, November 2011.

[37] J. P. Kim, W. S. Park, "Analysis and Network Modeling of an Aperture Coupled Microstrip Patch Antenna," IEEE Transactions Antenna Propagation, vol. 49, no. 6, pp 849-854, 2001.

[38] P. L. Sullwan and D. H. Schaubert, "Analysis of Aperture Coupled Microstrip Antennas," IEEE Transactions Antenna Propagation, vol. 34, no. 8, pp 977-984, 1986.

[39] H. Daniel and C. Terret, "Transmission Line Analysis of Aperture Coupled Microstrip Antenna," Electronics Letters, vol. 25, no. 18, pp- 1229-1230, August 1989.

[40] D. M. Pozar, "A Reciprocity Method of Analysis for Printed Slot and Slot-Coupled Microstrip Antennas," IEEE Transactions Antenna Propagation, vol. 34, no. 12, pp 1439-1446, 1986.

[41] R. Garg, B. Prakash, I. Bahl, and A. Ittipiboon, "Microstrip Antenna Design Handbook," Artech House, 2001.